ISTANBUL TECHNICAL UNIVERSITY ★ GRADUATE SCHOOL OF SCIENCE ENGINEERING AND TECHNOLOGY

DESIGN OF INORGANIC PEPTIDE BONDED FUSION BIOMOLECULES FOR TRACKING DISEASE RELATED PROTEINS

Ph.D. THESIS

Bertan Koray BALCIOĞLU

Department of Molecular Biology-Genetics and Biotechnology

Molecular Biology-Genetics and Biotechnology Programme

AUGUST 2014

ISTANBUL TECHNICAL UNIVERSITY ★ GRADUATE SCHOOL OF SCIENCE ENGINEERING AND TECHNOLOGY

DESIGN OF INORGANIC PEPTIDE BONDED FUSION BIOMOLECULES FOR TRACKING DISEASE RELATED PROTEINS

Ph.D. THESIS

Bertan Koray BALCIOĞLU
(521062208)

Department of Molecular Biology-Genetics and Biotechnology

Molecular Biology-Genetics and Biotechnology Programme

Thesis Advisor: Prof. Dr. Candan TAMERLER
Co-Advisor: Associate Prof. Berrin ERDAĞ

AUGUST 2014

İSTANBUL TEKNİK ÜNİVERSİTESİ ★ FEN BİLİMLERİ ENSTİTÜSÜ

HASTALIKLA İLİŞKİLİ PROTEİNLERİN İZLENMESİNDE ANORGANİK PEPTİT BAĞLARLA FÜZYON BİYOMOLEKÜLLERİN TASARIMI

DOKTORA TEZİ

Bertan Koray BALCIOĞLU
(521062208)

Moleküler Biyoloji-Genetik ve Biyoteknoloji Anabilim Dalı

Moleküler Biyoloji-Genetik ve Biyoteknoloji Programı

Tez Danışmanı: Prof. Dr. Candan TAMERLER
İkinci Tez Danışman: Doç. Dr. Berrin ERDAĞ

AĞUSTOS 2014

Bertan Koray BALCIOĞLU, a Ph.D. student of ITU Graduate School of Science, Engineering and Technology, student ID 521062208, successfully defended the thesis entitled "DESIGN OF INORGANIC PEPTIDE BONDED FUSION BIOMOLECULES FOR TRACKING DISEASE RELATED PROTEINS" which he prepared after fulfilling the requirements specified in the associated legislations, before the jury whose signatures are below.

Thesis Advisor :	**Prof. Dr. Candan TAMERLER** The University of Kansas	.....
Co-advisor :	**Assoc. Prof. Dr. Berrin ERDAĞ** TUBITAK MRC GEBI	.....
Jury Members :	**Prof. Dr. Dilek KAZAN** Marmara University	.....
	Prof. Dr. Beyazıt ÇRAKOĞLU	.....
	Prof. Dr. Z. Petek ÇAKAR Istanbul Technical University	.....
	Prof. Dr. Ayten YAZGAN KARATAŞ Istanbul Technical University	.....
	Assoc. Prof. Dr. Nevin KARAGÜLER Istanbul Technical University	.....
	Assis. Prof. Dr. Urartu ŞEKER Bilkent University	.....

Date of Submission : 23 July 2014
Date of Defense : 19 August 2014

To my spouse, my family, my best friend Ali, my friends and myself

FOREWORD

I am very pleased regarding the topic that we have chosen with my supervisors about my thesis. Therefore, I think that a nice work has aroused, but certainly not perfect and some improvements might be done. However, I think this is science… an everlasting hard work for trying to discover, to improve and to add a drop of knowledge into the scientific pool. Of course, all of these efforts are done for one main objective: the welfare of the human being…but also maybe a little bit to attenuate my curiosity.

I am grateful to my advisors, Ass. Prof. Dr. Berrin ERDAĞ and Prof. Dr. Candan TAMERLER for giving me the opportunity of doing this research and being my mentors all along my thesis. I am also grateful to all my colleagues (my friends) Dr. Aylin ÖZDEMİR-BAHADIR, Dr. H. Ümit ÖZTÜRK, K. Serkan UZYOL, Özlem İBRAHİMOĞLU, Duygu HINÇ which have supported me not only mentally but also by loading up our Laboratory works allowing me to work on my thesis. I have not to mention that much work was done after the working days and the week-ends.

I also want to thanks a lot Sibel ÇETİNEL, Burak ÇALIŞKAN, which have helped me nights and days for the SPR experiments at ITU-MOBGAM. I wish also to thank Yıldız ULUDAĞ for giving me advices regarding the interpretation of SPR results.

I would like also to make a special thank to a great Professor, Prof. Dr. M. Beyazıt ÇIRAKOĞLU (my MSc. Advisor and member of my thesis follow-up committee) and his wife Prof. Dr. Şeyda ÇIRAKOĞLU, to Prof. Dr. Petek ÇAKAR and Prof. Dr. Ayten YAZGAN KARATAŞ for their encouraging and supporting behaviors.

A special thank to our Laboratory technician Aydın BAHAR for helping me with the works since I have started my career in TÜBİTAK, already 14 years…

No work is done without money and infrastructure utilization, all the SPR experiment were done by using the infrastructure of ITU-MOBGAM. Therefore, I would like to thank the MOBGAM administration for allowing me to use the Institute instruments. My thesis was partially funded from a TUBITAK TARAL-1007 project entitled "The development of diagnostic kits for Hepatitis B infection by using serologic and molecular techniques" (2006-2010. However, the main funding was obtained from TUBITAK MRC project entitled "The development of anti-angiogenic humanized antibodies for blocking tumor vascularisation" achieved in the immunogenetic Laboratory at the Genetic Engineering and Biotechnology Institute. Therefore, I would like to thank again Ass. Prof. Dr. Berrin ERDAĞ for funding my thesis, without this money no work would be accomplished.

Finally, I would like to thank my childhood friend Ass. Prof. Ali Fıkırkoca (Ankara University), I am so sorry Ali; I was not able to finish my Ph.D. before you passed away… (25 June 2014). I would like to thank my family; my wife Ayçin, my mother Chantale, my dad Nurettin, my brother Kerem, my parents in Law (Necmiye and Neptün) and sisters in law (Yaprak, Yonca, Ayça and Gözde). They were always with me. Thank you very much.

July 2014

Bertan Koray BALCIOĞLU
(Senior Researcher, MSc.)

TABLE OF CONTENTS

Page

FOREWORD ..... **ix**
TABLE OF CONTENTS ..... **xi**
ABBREVIATIONS ..... **xiii**
LIST OF TABLES ..... **xv**
LIST OF FIGURES ..... **xvii**
SUMMARY ..... **xxiii**
ÖZET ..... **xxv**
1. INTRODUCTION **1**
1.1 Immunosensors 1
1.1.1 Optical immunosensors 5
1.1.1.1 Optical sensors using labels 5
1.1.1.2 Label free optical immunosensors 6
1.1.2 SPR spectrometer 8
1.1.2.1 Principle 8
1.1.2.2 Real-time monitoring 10
1.1.3 Biointerface 11
1.2 Inorganic binding peptides 15
1.2.1 Roles of proteins in biological materials 15
1.2.2 Inorganic binding peptides 17
1.2.3 Genetically engineered peptide-based applications 19
1.3 Hepatitis B virus 23
1.3.1 Epidemiology and virology 24
1.3.2 Detection of HBsAg 29
1.4 Detection probes for HBsAg 30
1.4.1 Anti-HBsAg monoclonal antibodies with Hybridoma technology 32
1.4.2 Recombinant antibodies with phage display technology 32
1.4.2.1 M13 Bacteriophage structure 32
1.4.2.2 Infection of M13 Bacteriophage 34
1.4.2.3 Displaying proteins on the phage surface 37
1.4.2.4 Phage display systems 38
1.4.2.5 Phage display applications 41
1.4.2.6 Random peptide libraries 42
1.5 “Self-Assembling Biosensing HBsAg Probes” 43
2. MATERIALS AND METHODS **47**
2.1 Materials 47
2.1.1 Strains 47
2.1.1.1 Bacterial strains genotype 47
2.1.1.2 Mouse strain 47
2.1.1.3 Mammalian cell lines 47
2.1.2 Vectors 48
2.1.3 Primers 48

2.2 Methods 48
2.2.1 Development of an anti-HBsAg single chain Fv recombinant antibody .. 48
2.2.1.1 Cloning of HBsAg in phagemid vector 48
2.2.1.2 Production of HBsAg displaying phages and phage ELISA 52
2.2.1.3 Mouse Immunization and ELISA from immunized mice sera 54
2.2.1.4 Statistical analysis 54
2.2.1.5 Construction of a recombinant antibody library 55
2.2.1.6 Selection of an anti-HBsAg scFv from the library 56
2.2.2 Development and characterization of an anti-HBsAg gold binding recombinant antibody 58
2.2.2.1 Cloning of the anti-HBsAg Lig7 recombinant antibody into pQE2 vector 59
2.2.2.2 Insertion of gold binding peptide coding region in the Lig7/pQE2 vector 61
2.2.2.3 Expression of the bifunctional recombinant antibodies 63
2.2.2.4 Purification of bifunctional antibodies from large scale culture and removal of His-Tag 65
2.2.3 The use of the recombinant antibodies as a biosensing probe 66
2.2.3.1 Binding studies using Surface Plasmon Resonance spectroscopy (SPR) 66
2.2.3.2 Monitoring HBsAg in *in-vitro* cell model 68
3. RESULTS AND DISCUSSION 71
3.1 Development of an anti-HBsAg single chain Fv recombinant antibody 71
3.1.1 Cloning of HBsAg in phagemid vector 71
3.1.2 Production of HBsAg displaying phages and phage ELISA 75
3.1.3 Mouse immunization and ELISA from immunized mice sera 77
3.1.4 Construction of a recombinant antibody library 79
3.1.5 Selection of an anti-HBsAg scFv from the library 82
3.2 Development and characterisation of an anti-HBsAg gold binding recombinant antibody 84
3.2.1 Cloning of the anti-HBsAg Lig7 recombinant antibody into pQE2 vector 84
3.2.2 Insertion of gold binding peptide coding region in the Lig7/pQE2 vector 86
3.2.3 Expression of the bifunctional recombinant antibodies 93
3.2.4 Purification of bifunctional antibodies from large scale culture and removal of His-Tag. 97
3.3 The use of the recombinant antibodies as a biosensing probe 102
3.3.1 Binding studies using Surface Plasmon Resonance spectroscopy 102
3.3.2 Monitoring HBsAg in *in-vitro* model 110
4. CONCLUSIONS AND RECOMMENDATIONS 113
REFERENCES 119
APPENDICES 135
CURRICULUM VITAE 143

ABBREVIATIONS

2D : Two dimension
3GBP : 3 repeats of Gold Binding Peptide 1
5GBP : 5 repeats of Gold Binding Peptide 1
ABTS : 2,2'- azino-bis (3-ethylbenzothiazoline-6-sulphonic acid)
AFM : Atomic Force Microscopy
Ag : Silver
AP : Alkaline Phosphatase
AuBP : Gold Binding Peptide
Au NP : Gold Nanoparticle
Bp : Base pair
BSA : Bovine Serum Albumin
CDR : Complementary Determining Region
CT : C-Terminal domain
Da : Dalton
DCC : Dicyclohexylcarbodiimide
Ds : Double Strand
E. coli : Escherichia coli
EDC : 1-ethytl-3-(-3-dimethiyaminopropyl) carbodiimide
ELISA : Enzyme Linked Immunosorbent assay
ER : Endoplasmic Reticulum
FBS : Fetal Bovine Serum
GATA : Gulhane Military Medical Faculty
GBP1 : Gold Binding Peptide 1
GEPI : Genetically Engineered Peptides for Inorganic
GFP : Green Fluorescence Protein
HABP : Hydroxyapatite Binding Peptide
HBcAg : Hepatitis B virus core antigen
HBeAg : Hepatitis B virus E antigen
HBsAg : Hepatitis B virus S antigen
HBV : Hepatitis B virus
HBx : Hepatitis B virus X protein
HCC : Hepatocellular Carcinoma
HIV : Human immunodeficiency virus
HRP : Horse Radish Peroxidase
HUVEC : Human Umbilical Vein Endothelial Cell
IPTG : Isopropyl-ß-D-thiogalactopyranosid
Ka : Adsorption rate
Kd : Desorption rate
K_D : Equilibrium dissociation constant
LB medium : Luria-Bertani medium
LSPR : Localised SPR
MBP : Maltose Binding Peptide

MDG : Mineral Directing Gelator
N1 or N2 : N-Terminal domain
NMR : Nuclear Magnetic Resonance
OD : Optical Density
ORF : Open Reading Frame
PBS : Phosphate Buffered Saline
PCR : Polymerase Chain Reaction
PEG : polyethylene glycol
Pd : Palladium
pNPP : Para-nitrophenylphosphate
PSA : Prostate specific antigen
Pt : Platinum
PtBP : Platinum Binding Peptide
QBP : Silica Binding Peptide
QCM : Quartz Crystal Microbalance
RF : Replicative form
RIU : Refractive index Unit
Rpm : Round per minute
SAM : Self-Assembled Monolayer
scFv : Single chain variable Fragment
SDS : Sodium Dodecyl Sulfate
SDSC : San Diego Supercomputer Center
SDS-PAGE : SDS- Polyacrylamide Gel Electrophoresis
SEM : Scanning Electron Microscope
SPR : Surface Plasmon Resonance
TiBP : Titanium Binding Peptide
TM : Transmembrane Domain
VEGF : Vascular Endothelial Growth Factor
VH : Variable Heavy
VL : Variable Light
WHO : World Health Organization

LIST OF TABLES

Page

Table 1.1: Comparison of Label-Free optical immunosensors 7
Table 1.2: M13 phages coat proteins 34
Table 2.1: PCR reaction for HBsAg amplification 48
Table 2.2: SfiI digestion reaction 49
Table 2.3: NotI digestion reaction 49
Table 2.4: Ligation reaction 50
Table 2.5: Colony PCR reaction for HBsAg 51
Table 2.6: DNA sequencing reaction 51
Table 2.7: Lig7 PCR amplification reaction 59
Table 2.8: NotI digestion of Lig7 60
Table 2.9: NdeI digestion of Lig7 60
Table 2.10: Ligation of Lig7 into pQE2 60
Table 2.11: PCR reaction for the amplification of GBP 61
Table 2.12: NotI and HindIII digestions 62
Table 2.13: Ligation reaction of Lig7 and pQE2 62
Table 2.14: Colony PCR reaction 63
Table 3.1: Enrichment of HBsAg specific scFv phage-displayed library. 83
Table 3.2: PCR amplification band size of each clone 90
Table 3.3: Refolding parameters of Lig7-GBP 99
Table 3.4: The μRIU ratio between 0.2 μM and 0.6 μM antibody concentrations (0.6μM/0.2μM) for the uptake and the adsorption 106
Table 3.5: Affinity calculations of the bifunctional antibodies 107

LIST OF FIGURES

Page

Figure 1.1 : SPR principle (Morgan, 1996). 9
Figure 1.2 : SPR angle shift caused by antigen binding to antibodies (Xu, 2010). .. 10
Figure 1.3 : SPR sensongram (Url-1). 10
Figure 1.4 : Biological material examples (Tamerler, 2010). 16
Figure 1.5 : Cross section of Sponge spicule of Rosella by SEM (Sarikaya, 2001). 17
Figure 1.6 : Two-dimensional array of immobilized 5GBP1-AP (Kacar, 2009)..... 20
Figure 1.7 : Fluorescence labeling of teeth with GFPuv-HAPB1 (Yuca, 2011). 21
Figure 1.8 : Immobilized proteins on gold NP arrayed surface (Hnilova, 2012). 22
Figure 1.9 : Cell adhesion mediated by TiBP1-RGDS peptide (Yazici, 2013). 23
Figure 1.10 : Dominant genotypes of HBV (Harkisoen, 2012). 25
Figure 1.11 : HBV genome representation. 25
Figure 1.12 : HBcAg and HBeAg representation (DiMattia et al., 2013). 27
Figure 1.13 : 3D representation of HBcAg and HBeAg (DiMattia, 2013). 27
Figure 1.14 : Hepatitis B virus surface antigens (Schadler, 2009). 28
Figure 1.15 : HBV life cycle (Rehermann, 2005). 29
Figure 1.16 : Genetic map of the Ff phage (Sambrook, 2001). 33
Figure 1.17 : Surface proteins of M13 phage (Paschke, 2006). 33
Figure 1.18 : pIII protein structure (Russel, 2004). 34
Figure 1.19 : Infection of E. Coli by Ff bacteriophage (Russel, 2004). 35
Figure 1.20 : Infection mechanism of E. Coli by Ff phage (Russel, 2004) 36
Figure 1.21 : The life cycle of the Ff phage (Rakonjac, 2011). 37
Figure 1.22 : Peptide display strategies (Smith, 1997). 38
Figure 1.23 : Phage display types (Smith, 1997). 40
Figure 1.24 : Chemically immobilized (A) and self-assembled oriented (B) scFv. . 45

Figure 2.1 : Cloning strategy..... 59

Figure 3.1 : PCR amplification of HBsAg gene with Sfi I ve Not I restriction enzyme site containing primers. Lane 1. M4 marker, Lane 2. ScFv marker, Lane 3-10., Lane 11. Control PCR product. 72
Figure 3.2 : Purification of Sfi I and Not I restriction enzyme site containing PCR products from agarose gel. Lane 1; M4 Marker, Lane 2-3; Agarose gel extracted PCR product. 72
Figure 3.3 : Control of pCANTAB5E phagemid vector and PCR products after Sfi I and Not I digestion. Lane 1; M4 marker, Lane 2; HBsAg, Lane 3; pCANTAB5E. The DNA band size was deduced from semi-log plotting. 73
Figure 3.4 : Colony PCR results of transformation colonies. Lane 1; M4 Marker, Lane 2; ScFv marker, Lane 3-6; Colony PCR products. 73

Figure 3.5 : A schematic representation of the emplacement of the HBsAg and the pCANTAB5E primers resulting of a PCR amplification.band of ~700 bp and ~850 bp, respectively. 74
Figure 3.6 : DNA and protein sequences of the HBsAg gene region cloned into the pCANTAB5E vector. The yellow region indicates the vector sequence, the underlined sequence correspond to SfiI restriction enzyme site and the red star indicates the end of translation. 74
Figure 3.7 : Sequence alignment of the cloned HBsAg and the HBsAg sequence selected from the reference sequence viral protein database (Hepatitis B virus isolate 4436-97 HBsAg protein (S) gene, complete) by CLUSTALW multiple sequence alignment. The blue color indicates total homology; green color indicates similar amino acids. 75
Figure 3.8 : Detection methods of M13 phages displaying HBsAg based on ELISA. 76
Figure 3.9 : Phage ELISA results of the first and second ELISA strategies. 76
Figure 3.10 : Immune response results of mice before the injection of phages and after each injection of 10^{12} phages. 78
Figure 3.11 : Schematic representation of an antibody and a single chain Fv. Orange color represent the light chain, and the blue color represent the heavy chain. Dark color represents the constant region, and light color represent the variable region. 79
Figure 3.12 : Schematic representation of the construction of a single chain Fv from variable domains of light (VL) and heavy (VH) chains and a linker. Orange color represent the light chain, and the blue color represent the heavy chain variable domain. The linker is represented by purple color flanked with short homologue sequences to VL or VH. 80
Figure 3.13 : PCR amplification results of VH and VL on 1.5% agarose gel. Lane 1; Thermo scientific Mass ruler Low Range DNA ladder (SM0383), Lane 2-3; Variable Heavy chain PCR, Lane 4-5; Variable Heavy chain PCR, Lane 6-7; Linker PCR.PCR amplification bands of ~350 bp for VH and ~320 bp for VL were obtained (Figure 3.13). Also, a single band of ~100 bp was also observed for the PCR amplification of the linker. These results confirmed the presence of a VH and a VL library. Primers dimers in the PCR product were purified with an agarose gel DNA extraction kit (Roche, Cat. No. 1 696 505) according to the manufacturer instructions and controlled on 1.5% agarose gel (Figure 3.14). 80
Figure 3.14 : Agarose gel purification results of VH and VL on 1.5% agarose gel electrophoresis. Lane 1; Thermo scientific Mass ruler Low Range DNA ladder (SM0383), Lane 2; Heavy chain variable region, Lane 3; Light chain variable region. 81
Figure 3.15 : The PCR amplification results after the fusion of the VH and VL libraries with the $(Gly\text{-}Gly\text{-}Gly\text{-}Gly\text{-}Ser)_3$ linker on a 1.2% agarose gel. Lane 1; Thermo scientific Mass ruler Low Range DNA ladder (SM0383), Lane 2-4; scFv fusion products. 81
Figure 3.16 : The scFv PCR amplification products after agarose gel extraction. Lane 1; Thermo scientific Mass ruler Low Range DNA ladder (SM0383), Lane 2-4; Purified scFv fusion products, Lane 5; Purified VH-Linker fragment, Lane 6; Purified VL-Linker fragment, Lane 7; Purified VH fragment, Lane 8; Purified VL fragment. 82

Figure 3.17 : ELISA results of HBsAg binding phage particles after two rounds of biopanning. The clones indicated in red (G5, K28 and K54) correspond to high HBsAg binding and the clones indicated in blue (G2, K2) correspond to low HBsAg binding phages. The green color correspond to negative control clones. 83
Figure 3.18 : ELISA results of the selected clones for HBsAg and BSA. 84
Figure 3.19 : The multiple cloning sites of the pQE2 expression vector (Qiagen)... 84
Figure 3.20 : Modification of the Lig7 C-terminal region. Glutamine (Q) indicated in red was added to the Lig7 sequence to stop the cleavage of the Tagzyme enzyme. 85
Figure 3.21 : Colony PCR results from 14 randomly selected transformant colonies. Lane 1; Thermo scientific Mass ruler Low Range DNA ladder (SM0383), Lane 2-14; different transformation colonies, Lane 15; Control PCR of Lig7 scFv from the original Lig7/pDUCK1 vector. ... 85
Figure 3.22 : DNA and protein sequence results retrieved from the San Diego Supercomputer Center (SDSC) Biology Workbench Internet website. Color code for restriction enzyme site; orange; NdeI, green; NotI, blue; HindIII. 86
Figure 3.23 : Results of PCR amplification from the pDrive-5GBP vector using primers containing NotI and HindIII restriction enzyme sites. Lane 1; Thermo scientific Mass ruler Low Range DNA ladder (SM0383), Lane 2-3; PCR products. 87
Figure 3.24 : Schematic representation of the GBP_forward_NotI_with_tail and GBP_reverse_HindIII_with_tail primers annealing emplacement on pDrive-5GBP vector. 88
Figure 3.25 : PCR amplification results of 5GBP by using the "GBP_forward_NotI_with_tail" and "GBP_reverse_HindIII_with_tail" primers. Lane 1; Thermo scientific Mass ruler Low Range DNA ladder (SM0383), Lane 2; empty well, Lane 3-12; PCR amplifications. 88
Figure 3.26 : PCR amplification results of 5GBP by using the "GBP_forward_NotI_with_tail" and "GBP_reverse_HindIII_with_tail" primers. Lane 1; Thermo scientific Mass ruler Low Range DNA ladder (SM0383), Lane 2; empty well, Lane 3-12; PCR amplifications. 89
Figure 3.27 : Agarose gel image of the colony PCR made with GBP1 specific primers set. Lane 1; Thermo scientific Mass ruler Low Range DNA ladder (SM0383), Lane 2-17; transformation colonies from 1 to 16. ... 89
Figure 3.28 : Agarose gel image of the PCR amplification products. Lane 1; Thermo scientific Mass ruler Low Range DNA ladder (SM0383), Lane 2, 6, 11; clone 7, Lane 3, 7, 11; clone 6, Lane 4, 8, 12; clone 5, Lane 5, 9, 13; clone 1, Lane 14; Thermo scientific Mass ruler High Range DNA ladder (SM0393). 90
Figure 3.29 : DNA sequence alignment of the four clones at the 3' end. The green and purple colors indicate the GBP1 peptide encoding region. 92
Figure 3.30 : Protein sequence alignment of the four clones. The green and purple colors indicate the GBP1 encoding region. The stars correspond to 100% amino acid homology for each clone at the same amino acid emplacement. 92
Figure 3.31 : Coomassie staining for bifunctional Lig7 antibodies expression in BL21(DE3) cells. T0: before expression, T4: 4 hours of induction. Lane 1; Fermentas PageRulerTM plus Prestained protein Ladder (SM1811),

Lane 2; Lig7-5GBP T0, Lane 3, Lig7-5GBP T4, Lane 4; Lig7-3GBP T0, Lane 5; Lig7-3GBP T4, Lane 6; Lig7-GBP T0 (clone 6), Lane 7; Lig7-GBP T4 (clone 6), Lane 8; Lig7-GBP T0 (clone 7), Lane 9; Lig7-GBP T4 (clone 7), Lane 10; control scFv T4. 93
Figure 3.32 : Western blot image for bifunctional Lig7 antibodies expression in BL21(DE3) cells. T0: before expression, T4: 4 hours of induction. Lane 1; Fermentas PageRulerTM plus Prestained protein Ladder (SM1811), Lane 2; Lig7-5GBP T0, Lane 3, Lig7-5GBP T4, Lane 4; Lig7-3GBP T0, Lane 5; Lig7-3GBP T4, Lane 6; Lig7-GBP T0 (clone 6), Lane 7; Lig7-GBP T4 (clone 6), Lane 8; Lig7-GBP T0 (clone 7), Lane 9; Lig7-GBP T4 (clone 7), Lane 10; control scFv T4. 94
Figure 3.33 : Coomassie staining results for the bifunctional Lig7 antibodies expression in M15[pREP4] cells. T0: before expression, T4: 4 hours of induction. Lane 1; Fermentas PageRulerTM plus Prestained protein Ladder (SM1811), Lane 2; Lig7-5GBP T0, Lane 3, Lig7-5GBP T4, Lane 4; Lig7-3GBP T0, Lane 5; Lig7-3GBP T4, Lane 6; Lig7-GBP T0 (clone 6), Lane 7; Lig7-GBP T4 (clone 6), Lane 8; Lig7-GBP T0 (clone 7), Lane 9; Lig7-GBP T4 (clone 7), Lane 10; control scFv T4. The bands entoured with a black rectangle correspond to protein expression. 95
Figure 3.34 : Western blot image for the bifunctional Lig7 antibodies expression in M15[pREP4] cells. T0: before expression, T4: 4 hours of induction. Lane 1; Fermentas PageRulerTM plus Prestained protein Ladder (SM1811), Lane 2; Lig7-5GBP T0, Lane 3, Lig7-5GBP T4, Lane 4; Lig7-3GBP T0, Lane 5; Lig7-3GBP T4, Lane 6; Lig7-GBP T0 (clone 6), Lane 7; Lig7-GBP T4 (clone 6), Lane 8; Lig7-GBP T0 (clone 7), Lane 9; Lig7-GBP T4 (clone 7), Lane 10; control scFv T4. 95
Figure 3.35 : Coomassie staining results for the large scale production of the bifunctional Lig7 antibodies in M15[pREP4] cells. T0: before expression, T4: 4 hours of induction. Lane 1; Fermentas PageRulerTM plus Prestained protein Ladder (SM1811), Lane 2; M15[pREP4] T0, Lane 3, Lig7-GBP T4, Lane 4; Lig7-3GBP T0, Lane 5; Lig7-5GBP T4. 96
Figure 3.36 : Western blot results for the large scale production of the bifunctional Lig7 antibodies in M15[pREP4] cells. T0: before expression, T4: 4 hours of induction. Lane 1; Fermentas PageRulerTM plus Prestained protein Ladder (SM1811), Lane 2; M15[pREP4] T0, Lane 3, Lig7-GBP T4, Lane 4; Lig7-3GBP T0, Lane 5; Lig7-5GBP T4. 96
Figure 3.37 : Coomassie staining and western blot results of periplasmic extraction from large-scale production of the bifunctional antibodies in M15[pREP4] cells. Lane 1; Fermentas PageRulerTM plus Prestained protein Ladder (SM1811), Lane 2; Lig7 scFv, Lane 3; Lig7-GBP, Lane 4; Lig7-3GBP, Lane 5; Lig7-5GBP. 97
Figure 3.38 : Coomassie staining of Cobalt affinity purified periplasmic extraction (lane 2-5) and solubilized inclusion bodies (lane 6-9) from large scale production of the bifunctional antibodies. Lane 1; Fermentas PageRulerTM plus Prestained protein Ladder (SM1811), Lane 2; Lig7 scFv, Lane 3; Lig7-GBP, Lane 4; Lig7-3GBP, Lane 5; Lig7-5GBP, Lane 6; Lig7 scFv, Lane 7; Lig7-GBP, Lane 8; Lig7-3GBP, Lane 9; Lig7-5GBP. 98

Figure 3.39 : Coomassie staining results of Lig7-GBP after different dialysis conditions. Lane 1; Marker, Thermo Scientific 26619, Lane 2; DB + 0.5 M Urea + 400 mM L-Arg, pH10.0, Lane 3; DB alone, pH10.0, Lane 4; DB + 400 mM L-Arg, pH10.0, Lane 5; DB + 0.5 M urea, pH10.0, Lane 6; DB + 400 mM L-Arg + 0.4% Triton X100, pH10.0, Lane 7; DB + 0.5 M Urea + 0.4% Triton X100, pH10.0, Lane 8; DB + 0.5 M Urea + 400 mM L-Arg, pH8.0, Lane 9; DB + 0.5 M Urea + 400 mM L-Arg, pH6.3. 100
Figure 3.40 : Coomassie staining of concentrated soluble Lig7 and Lig7-GBP, Lane 1; Ladder, Thermo scientific, Cat.No. 26619, Lane 2; empty, Lane 3; Lig7-GBP, Lane 4; Lig7 scFv. 100
Figure 3.41 : Coomassie staining of DAPase digestion products, 1; Ladder, Thermo scientific, Cat.No. 26619, Lane 2; Lig7 scFv, Digestion time: Lane 3; 15 min, Lane 4; 30 min, Lane 5; 45 min, Lane 6; Lig7-GBP, Digestion time: Lane 7; 15 min, Lane 8; 30 min, Lane 9; 45 min, Lane 10; DAPase enzyme. 101
Figure 3.42 : SPR binding sensograms of Lig7-GBP on gold coated sensor chip. Cyan; 0.4 µM, Green; 0.3 µM, Purple; 0.2 µM. 102
Figure 3.43 : SPR binding sensorgrams of Lig7-3GBP on gold coated sensor chip. Dark Blue; 0.6 µM, Cyan; 0.4 µM, Green; 0.3 µM, Purple; 0.2 µM. 103
Figure 3.44 : SPR binding sensorgrams of Lig7-5GBP on gold coated sensor chip. Dark Blue; 0.6 µM, Cyan; 0.4 µM, Green; 0.3 µM, Purple; 0.2 µM. 103
Figure 3.45 : Figure describing the uptake and the adsorption values of the bifunctional antibodies flown on the gold-coated SPR sensor chip. .. 104
Figure 3.46 : The uptake of the fusion recombinant antibodies on gold coated SPR sensor chip in refractive index unit. 104
Figure 3.47 : The adsorption of the fusion recombinant antibodies on gold coated SPR sensor chip in refractive index unit. 105
Figure 3.48 : SPR sensorgram of Lig7-GBP (0.3µM) adsorption on the sensor chip and the binding of HBsAg binding to Lig7-5GBP. 106
Figure 3.49 : SPR sensorgram of HBsAg binding to Lig7-5GBP adsorbed on the sensor chip. The bifunctional Lig7-5GBP at 0.3µM concentration was adsorbed on the SPR sensor chip. Three different HBsAg concentration was flown over the sensor chip (Blue color; 200 nM, Green color; 150 nM, Purple color; 100 nM). 107
Figure 3.50 : ELISA results of HBsAg for culture medium of different mammalian cells after transfection. 110
Figure 3.51 : Fluorescence microscope images (10X) of HeLa cells transfected with HBsAg-pCEP4 vector. A; Bright Field, B; A4 filter, C; RFP filter. .. 111
Figure 3.52 : Fluorescenct microscope images (40X) of HeLa cells transfected with HBsAg-pCEP4 vector. A; Bright Field, B; A4 filter, C; RFP filter. .. 111

Figure A.1 : pCANTAB5E vector. 138
Figure A.2 : pQE2 expression vector (TAGzyme handbook, Qiagen). 139
Figure A.3 : MassRuler Low Range, DNA Ladder, ready-to-use, SM0383, Thermo Scientific. 140
Figure A.4 : MassRuler DNA Ladder, High Range, ready-to-use, SM0393, Fermentas. 141
Figure A.5 : PageRuler^{TM} Plus Prestained Protein Ladder, SM1811, Fermentas... 142

DESIGN OF INORGANIC PEPTIDE BONDED FUSION BIOMOLECULES FOR TRACKING DISEASE RELATED PROTEINS

SUMMARY

Detecting disease-related antigens could save lives; Therefore, researchers are constantly in an urgency to find ways for increasing sensitivity as well as speeding up detection. First, the substrates used for colorimetric reaction were replaced with the chemiluminescent ones allowing a more sensitive detection in a shorter time. Next, the reducing the number of detection steps was targeted. Simulatenously, single step detection strategies were developed by introducing covalent coupling of the fluorescent molecules or by bioconjugating fluorescence proteins to the antibody. Due to the restricted orientation control in these approaches, novel protocols are constantly being searched to improve the diagnostic systems.

Surface Plasmon Resonance (SPR) spectroscopy is a label-free technique offering real-time monitoring of noncovalent interactions of protein-protein, protein-DNA and many other biomacromolecules in relatively short times. The principle relies on an electron charge density that arises at the surface of a metallic film, e.g. gold and silver, when the collective oscillation of the electrons is stimulated by incident light. The adsorption of the molecules detected as a refractive index change at the metal film surface. Since the interactions followed by the variation of plasmon resonance on the sensing surface of the chip, no label such as enzyme or fluorescent molecules are necessary.

Despite the success of SPR based detection systems, they have several drawbacks. Proteins or antibodies, which are used as capture agents, must be covalently coupled to the gold surface via chemical reactions. And the second drawback which is also present in ELISA-based detection systems is the coating of the capture molecules without any orientation control. In biological systems, molecular structure is the key to the functionality, any obstruction due to disorientation may affect the detection efficiency immensely.

This study focuses on developing a novel approach to enhance the adsorption of the antibodies by controlling their binding on SPR chips. This approach eliminates the covalently coupling of the capture molecules. Furthermore, it provides the capture molecules to be biologically self-assembled to the sensing surface in an oriented manner. As a case study, we used Hepatitis B virus surface antigen as the disease-tracking target to create self-assembled sensing surface.

Hepatitis B virus (HBV) is one of the major causes of chronic Hepatitis, cirrhosis and liver cancer (hepatocellular carcinoma, HCC). According to World Health Organization (WHO) the number of infected people is about 2 billion. From these infected people approximately 240 million are chronically infected, and about 600,000 people die every year due to the consequences of HBV. HBV infects human hepatocytes, which results in the release of infectious virions and excessive hepatitis

B surface antigens (HBsAg) to the blood stream. Therefore, the presence of HBsAg in circulating blood is an indicator of HBV infection. The HBsAg specific ELISA kits are routinely used throughout the world for the detection of HBV infection. Nevertheless, this method requires a second anti-HBsAg antibody, which is different from the HBsAg capture antibody, and it requires approximately 3 hours for the detection of HBsAg. Consequently, HBsAg detection was selected as a model to develop our novel SPR based biosensor strategy.

For this purpose, an anti-HBsAg single chain variable fragment (scFv) recombinant antibody was first developed by the Immunogenetics Laboratory (Genetic Engineering and Biotechnology Institute, Marmara Research Center) This antibody was then genetically fused with a gold binding peptides (GBP1) characterized by Tamerler's group. The bifunctional recombinant antibody contains both gold bindings as well as anti-HBsAg was successfully generated and used as a biosensing probe. The probe molecule was demonstrated to biologically self-assemble on the surface in a single step process. With this probe, we detected HBsAg using and SPR spectroscopy, resulting an equilibrium dissociation constant of 0,6 nM.

HASTALIKLA İLİŞKİLİ PROTEİNLERİN İZLENMESİNDE ANORGANİK PEPTİT BAĞLARLA FÜZYON BİYOMOLEKÜLLERİN TASARIMI

ÖZET

Hastalıklarla ilişki antijenlerin belirlenebilmesi hayat kurtarır. Bu nedenle araştırmacılar sürekli olarak daha hassas ve hızlı tanı sistemleri geliştirmek için çalışmaktadırlar. İlk olarak, ELISA yöntemi gibi tanı sistemlerinde standart olarak kullanılan kolorimetrik substratlar daha hassas ve hızlı görüntüleme sağlayan kemilüminesan subtratlar ile değiştirilmeye başlanmıştır. Bazı çalışmalar ise tanı sistemlerindeki aşamaların azaltılması konusuna yönelmiştir. Algılayıcı moleküller olan antikorlara kovalent olarak bağlanmış kuantum dot'lar gibi floresan moleküller veya genetik füzyon olarak bağlanmış yeşil floresans protein (GFP) aracılığıyla tek aşamalı tanı sistemleri geliştirilmiştir. Günümüzde ise farklı tanı stratejilerin ile yeni cihazların geliştirilmesi söz konusu olmaktadır.

Yüzey plazmon rezonans (SPR) spektrometreleri protein-protein etkileşimlerini gerçek zamanda takip etmeyi sağlayan cihazlardır. Bu cihazlar sayesinde protein-protein etkileşimlerinin kinetik hesaplamalarının yapılması dışında ayrıca daha kesin sonuçlar elde edilmesini sağlanmaktadır. SPR cihazların temeli SPR çipi yüzeyinde bulanan ince altın tabakasının yaydığı yüzey plazmon rezonanslarına dayanmaktadır. SPR çipinin alt tarafında bulunan bir prizmanın içerisinden geçen bir ışık süzmesi gönderilmektedir. Işık süzmesinin altın tabakaya çarptıktan sonra ışık süzmesinin yansıma açısı ölçülmektedir. SPR çipi üzerinde proteinlerin geçişi sağlandığı zaman çip yüzeyine bağlanan proteinler altın tabakanın yaydığı yüzey plazmon rezonansını etkileyerek ışık süzmesinin yansıma açısını değiştirmektedir. Ölçülen yansıma açısındaki değişiklik çip yüzeyinde bağlanan protein miktarı ile doğru orantıda olmasından dolayı çip yüzeyinde etkileşime giren protein miktarı belirlenebilmektedir. Protein-protein etkileşimleri, SPR çipi yüzeyinde oluşan yüzey plazmon rezonans değişimine dayalı olması nedeniyle diğer tanı sistemlerinde gereken enzim veya floresans molekül gibi işaretleyici moleküller ihtiyaç duyulmaması SPR'a dayalı tanı sistemlerinin en büyük avantajıdır.

SPR temelli tanı sistemleri umut vaat edici olmalarına karşın birkaç dezavantajları bulunmaktadır. Protein-protein etkileşimlerinin incelenebilmesi için öncelikle bir proteinin altın kaplı çip yüzeyine bağlanması gerekmektedir. Bu bağlama işlemi, öncelikle çip yüzeyinde bulunan altın tabakasının kullanım türüne göre farklı kimyasal kaplama molekülleri ile protein bağlaması için aktif hale getirilmesi gerekmektedir. Daha sonra da proteinlerin amino veya karboksi gruplarından bağlamak için ayrıca kimyasal reaksiyonlar gerekmektedir. Uygulanan bu kimyasal reaksiyonların bağlanacak proteinler üzerinde olumsuz etki gösterebileceği göz ardı edilemez. Diğer dezavantaj ise ELISA için de geçerli olmakla birlikte çip yüzeyine bağlanan proteinlerin yönlendirilmemiş olmasıdır. Bu nedenle bazı proteinlerin diğer proteinlere bağlanma bölgeleri, oluşturulan bağ nedenliyle perdelenmiş olur ve hedef molekülün tanısında veri kaybına neden olabilmektedir.

Bu çalışma, kimyasal reaksiyonlar kullanmadan ve kendilerini yönlendirmiş bir şekilde SPR çipi yüzeyine bağlayabilen antikor yapıların geliştirilmesine odaklanarak SPR'a dayalı tanı sistemlerinde bir iyileştirilmeye gidilmesini hedeflemektedir. Hastalıklarla ilişkili proteinlerin takibinin yapılması için tasarlanacak sistem için model olarak Hepatit B virüsü yüzey antijenine bağlama özelliği olan bir rekombinant bir antikor kullanılacaktır.

Hepatit B virüsü (HBV), Kronik Hepatit, siroz ve karaciğer kanserinin (hepatoselüler karsinoma, HCC) başlıca sebeplerindendir. Dünya sağlık örgütüne göre yaklaşık 2 milyar kişi HBV tarafından enfekte edilmiş ve enfekte edilen kişilerden 240 milyonunun enfeksiyonu kronikleşmiş durumdadır. Her yıl yaklaşık 600.000 kişi HBV'ye dayalı hastalıklardan hayatını kaybetmektedir.

HBV, insan hepatositlerini enfekte ederek enfeksiyöz virionların ve yoğun miktarda hepatit B yüzey S antijeninin (HBsAg) kan dolaşım sistemine bırakılmasına neden olmaktadır. Bu nedenle dolaşım sisteminde HBsAg'nin varlığı HBV enfeksiyonu belirtecidir.

HBV enfeksiyonu rutin olarak HBsAg'ye spesifik ELISA kitleri ile belirlenmektedir. Bu kitler dünya çapında yaygın olarak kullanılmaktadır. Fakat, bu kitler kullanılarak HBsAg varlığı ancak 3 saat gibi bir sürede tespit edilebilmektedir. Daha da önemlisi bu tür tanı sistemlerinde algılayıcı bir anti-HBsAg dışında bir de işaretleme için farklı bir anti-HBsAg antikoru gerekmektedir. Bu sebepten dolayı kitlerin maliyetini artırmaktadır. Bu nedenlerden dolayı oluşturulmak istenen yeni SPR temelli biyosensör stratejisi için HBV enfeksiyonu tanısı model olarak seçilmiştir.

Bu kapsamda, öncelikle HBsAg'ye bağlanma özelliği olan rekombinant antikor geliştirmek amacıyla Faj gösterim teknolojisi kullanılmıştır. Faj gösterim teknolojisi ile rekombinant antikor geliştirmek için standart olarak deney farelerinin saf hedef antijen ile bağışıklanması gerekmektedir. Bu çalışmada ise, ilk yenilikçi yaklaşım olarak maliyeti yüksek olabilecek saf antijenlerin kullanılmasından ziyade bağışıklamalar için yüzeyinde HBsAg'yi sunan bakteriyofajlar kullanarak farelerin bağışıklanmasını sağlamak olmuştur. Fajların, hayvan bağışıklama çalışmalarında adjüvan olarak kullanıldığı bilinmektedir. TÜBİTAK Hayvan Deneyleri Yerel Etik Kurulundan onay alındıktan sonra Hepatit B yüzey antijeni geni polimeraz zincir reaksiyonu (PZR) ile çoğaltılmış ve bir fajmit vektöre klonlanmıştır. Sonrasında E. *coli* TG1 suşuna rekombinant vektör kimyasal transformasyon ile aktarılmıştır. Daha sonra HBsAg'nin faj yüzeyinde expresyonu sağlanmış ve bu fajlar fare bağışıklamasında kullanılmıştır. Ardı ardına yüzeyinde HBsAg sunan fajlar ile yapılan üç enjeksiyon sonrasında farelerin oluşturduğu anti-HBsAg immün yanıta ELISA (Enzyme-linked immunosorbant assay) yöntemi ile bakılmıştır. Yapılan enjeksiyonlar sonucunda farelerde immün yanıt oluştuğu gösterilmiştir. Bu çalışmalar Uluslararası atıf endeksine giren "Advances in Biosciences and Biotechnology" dergisinde yayınlanmıştır.

Bağışıklama sürecinden sonra immün yanıt gösteren farelerin dalağı alınmış ve antikor üreten B lenfositlerinden RNA izolasyonu yapılmıştır. RNA'ların cDNA'ya çevrilmesiyle bir cDNA kütüphanesi oluşturulmuştur. PZR yöntemi ile cDNA kütüphanesinden antikor ağır ve hafif değişken bölgeleri çoğaltılmış ve tek zincir rekombinant antikor (single chain variable fragment, scFv) gen kütüphanesi oluşturulmuştur. Elde edilen kütüphane fajmit vektöre klonlanmış ve *E. coli* TG1 bakterilerine kimyasal transformasyon ile aktarılmıştır. Daha sonra yüzeylerinde antikor kütüphanesi sunan fajlar elde edilmiş ve bu kütüphane HBsAg'ye karşı

taranmıştır (Biopanning). HBsAg'ye bağlanan fajlar seçilmiş ve tekrar bir biopanning aşamasından geçilerek kütüphanesinin zenginleşmesi sağlanmıştır. Üç zenginleştirme aşamasından sonra faj klonlarının ayrı ayrı HBsAg'ye bağlanmaları ELISA ile kontrol edilmiştir. HBsAg'ye bağlanma özelliği olan antikorlar seçilmiş olmasına karşın TÜBİTAK Marmara Araştırma Merkezi Gen Mühendisliği ve Biyoteknoloji Enstitüsü immünogenetik Laboratuarında daha önceden oluşturduğumuz Lig7 anti-HBsAg rekombinant antikoru kadar iyi bağlanma göstermediklerinden biyosensör çalışmalarına Lig7 antikoru ile devam edilmesine karar verilmiştir.

Lig7 antikoru PZR ile çoğaltıldıktan sonra pQE2 bakteriyel ekspresyon vektörüne klonlanmıştır. Bu ekspresyon vektörünün özelliği, protein saflaştırma çalışmalarında kolaylık sağlayan Histidin kuyruğunun (His-Tag) daha sonra Histidin kuyruğu ile protein arasına yerleştirilmiş proteaz kesim bölgesi sayesinde Histidin kuyruğunun çıkarılabilmesidir. Bu sayede üretilen proteinin orijinal yapısına en yakın olabilecek şekli elde edilebilmektedir. Lig7 geni pQE2 vektörüne klonlandıktan sonra genetik füzyon olacak şekilde Prof. Dr. Candan TAMERLER ve grubunun (Moleküler Biyoloji- Genetik ve Biyoteknoloji Araştırma Merkezi, İstanbul Teknik Üniversitesi) karakterize etmiş olduğu altına bağlanma özelliği olan GBP1'yi (Gold Binding Peptide-1) kodlayan gen rekombinant vektöre klonlanmıştır. Klonlamalar sonrasında genetik füzyon yapı DNA dizi analizi ile kontrol edilmiş ve üç farklı füzyon yapı belirlenmiştir. Bu genetik füzyonların, Lig7 ile birleşmiş farklı GBP1 tekrarlarından (tek GBP1, 3'lü tekrar ve 5'li tekrar) olduğu tespit edilmiştir. Lig7 antikoru ile üç Lig7 GBP1 füzyon yapıları eksprese edilmiş ve His-tag aracılığı ile saflaştırılmıştır. Saflaştırılan altına bağlanma özelliği kazandırılmış anti-HBsAg bifonksiyonel rekombinant antikorların altın kaplı SPR çiplerine bağlanmaları Reichert SPR spektrometresiyle kontrol edilmiş ve bağlanmaları teyit edilmiştir. Daha sonra, çip yüzeyine yönlendirilmiş şekilde bağlanmış bifonksiyonel antikorların HBsAg'yi bağlama özellikleri yine SPR spektrometresiyle kontrol edilmiş ve HBsAg'nin çip yüzeyine tutulduğu gösterilmiştir.

SPR spektrometresi ile yapılan kinetic çalışmalar sonucunda Lig7-GBP1, Lig7-3GBP ve Lig7-5GBP füzyon antikorlarının altına bağlanma kinetiği çok farklılık göstermemesine karşın GBP1 tekrar sayısının HBsAg'nin bağlanması açısından kayda değer farklılıklar gösterdiği tespit edilmiştir. Füzyon antikor yapılarının HBsAg için denge ayrışma sabitleri Lig7-GBP1, Lig7-GBP3 ve Lig7-5GBP için sırasıyla 315 nM, 30 nM ve 0,6 nM olarak belirlenmiştir. Bu değerlere bakıldığında GBP1 tekrarının artmasıyla antikorun HBsAg'ye olan "afinitesinin" arttığı görülmüştür. Ancak anti-HBsAg Lig7 antikoru her bir füzyon yapı için aynı olduğundan bağlanmadaki bu farkın antikorun HBsAg'nin bağlanmasına ne kadar elverişli olduğunun bir göstergesi olarak kabul edilmiştir. Bu nedenle altın çip yüzeyine yönlendirilmiş şekilde adsorbe edilmiş Lig7-5GBP bifonksiyonel antikorun konformasyonel olarak diğer iki antikora göre HBsAg'yi bağlamak için daha uygun olduğu görülmüştür. Antikorların altına bağlanma kinetiklerinin yaklaşık aynı olduğu düşünülürse tekrar sayınının altına bağlanma özelliğini arttırmasından çok, anti-HBsAg Lig7 antikorunun uygun konformasyonda sunulmasında etkili olduğu gözlemlenmiştir. Kimyasal bağlar oluşturarak SPR çipi üzerine bağlanmış Lig7'nin HBsAg'yi bağlama denge ayrışma sabitinin 31,4 nM olduğu hesaplanmıştır. Bu değerin, Lig7-3GBP'nin HBsAg için olan denge ayrışma sabiti ile yaklaşık aynı olduğu, Lig7-GBP ile karşılaştırıldığında ise daha düşük olduğu görülmüştür. Fakat Lig7-5GBP'nin HBsAg'ye olan afinitesinin kimyasal olarak bağlanmış Lig7'den de

yaklaşık 50 kat daha iyi olduğu görülmüştür. Bu sonuçlar da, tez çalışmalarının dayandığı, bifonksiyonel rekombinant antikorların yönlendirilmiş şekilde altın kaplı SPR çiplerinin üzerine kaplanarak SPR sistemlerinde biyosensör uygulamalarının iyileştirilmesi hipotezinin doğruluğunu göstermiştir.

Sonuç olarak bu çalışmada, genetik olarak altına bağlanma özelliği kazandırılmış bir rekombinant antikorun yönlendirilmiş bir şekilde altın kaplı SPR Çipleri yüzeyine bağlandığı gösterilmiş, ve bu antikorun SPR spektrometresine dayalı tanı sistemlerinde kullanılabileceği ve hatta bir iyileştirme sağladığı gösterilmiştir.

1. INTRODUCTION

The detection of disease-related proteins can save lives. Tracking these proteins is crucial for the diagnosis and the prognosis of the diseases. There is a race between companies for the development of more sensitive, selective and cost-effective detection systems than the gold standard; the Enzyme-linked Immunosorbent Assay (ELISA). ELISA is a well-established detection method widely used all around the world since its development (Van Weemen, 1971). Since technology evolves rapidly, especially in the microfluidic field, new detection systems with higher performance are expected from the field. Therefore, the development of new cost and time effective devices with higher selectivity has a great importance. The interface between the sensor device and the target molecule is one of the key element for improving the detection systems.

Here, will be discussed the two components of immunosensors, the transducers, the biosensing probes and the interface between transducers and biosensing probes, the most important and challenging part.

Then a new way of thinking for attaching biomolecules on solid surfaces by self-assembly for tracking disease related proteins will be defined. The hypothesis will be transposed to the development a new biosensing interface for the surface antigen detection of the Hepatitis B virus (HBV), the major cause of chronic hepatitis, cirrhosis and liver cancer.

1.1 Immunosensors

Immunosensors correspond to a small section of the biosensors family which are devices developed for the detection of a variety of molecules in a defined environment (Morgan, 1996). In a general view, biosensors are composed of two elements, the bioreceptor, the recognition element and the transducer which converts the recognition event into a measurable signal (Morgan, 1996). A wide variety of transducer technology is used in biosensor systems, such as electrochemical

biosensors (potentiometric, amperometric or conductometric), piezoelectric biosensors (crystal resonance frequency, surface transverse wave or surface acoustic wave), optical biosensors (surface plasmon resonance, fiber optic, light addressable potentiometric, bioluminescent or resonant mirror) and thermistor biosensors. Bioreceptors are biological entities able to detect, sense different type of molecules such as glucose, antigens, antibodies, proteins, toxins. Some examples of bioreceptors from many others can be given. Enzymes can catalyze an analyte into a detectable product, or they can be inhibited by the catalyst. Nucleic acids (aptamers) can be used as a sensing probe for the detection of ligands, also whole cells can be used for monitoring the apoptotic or proliferative effects of analytes or proteins on cells. Non-enzymatic proteins such as receptor present in cells or proteins implicated in different cell signaling pathways are other examples of bioreceptor. However, the most widely and commonly used recognition molecules are the antibodies or the antigens (Homola, 2008).

Immunosensors are biosensors in which the bioreceptors consist of an antigen or an antibody. Depending on the detection purpose, a wide variety of antibodies or antigens are present on the market. Medical diagnostic markers (hormones, steroids), drugs (therapeutic and abused), bacteria, environmental pollutants (pesticides) can be detected by using an appropriate antibodies (Elliott, 2001; Murugaiyan, 2014; Yanez-Sedeno, 2014). Antibodies and antigens are used for the detection of their complementary partners for many years for immunological detection systems (Immunoassays); they are the key elements for the sensitivity and the selectivity of these detection systems. ELISA is the predominant analytical technique for quantitative measurement and is considered as “gold standard” for most of the detection systems (de la Rica, 2012; Zhao, 2013). However, other methods such as immunoblotting and immunochromatography base detection systems are commonly used for detection (Gopinath, 2014). These immunoassay methods have high specificity and selectivity and have a broad biological matrices panel owning these properties to the chemical binding and the spatial conformation of antibodies (Van Weemen, 1971; Gopinath, 2014). These methods are also easy to interpret with a minimum training which is one of the most desired property for detection systems. Unfortunately, these immunoassay have some drawbacks such as the necessity of many antibodies, a time-consuming experimental process (except for the immunochromatography) and the lack of multiplex detection possibility. Some

improvement in immunoassay methods have been performed with the technological development in the field of fluorescence, chemiluminescence emissions detections systems. They have allowed the increase of sensitivity of the immunoassays such as the detection of prostate specific antigen or cardiac biomarkers (Oh, 2009; Kim, 2014; Wang 2013). Improvements regarding immunoassays are still going on, recently a microfluidic immunoblotting method was developed for profiling inflammatory responses. Also, a plasmonic ELISA system allowing ultrasensitive detection with the naked eyes of prostate serum albumin (PSA) and HIV-1 capsid antigen p24 was developed (de la Rica, 2012).

The fundamental principal of immunoassay consists about the immobilization of antibodies or antigens to be detected on a Solid phase matrice which facilitates the separation and washing steps during the experiments. Then, the complementary antigen or the antibody conjugated with a wide range of labels, such as radioisotopes, fluorescent and luminescent molecules, light scattering molecules, enzymes are detected (Gopinath, 2014). Sandwich ELISA and immunochromatography systems have an extra layer of a second bioreceptor allowing the immobilization of the target molecules on a solid support thus increasing the selectivity and sensitivity of the detection (Pei, 2012).

Immunosensors, like immunoassays, detect antibody – antigen interactions. However, in contrary to immunoassays the detection of the binding is directly intercepted by the transducer integrated with the device. Therefore, allowing a real-time monitoring of the binding interactions. This real-time monitoring is supported by means of the development of fluidics systems. Real-time monitoring of antibody-antigen interactions makes possible the determination of the binding kinetics. Immunosensors have also, other advantages such as the possibility of multiplexing the detection molecules. They offer the opportunity of regenerating the sensor surface enabling the its reuse the for several times (Vaisocherova, 2009).

Various immunosensors with different transducer systems have been developed and are used for different purposes. Electrochemical immunosensors are based on the recognition of electrochemical signal variations generated between the electrodes during the interaction the antibody and antigen interaction. The advantages of electrochemical immunosensors are the possibility of easily miniaturizing the electrodes and the possibility of their mass production. Four groups of electrochemical immunosensor can be sited such as potentiometric, impedimetric,

conductometric and amperometric immunosensors, the later being the most to be used. Most of the electrochemical immunosensors applications are focused on the detection of small molecules especially in the fields of environmental pollution due the portability, the direct identification and quantification of compounds of this kind of sensors. Recently, an electrochemical immunosensor intended to determine alcohol consumption was developed. The Ethyl glucuronide molecule, a biomarker for alcohol consumption, produced by the nonoxidative ethanol metabolism was detected by an anti-Ethyl glucuronide antibody immobilized on gold electrodes. Besides the detection of small molecules electrochemical immunosensors are recently being used for the detection of mouse or goat antibodies from sera or microorganisms such *Francisella*, *Salmonella*, *Escherichia* and *Bacillus* (Skladal, 2013).

Another immunosensor type using different transducer systems is the piezoelectric immunosensor such as quartz crystal microbalance. The first piezoelectric sensors were used as gas phase sensors then the system was adapted to the detection in the liquid phase enlarging its properties to the detection of biomolecules. The system consists on the detection of mass transfer on the gold electrodes by monitoring the frequency of its quartz crystal resonator. Briefly, an alternating current between the piezoelectric sensor causes the oscillation of the quartz crystal which is detected as a frequency signal. Once a molecule such as a bioreceptor is conjugated to the gold electrodes the change in the frequency allows the determination of mass density of the bioreceptor. Overflown analytes on bioreceptors conjugated electrodes cause the binding of these analytes to their receptor causing again a frequency variation allow to determine this time the quantity of analytes bound to the bioreceptor. The monitoring of dissipation (QCM-D) offering to the system to give information about the viscoelasticity of the samples was integrated in year 1996. Several examples regarding the applications of piezoelectric immunosensors were given by Gopinath (2014) such as the detection of IgG or the alanine aminotransferase enzyme (Gopinath, 2014; Wu, 2011; Zhang, 2008). Recently, a piezoelectric immunosensor system was developed for the detection of a mutagenic and carcinogenic molecule frequently used in agriculture, the 2,4-dichlorophenoxyacetic acid. The detection of this small molecule was monitored by enhancing the response signal by the use of gold nanoparticles. Therefore, researches related to the improvement of piezoelectric immunosensors are still going on.

The last type and the most commonly used immunosensors are the optical immunosensor which will be discussed below in more details.

1.1.1 Optical immunosensors

Optical immunosensors uses optical transducers which are designed to detect linear optical phenomenon such as adsorption, polarization, rotation, interference, bioluminescence and chemiluminescence, but also non-linear phenomena such as harmonic generation.

Early optical systems were based on spectrophotometry measurements. Enzymes were immobilized on columns, and the absorbance change generated in the local environment caused by the catalysis of the enzymes substrate. Later on, reagent phase was immobilized on the sensor surface, and a change in optical properties due to the binding of the analytes was monitored (Murugaiyan, 2014).

The lack of requirement of reference electrode, the increased versatility, the speed and the reproducibility of the measurements have made of the optical immunosensor systems the most suitable detection systems for clinical applications, in vivo monitoring and the measurement of hazardous materials. The main drawback of optical immunosensors is the cost and the dimension of the devices, which are under investigation for the development of cost-effective devices with smaller dimensions.

Optical immunosensors can be divided into two groups the one which need labelled antibodies or antigens and the one which can perform a label-free detection.

1.1.1.1 Optical sensors using labels

Some immunosensors are designed to monitor fluorescence; luminescence such as bioluminescence and chemiluminescence generated from labels integrated to the detection process (Chen, 2010; Gopinath, 2014). Luminol-peroxidase reaction can be shown as one example for chemiluminescence sensing where the oxidation of luminol by horseradish peroxidase produces light that is detected by the appropriate optical transducer. This chemiluminescence sensor was used for the detection of an endocrine disrupting compound with a possible carcinogenic effect, the 17-β estradiol molecule, in natural water and human serum. Chemiluminescence sensors were also used for the detection of antibodies, estradiol, total IgG and antigens (Starodub, 1994; Seia, 2012, Chen, 2011).

These optical labels are mainly used for increasing the detection limits of the target molecules. Recently a fluorescent based immunosensor was developed for the serodiagnosis of canine *Leishmaniasis* combining immunomagnetic separation and Flow Cytometry. The immunosensor with increased sensitivity was even able to detect pathogen-specific antibodies in asymptomatic animals (Sousa, 2013).

Even if high sensitivity is acquired with optical labels the indirect optical immunosensors have some drawbacks like the replenishment of the luminescence or fluorescence during long-term measurement. The necessity of having luminescent compound in excess is another drawback regarding the increase of the detection cost (Sun; 2014). Moreover, finally the narrow excitation bands and the broad emission bands with red spectral tails of the fluorescent molecules limit the possibility of multiplex detection. Quantum dots conjugated to antibodies overcome some of these problems. Quantum dots are nanoparticles with stable and intense fluorescence allowing multiplex detection; these nanoparticles have been used in different diagnostic systems such as carbohydrate or toxins detection. However, the major problems of quantum dots are their hydrophobic properties and their toxicity. Therefore, an intense optimization of surface functionalisation is necessary for stabilizing the particles in a hydrophilic environment and for preventing their toxic effects. These restrictions have pushed the researchers to improve label-free immunosensor systems already discovered in the 90's, but under-exploited until the years 2000 (Morgan, 1996). Since year 2000, label-free, direct optical sensing systems have gained tremendous importance in biomolecular interaction characterisation and quantification (Homola, 2008).

1.1.1.2 Label free optical immunosensors

Label-free optical immunosensors are based on the monitoring of refractive index changes which corresponds to the changes in the dielectric permittivity on the sensor surface. Biological molecules such proteins, DNA, cells have a dielectric permittivity superior to the air and water causing a reduction of the propagation velocity while the electromagnetic fields pass through them. Briefly, a light (a laser, light emitting diode, incandescent light bulb) is directed towards the sensing surface and then the light beam is either reflected or transmitted through the sensor. The light emerging from the device is then monitored. Direct optical sensors have the advantage of

being less sophisticated in instrumentation compared to indirect optical sensors where in addition to the transducer a fluorescence excitation systems are necessary. Therefore, label-free optical immunosensors can be fabricated at lower cost in a smaller size compared to the other type of optical immunosensors.

There is a variety of direct optical sensors such as resonance wave grafting which employ the evanescent wave generated by the resonant coupling of light. Ellipsometric and oblique incidence reflectivity difference sensors are based on the monitoring of changes in phase and magnitude of the reflectivities of polarized monochromatic light due to the physical and chemical changes on the sensor chip surface. Reflectometric interference spectroscopy is an other example for label-free optical immunosensors. The sensor determines the change in thickness and refractive index of the dielectric layer by the interference of the incident light caused by double reflection at the surface (Sun, 2014). The last and most commonly used label-free optical detection system is the surface plasmon resonance (SPR). The SPR immunosensors are discussed in more details in the next section. All these detection techniques have several strengths and weaknesses which are described in Table 1.1.

Table 1.1 : Comparison of Label-Free optical immunosensors (Sun, 2014).

Techniques	Strengths (Application Suitability)	Weaknesses	Max. Throughput
Surface Plasmon Resonance	• Real-time measurements • End-point measurements (in imaging) • Sensitive to conformational changes	Restricted to gold-coated surfaces	~400 features
Ellipsometry based OI-RD	• Real-time measurements • End-point measurements (in imaging) • Not restricted to gold-coated surfaces • Simple instrumentation • Large field of view	Insensitive to conformational changes	Up to tens of thousands of features
Reflectometric Interference Spectroscopy	• Real-time measurements • Very high sensitivity • Fast determination of binding kinetics	Commercial instruments are expensive and complex	Compatible with 384-well microplates
Resonant Cavity	• Real-time measurements • End-point measurements (in imaging)	Low sensitivity	~tens of features
Resonant Waveguide Grating	• Real-time measurements • Fast determination of binding kinetics	Commercial instruments are expensive and complex	Compatible with 384-well microplates

1.1.2 SPR spectrometer

SPR was developed in the early 1990s as a technique for biomolecular interaction analysis (Malmqvist, 1993). Since then this technology is continually improving in the term of technology and its applications. The variety of molecules that can be immobilized on the sensor surface of SPR has allow the device to be used in different purposes such as affinity analysis, kinetic analysis, concentration assays, binding stoichiometry determination, thermodynamic analysis, study of interaction mechanism, routine screening and epitope mapping of peptides, virus particles and antibodies. Therefore, SPR biosensors have become key system for the characterization and the quantification of biomolecular interactions (Homola, 2008; Kim, 2006). Consequently, many publications have been made regarding the applications of SPR in the fields of medical diagnostics, environmental monitoring and food safety (Sun, 2014; Gopinath, 2014; Xia, 2010). Within all the biosensor systems, SPR spectrometers were the first biosensor to be commercialized (Englebienne, 2003; Van der Merwe, 2001). The main reason for the great interest in SPR is that SPR is a label-free system with very high sensitivity, which provides extensive information about the kinetics between two interacting molecules.

1.1.2.1 Principle

The SPR technology is based on the excitation ability of surface plasmons present in the metal film (Figure 1.1). Surface plasmons can be defined as electrons at the surface of a metal that behave differently from those in the bulk of the metal. Even if the physical aspect of SPR is quite complicated the principal is quite simple (Englebienne, 2003; Homola, 2008). The SPR spectrometer consists of a light source, a detector, a transduction surface (usually gold-film), a prism and a flow system (Xu, 2010). Briefly a light beam is directed through the layer of higher refractive index (prism) to the interface between the high and low (sample) refractive index media (Figure 1.1). When the angle of the incident beam exceeds the critical angle, the light is totally internally reflected back out of the device. In the material of lower refractive index (sample), a high-frequency electromagnetic field is generated, known as an evanescent wave. This wave penetrates into the sample medium for a short distance with exponentially decreasing amplitude. At the resonance angle (σ), the absorption of light energy by the surface plasmons during resonance causes a

sharp decrease in the intensity of the reflected light which implies biomolecular interactions. The resonance angle is determined by the wavelength and polarization state of the incident light, as well as by the refractive indices of the prism, the metal and the sample layers of the system. When all factors are maintained constant the resonance angle measures the refractive index at the surface of SPR system.

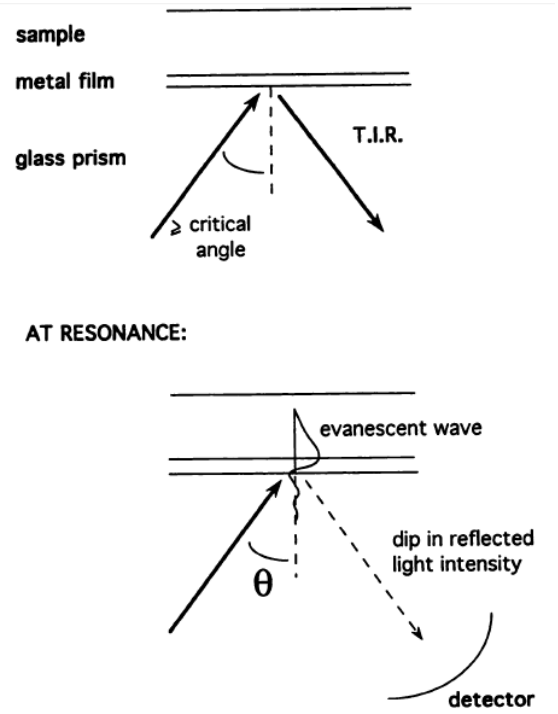

Figure 1.1 : SPR principle (Morgan, 1996).

Biomolecules which interact, at the gold interface, with the evanescent wave cause a reduction in intensity of the reflected light beam. This decrease reflects the changes in mass caused by biomolecules adsorbed on the gold layer. Therefore, SPR is a noninvasive method which allows real-time monitoring of interactions between injected analytes and immobilized biomolecules (Figure 1.2)(Xu, 2010).

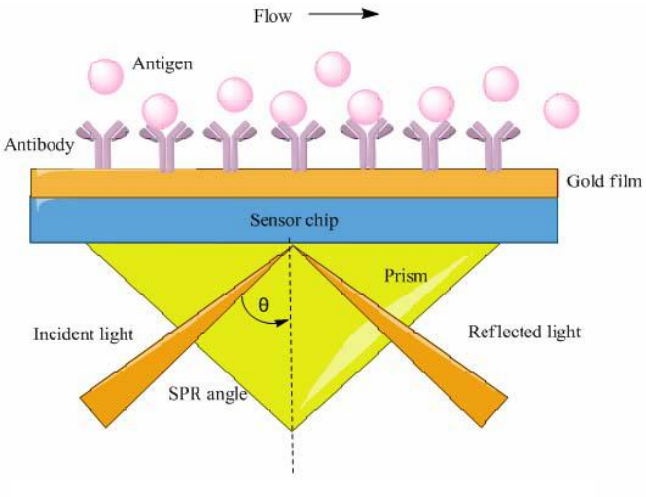

Figure 1.2 : SPR angle shift caused by antigen binding to antibodies (Xu, 2010).

1.1.2.2 Real-time monitoring

Once the sensor slides are ready for the detection, the sample to be analysed is injected into the instrument and flow over the sensor surface. When the antigens present in the sample bind to the immobilized antibodies (association) (Figure 1.3), there is an increase in the refractive index unit (RIU) which can be monitored from the computer. In the same way, dissociation of the antigens is monitored, the difference of RIU before and after dissociation indicates the presence of antigen in the sample. The slides are then regenerated for further analysis. The data collected from the SPR sensograms can be easily transferred to SPR data analysis software where the binding kinetics are calculated according to the association and dissociation curves.

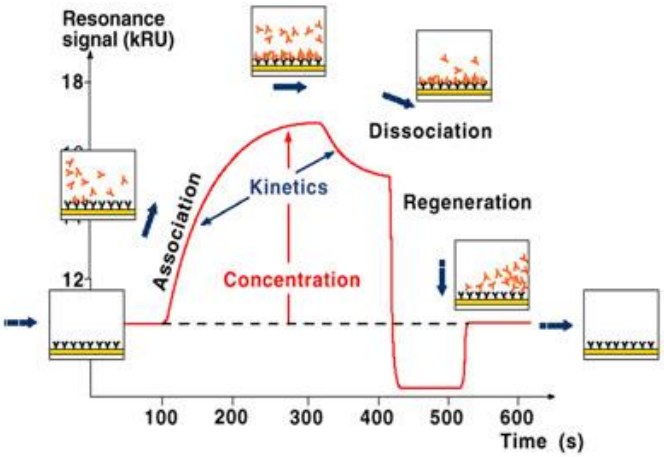

Figure 1.3 : SPR sensongram (Url-1).

1.1.3 Biointerface

Since many years material sciences, electronics and biotechnology have evolved in their areas and have reached a quite significant level. Unfortunately, it becomes more and more difficult to develop a cutting edge discovery in these fields. Then appeared the idea of integrating the properties of biological materials to inorganic materials for the development of a new generation of materials: biomaterials. Even if this concept was actually applied for many years in the diagnosis systems, like ELISA, where the antibodies or antigens are attached to plastic based ELISA plates, biomaterial field has found its place with the development of detection systems and nanotechnology. Suddenly, an increasing interest in the biomaterial field has emerged bringing with it an immense area to be elucidated, biointerface.

Biointerface: A surface forming a common boundary between a cell, a biological material and another material.

An ideal immunosensor is a mobile, cost effective sensor with high sensitivity, high accuracy, high selectivity. The development regarding the detection devices was cited above, but the manufacturing of a viable immunosensor necessitates correct choice of a solid surface and the development of an appropriate surface chemistry for the attachment of proteins. The critical part of immunosensors is to preserve the integrity, the native conformation and the biological function of the protein to be immobilized on the surface. A well orientation immobilized protein would increase the efficiency of the immunosensors (Goddard, 2007) as a non-oriented immobilized protein would decrease the efficiency.

Adsorption is the first method for protein immobilization. Adsorption can be done physically, physisorption, or chemically, chemisorption, rearrangement of electron density between the proteins and the sensor surface. Physisorption consists on the formation of weak interactions such as Van der Walls, non-selective ionic, electrostatic and hydrophobic interactions. Even if these interactions are enough to immobilize the proteins easily on the surface, the immobilization process is uncontrolled causing an inhomogeneous orientation of immobilized proteins. Also, with time these proteins might unfold for minimizing interfacial interaction energy by rearranging hydrophobic domains. The uncontrolled immobilization process is also prone to the immobilization of undesired protein contaminants on the immunosensor surface decreasing the sensors efficiency.

The immobilization of proteins by covalent bonds is a second approach. This approach is the most commonly used method. However, specific care must be taken for a successful immobilization. First of all, proteins functional groups (-COOH, -NH2, -SH), suitable for immobilization, must be defined. Secondly, an appropriate surface functionalization molecule (spacer) must be determined to preserve the integrity of the protein without disturbing its function. Therefore, the amount of functionalization molecule must be optimized. Insufficient quantity of functionalization molecule might cause a loss of protein activity by placing proteins in direct contact with the hydrophobic layer causing uncontrolled adsorption of the protein or protein contaminants. Overloaded functional groups might cause steric repulsion causing proteins deactivation (Goddard, 2007). The length of the spacer is another factor influencing the conformation of the protein. The longer the spacer is, the higher is the protein load on the immunosensor surface and the better is the conformational integrity; Therefore, the better is the immunosensor sensitivity (Hosseini, 2014).

Other surface functionalization methods such as sol-gel method, a relatively mild procedure consisting of entrapping protein in the swelling gel network can be cited. Even if this method confers an improved resistance of proteins toward chemical and thermal denaturation, and have a high protein loading capacity, the method have also many disadvantages. For example, the possibility of a direct contact of the protein with the sensor surface can cause protein deactivation because of the surface hydrophobicity. Another problem is that there is no intermolecular interaction between the gel and the surface, therefore, a good functionalization in necessary (Prashar, 2012). The protein immobilization is uncontrolled, therefore, the proteins are not oriented, and contaminant proteins might be co-entrapped with the target protein. Finally, sol-gel method produces toxic wastes that might cause an environmental problem on an industrial scale.

Plasma treatment compared to sol-gel is not toxic, and no corrosive solvents are needed. This method allows the deposition of an extra thin uniform functional coating of different shapes, surface charges, surface hydrophylicities allowing efficient protein immobilization on sensor surfaces.Many biological applications. However, this method has some drawbacks such as the loss or re-orientation of functional groups, and surface ageing related to storage conditions. The method

based on vacuum technology requires a strict process control regarding the risk of contamination the reproducibility problems (Prashar, 2012).

Surface functionalization with self-assembling monolayers (SAMs)

SAMs consist on the spontaneous organization of chemical molecules into a highly ordered larger functional structure. They are used as intermediate molecules for functionalizing metal surfaces such as gold, platinum, palladium, silver, copper but also polymer surfaces such as polystyrene, polydimethylsiloxane (PDMS), Polymethacrylate (PMMA), by covalent bonding (Hosseini, 2014; Arya, 2009). SAMs are excellent systems to study interfacial reactions due to the one molecule thick layer. Therefore, they are widely used in biotechnology, drug discovery, material sciences, polymer synthesis, surface science from full homogeneous functionalisation to gradual variation of physicochemical properties (Koepsel, 2012; Arya 2009; Nicosia, 2014).

The formation of ordered films depends on the geometry, the electrostatic and the dipole-dipole interactions of the alkane and the tail groups such as acids (-COOH) or amines (-NH2) within the monolayer and the affinity of the head functional group (Thiols, silanes) to the substrate (Chechik, 2000).

SAMs are characterized by several methods allowing the detection of surface coverage defects. The characterization is made by physical measurement such as contact angle and wettability that permit a fast evaluation of the hydrophilicity of the SAM, which is necessary for correct protein immobilization. Also, several more sophisticated instruments are used for deeper characterization regarding the binding efficiency and the surface topology of functionalized immunosensor chip. These devices are ellipsometry, X-Ray photon spectroscopy, infrared spectroscopy, QCM, surface enhanced Raman spectroscopy, Atomic force microscopy, scanning tunneling microscopy, fluorescence spectrometry, SPR (Prashar, 2012).

Alkanethiol (organosulfur molecule) monolayers on the gold surface are the most studied assembling reactions (Prashar, 2012; Nicisia, 2014). Because they form a strong bond with gold but thiol SAMs can also be used for other metallic surfaces such as platinum, copper, palladium and silver (Arya, 2009).

Alkanethiolates have an –SH functional head group allowing a strong binding with gold. The stability of the thiol SAM depends tremendously with the length of the alkane group. Highest organization in SAM was observed with thiol SAM containing 10 to 20 Carbon atoms (Prashar, 2012).

SAMs tail groups give some properties like biocompatibility, corrosion, wettability, adhesion, friction, resistance to the interfacial surface (Nicosia, 2014). Three functional groups are mainly utilized at the tail terminal. Alkanethiolates containing an amino group tail such as the 11-amino-1-undecanethiol molecule are widely used for redox studies The terminal amino group can be activated with acylating reagents such as active esters, acid chlorides or quinones. Carboxylalkanethiols are used for the immobilization of proteins by forming amide bonds by using carbodiimides such as dicyclohexylcarbodiimide (DCC) or 1-ethyl-3-(-3-dimethylaminopropyl) carbodiimide (EDC) (Chechik, 2000). Hydroxylalkanethiols are mostly used as dilution or blocking reagents to prevent unspecific protein adsorption for immunosensor applications (Prashar, 2012).

Silane monolayers are used for the functionalization of glass, silica (SiO2) surface. Single Alkylsilane molecules form less perfect layer than thiols, but trifunctional silanes have a better SAM formation property, but there is a risk of 3-dimensional structure formations. Organosilane SAMs have importance in the photoresist industry and the silicon technology.

SAM looks to have many advantages that make them suiTable for surface functionalisation, but they have some considerable drawbacks.

First of all, SAM fabrication can be labor intense because it forms a stable layer. Therefore, contaminant molecules, unwanted by-products or unreacted molecules cannot be removed selectively from the surface, causing severe surface impurity problems, Therefore, changing the homogeneity of the SAM. This problem is even more critical when successive reactions are performed (Chechik 2000; Koepsel, 2012). It has been also demonstrated that sulfur can induce corrosion of Au (111). The strong interaction between gold (Au) atoms and sulfur weakened the Au-Au interactions. This causes the removal of some Au atoms from the surface and which incorporates into the growing 2D phase producing etch pits and irregular shaped au-Sulfur islands. The stability of SAM is another point to consider, SAMs undergo photooxidation during exposure to ultraviolet light that causes the desorption of the thiol groups from the surface. The final stability of monolayers for short temperature excursions are small compared to typical microfabrication processing conditions (Celestin, 2014).

Also, thiol SAMs on the gold surface are well packed and have a quasi-crystalline structure when the tail group has a long alkane chain. However, if bulky and charged

groups are incorporated to SAMs disruption of the molecules from the surface due to the steric effect and electrostatic repulsion is possible (Chechik, 2000). Another problem is the time necessary for the formation of accepTable SAMs. Even if the binding of alkanethiols on gold surface is very fast, the time necessary to obtained a highly organized compact SAM vary between 12 -18 hours. This can increase up to 48 hours for 11-mercaptoundecanoic acid (Prashar, 2012; Marques de Oliveira, 2011). Finally, the most important drawback is that proteins are immobilized on the surface in a non-oriented manner causing a severe reduction in the availability of proteins functional groups such as the recognition sites of antibodies. In consequence, a decrease in the immunosensor efficiency is expected.

Considering all the defects regarding chemically based material surfaces functionalization processes, there is an urge for new functionalization strategies. Bio-functionalization offers an enormous potential in the functionalization area with its easy to handle single-step self-assembling protein immobilization process. Biological self-assembling layers offered highly ordered, stable and oriented homogenous biocompatible structures by using green technology (Yazici, 2013; Hnilova, 2012).

1.2 Inorganic binding peptides

Proteins are the fundamental elements for life. These proteins have very broad functions that may consist of structural integrity of tissues (collagen) and enzymatic activity for cell survival or gene expression regulation. Therefore, they can interact with various organic molecules such as other proteins, DNA, carbohydrates, lipids. But there is the other aspect of proteins that is forgotten. Living organism are producing biological hard tissues such as bones, teeth, hairs, nails but also nacre or spicules with the intervention of proteins. Therefore, these inorganic binding proteins inspired from nature or their molecular derivatives might help to develop new high-tech organic-inorganic hybrid materials by using molecular biology, bioinformatics for the nanotechnology industry.

1.2.1 Roles of proteins in biological materials

Biological hard tissues are complexes structures composed of sensitively balanced mixture between organic and inorganic molecules. These structures can even be found in single cell organism such as bacteria. Aquasprillum magnetotacticum is one

of the possible examples (Figure 1.4A). This bacteria has organelles containing magnetite (Fe_3O_4) nanoparticles which help the bacteria navigation through the sensing of earth's magnetic field (Frankel, 1991). This phenomenon is called magnetotaxis. The extraordinary facts are that these biologically produced nanoparticle have equivalent size (50 nm) and same cubo-octahedral shape allowing the maximum sensing ability of the earth's magnetic field (Tamerler, 2010).

The protective shell of mollusks is another example for the structural perfection of biological hard tissues (Figure 1.4B). The layered shell structure of mollusks composed of aragonite (orthorhombic $CaCO_3$) and the biopolymer mixture of proteins and polysaccharides gives the shell the unique toughness and fracture strength among all ceramic based materials (Fong, 2003; Sarikaya, 1992).

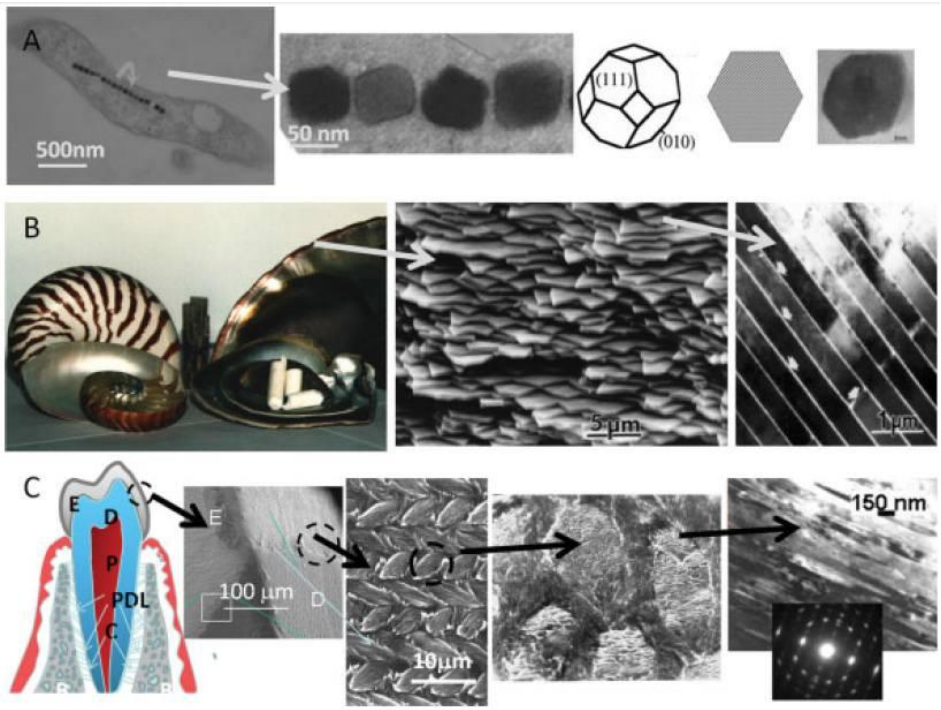

Figure 1.4 : Biological material examples (Tamerler, 2010).

Sponges (Rosella racovitzea) also are producing inorganic materials such as spicules (Figure 1.5). These silica-based fibers with star-shaped tips are collecting the light and transfer it into the inner part of the sponge allowing sponges survival (Sarikaya, 2001).

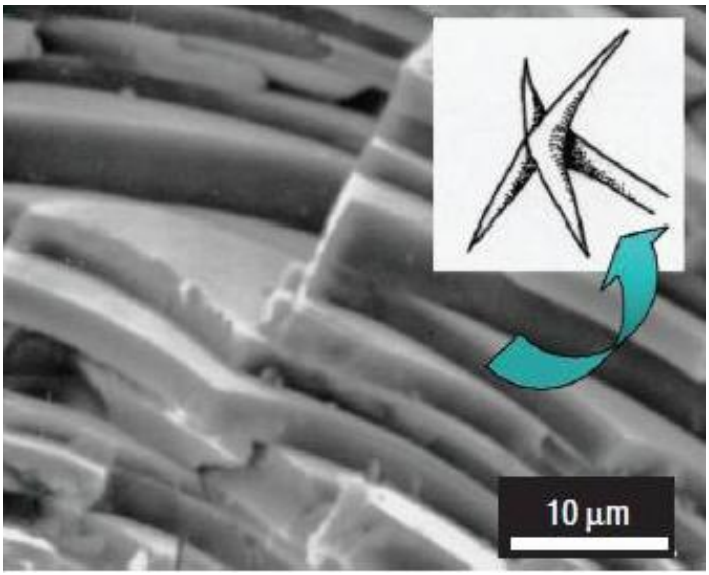

Figure 1.5 : Cross section of Sponge spicule of Rosella by SEM (Sarikaya, 2001).

The last example is mammalian tooth (Figure 1.4C) that is one of the most complex structure comprising layers of different tissues. Enamel is the protective outer layer of the tooth that is the hardest material in the body. Enamel has a very particular woven-like fiber structure, composed of tightly controlled shape and size of hydroxyapatite crystallites. Enamel is integrated to dentin, the later is the softer bone-like tissue involved in absorbing external physical stress. All these inorganic tissues are generated by a panel of proteins. Some of these proteins are involved in nucleation, others are implicated in growth and assembly.

Therefore, if proteins are highly involved in the production of various inorganic materials by controlling the shape, the size and the strength of produced crystallites, then why not mimicking their activity? So the term of "molecular biomimetics" has arisen (Sarikaya, 2003). Since then, mechanism involved in the formation of biologic inorganic materials are investigated and especially, at the first step, proteins or peptides implicated in the recognition of inorganic compounds.

1.2.2 Inorganic binding peptides

The first term of metal recognition polypeptides was employed in year 1997 by Stanley Brown regarding the selection of polypeptides able to bind gold and chromium (Brown, 1997). Brown has generated a repeating peptides library and displayed the library on the surface of *Escherichia coli*. Then the cell surface displayed library was screened either against gold or chromium and cells adhering to

gold or chromium surfaces were selected. The library was enriched with several enrichment cycles, and the polypeptides encoding inserts were amplified by PCR. The PCR amplified inserts were recloned into an alkaline phosphatase (AP) vector for facilitating the soluble expression of the polypeptides. The gold binding property of the peptides fused with AP was analyzed by a modified Scatchard method. Later on, new cell surface displayed polypeptides libraries were constructed for the selection of polypeptides which have an effect on gold crystals formation (Brown, 2000). They have found that two different peptides with some commons sequences were accelerating colloid appearance of gold. Referring to these experiments, the authors have suggested a mechanism in the formation of the crystalline phases of hard tissue.

Cell surface display method was the pioneer for the selection of genetically engineered polypeptide for inorganic (GEPI). Up to now, cell surface display has been used to identify peptides recognizing zinc oxide, cuprous oxide, iron oxide and zeolites. New inorganic binding peptides were discovered by M13 phage-displayed peptide libraries. Metal binders such as silver (Ag), platinum (Pt) and palladium (Pd) binding GEPI's were selected by using 12-mer or disulphide-constrained 7-mer peptide libraries (Naik, 2002; Sarikaya, 2003). But also peptides specific to Titanium oxide (Sano, 2003; Sano, 2005), semiconductors (GaN, ZnS, CdS (Lee, 2002), minerals (hydroxyapatite, graphite, calcite, sapphire (Krauland, 2007) were selected from peptide libraries (Gaskin, 2000; M. Gungormus, 2008; So, 2012; Whaley, 2000). The most important and critical point for the selection of inorganic peptides is the composition or the structure of the target material during the selection process. Because of inorganic material heterogeneity at atomic and crystallographic level, several peptides with different sequences might be selected, each of them specifically binding different state or size of the inorganic compounds (Sarikaya, 2003).

Most of the selected inorganics binding peptides were used as it is. But some peptides were further engineered by computational biomimetics approaches. Amino acid sequences of peptides might be a very effective data for understanding the binding mechanism of inorganics binding peptides. The inspection of the sequence of the noble-metal binders showed that the serine and the threonine amino acids were important for binding, possibly by their aliphatic hydroxyl groups. Interestingly two amino acids which are known to bind to transition metal ions, cysteine and histidine, were mostly absent in these sequences (Slocik, 2002). The same inspection was

made for non-metal binding sequences Therefore, the phage display or cell surface display technologies have given the opportunity to predict which amino acids were important for binding to metals or non-metals (Sarikaya, 2003). This knowledge was useful for molecular modelling studies. The structure of the 3-repeat gold-binding peptide GBP1 was determined *in silico* and then this structure was placed on gold atomic lattices (Au 111) for visualisation the potential interaction between them (Braun, 2002). In consequence, second generation of peptides with higher binding ability and specificity were selected with the help of bioinformatics tools and/or experimental mutagenesis (Tamerler, 2010). Material-specific scoring matrices were produced by combining sequence alignment techniques (Oren, 2007; Tamerler, 2009). These matrices were used to develop a bioinformatics method allowing the design of new peptides with a high affinity and specificity. This methodology was validated by the design of new peptides with high affinity to quartz (Oren, 2007).

Even if molecular modelling and bioinformatics might help to understand binding interactions, more precise structural analysis are required such as nuclear magnetic resonance spectroscopy. But also other characterization methods are necessary for determining the affinity (quartz crystal microbalance (QCM) and surface plasmon resonance spectroscopy (SPR)) and selectivity (fluorescence microscopy, atomic force microscopy (AFM)). Such that the binding properties of GBP1, platinum binding (PtBP1) and silica binding (QBP) peptides to respectively gold, platinum and silica were determined by SPR (Seker, 2007; Seker, 2009; Tamerler, 2006a; Tamerler, 2006b). The binding of GBP1 was also confirmed by QCM was determined with SPR (Tamerler, 2006a; Tamerler, 2006b).

1.2.3 Genetically engineered peptide-based applications

GEPI have been widely used for a wide range of applications, mainly on the biofunctionalization of materials (Seker, 2011; Tamerler, 2010). GEPI were used for the immobilisation of anti-fouling polymer such as poly(ethylene glycol), integrin-binding RGD, enzymes (alkaline phosphatase, L-lactate dehydrogenase), fluorescence protein (Green fluorescence protein) on different solid surfaces such as gold, titanium or silica. GEPI fused with DNA binding proteins were also used for targeting nanoparticles to DNA by this way demonstrating that complex nanoarchitecture through DNA-protein-nanoparticle can be constructed (Cetinel,

2013; Sedlak, 2010; Khatayevich, 2010; Tamerler, 2010). Some of these applications are explained in more details further.

An enzyme, such as Alkaline phosphatase (AP) was successfully immobilised on the gold surface through Gold binding peptide (Kacar, 2009). Several alkaline phosphatase fusion construct with different copy number of GBP were expressed and purified. These fusion enzymes were then immobilized on a pattern by adsorption with the use of microcontact printing (Figure 1.6), and the enzymatic activity of AP was demonstrated.

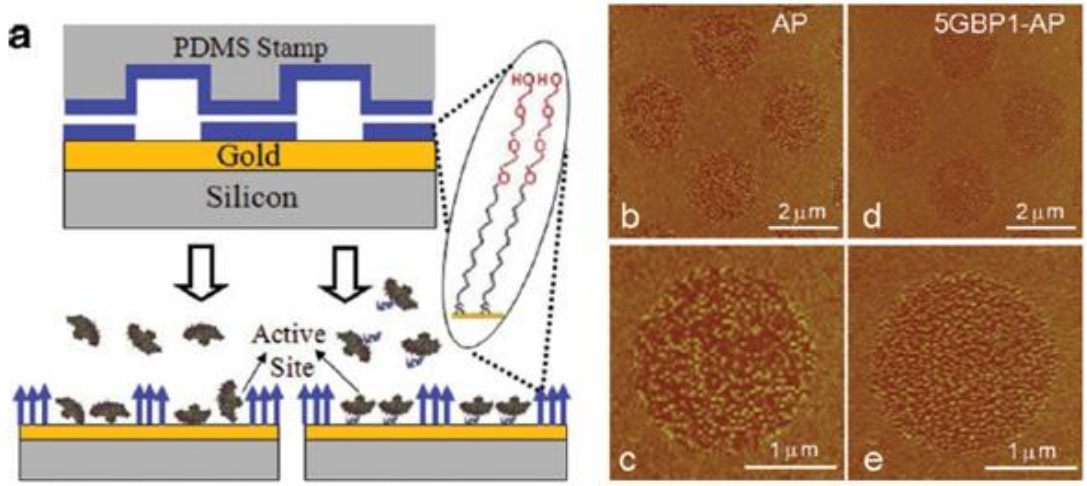

Figure 1.6 : Two-dimensional array of immobilized 5GBP1-AP (Kacar, 2009).

GEPI against hydroxyapatite was selected with phage display technology. One strong hydroxyapatite binder peptide (HABP1) was selected, and the effect of this peptide on biomineralisation of hydroxyapatite was observed with SEM for 28h. HABP1 significantly influenced hydroxyapatite crystal formation by generating larger crystals. Consequently, genetically engineered peptides for inorganics have the potential to be used in tissue regeneration (Gungormus, 2008). Then a fusion peptide (MDG1, Mineral Directing Gelator), wherein the HABP1 peptide and a peptide implicated in hydrogel formation, was synthesized. It was shown that MDG1 gels were capable of directing the formation of hydroxyapatite (Gungormus, 2010).

Yuca (2011) have engineered a hydroxyapatite binding fluorescent protein for monitoring biomineralisation. They have genetically linked the DNA encoding the HABP1, hydroxyapatite-binding peptide, with green fluorescence proteins gene and expressed the fusion protein in *E.coli*. The fluorescence of the construct was verified under a fluorescence microscopy, and the affinity of the engineered protein to

hydroxyapatite was determined by quartz crystal microbalance spectroscopy (Figure 1.7).

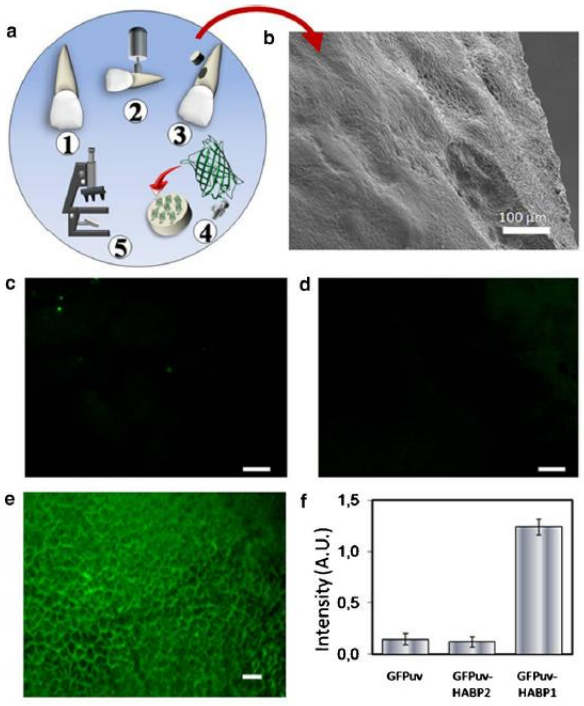

Figure 1.7 : Fluorescence labeling of teeth with GFPuv-HAPB1 (Yuca, 2011).

Quartz binding peptide (QBP) was used as molecular linker (Kacar, 2009). The quartz binding peptide was conjugated with fluorescein or biotin and then printed by microcontact on quartz surface. The immobilized QBP-fluorescein fusion protein was directly monitored by fluorescence microscopy. The QBP-biotin fusion construct was monitored with the help of streptavidin conjugate fluorescent quantum-dot. By this way, it was demonstrated that inorganic solid-binding peptides could be used as ink for microcontact printing as well as linker for self-assembly.

Hnilova (2012) have developed a gold and quartz binding bifunctional peptide by the fusion of the QBP with AUBP1, a gold binding peptide. This bifunctional peptide was able to assemble gold nanoparticles on a silica surface. The group has also succeeded to synthesize nano-metallic particles in situ on the peptide pattern (Hnilova, 2012).

The same group has also demonstrated a bio-enable self-assembly technique by using a gold binding peptide (AuBP1) tag (Hnilova, 2012). They have used this technique for multi-layered protein formation and nanometallic assembly. For this purpose, they have fused the AuBP1 gold binding peptide with maltose binding protein

(MBP) using different linkers. Then they have measured the binding affinity of the construct to gold. The equilibrium dissociation constant (K_D) of the AuBP1-MBP fusion protein was determined between 0,02 and 0,04 μM, differing because of the detection method used (SPR and localised SPR (LSPR)) and the linker sequence inserted. They have immobilized the gold and quartz binding bifunctional peptide on a silica surface, then gold nanoparticles successively. As the third layer, they have immobilized the gold binding AuBP1-MBP construct and finally, they have immobilized an Alexa-488 conjugated anti-MBP antibody as a monitoring agent. Therefore, they have successfully immobilized a combination of organic and inorganic layers on the surface of silica, demonstrating as a matter of fact a new layer-by-layer coating method (Figure 1.8).

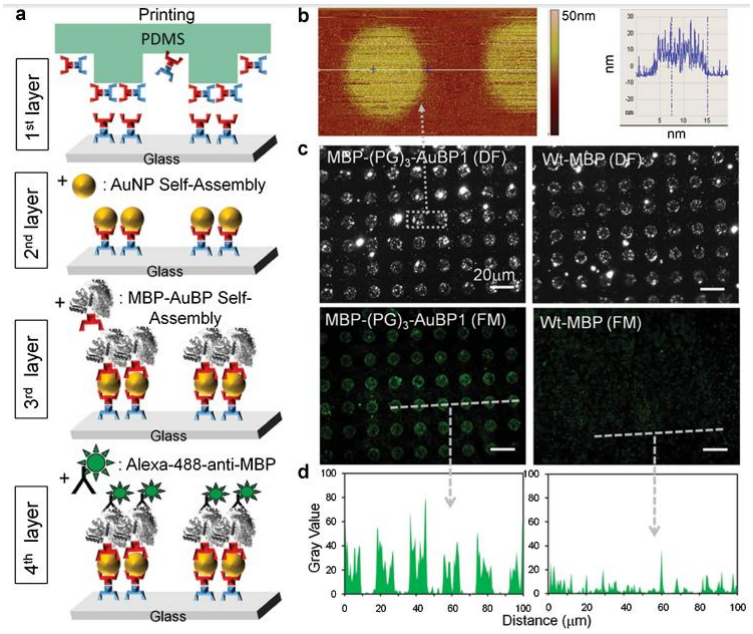

Figure 1.8 : Immobilized proteins on gold NP arrayed surface (Hnilova, 2012).

Recently, Yazici (2013) have developed two titanium binding bi-functional peptides with an integrin recognizing peptide motif, RGDS. They have shown that the functionalization of titanium surface with these peptides significantly enhanced osteoblasts and fibroblasts bioactivity. Briefly, they have screened a cell surface displayed peptide library against Titanium. They selected 60 unique peptides with titanium binding ability. Out of them two strong titanium binding peptides (TiBP1 and TiBP2) were identified and characterized for their molecular structures by circular dichroism spectroscopy and molecular modeling studies. The affinity of the peptides to titanium was measured by QCM and dissociation constant (Kd) of

0.9±0.12 μM for TiBP1 and 0.18±0.03 μM for TiBP2 was calculated. Then they have synthesized new TiBP1 and TiBP2 peptides containing RGDS peptide motif, and they have shown the increases of NIH3T3-E1 preosteoblast cells adherence and proliferation on titanium surfaces functionalized with TiBP1-RGDS and TiBP-RGDS (Figure 1.9).

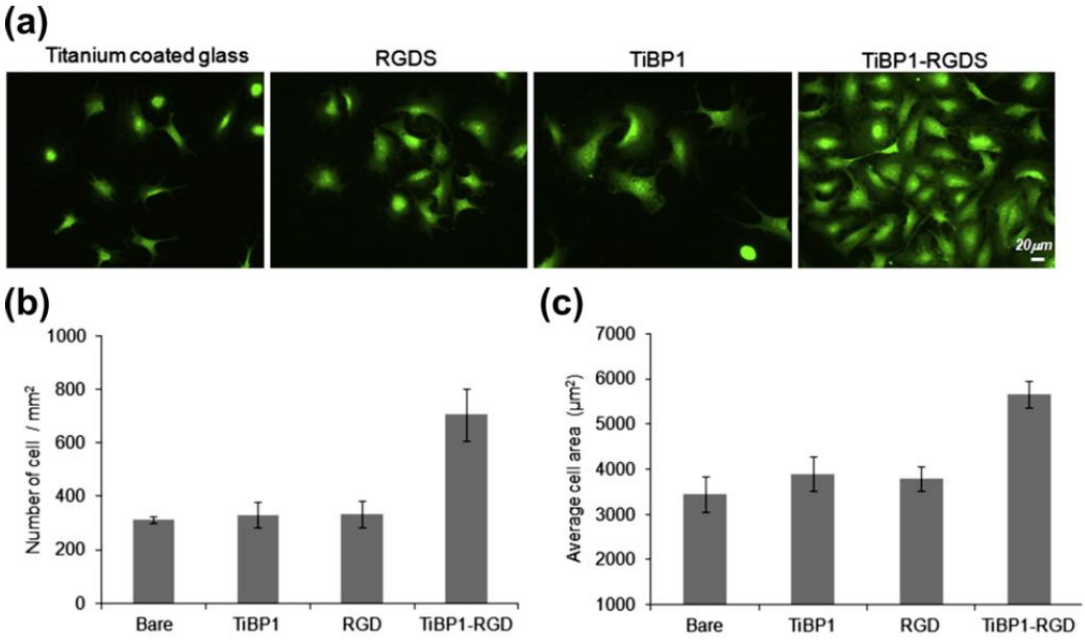

Figure 1.9 : Cell adhesion mediated by TiBP1-RGDS peptide (Yazici, 2013).

In conclusion, GEPIs have proven their metal-binding ability and their potential to be used as self-assembled linkers between inorganic surfaces and proteins. This property is opening a new vision about the immobilization of antibodies on biosensors surfaces for the detection of disease-related proteins such as the Hepatitis B virus Surface antigen.

1.3 Hepatitis B virus

Hepatitis B virus (HBV) is one of the major causes of chronic Hepatitis, cirrhosis and liver cancer (hepatocellular carcinoma, HCC) in the World.It is forecasted that it will be in higher ranks in the next two decades (World Health Organization, WHO, Executive board 126th session EB126/15, 2009). According to WHO (Fact sheet No: 204, 2013) the number of infected people is about 2 billion. From these infected people approximately 240 million are chronically infected, and about 600,000 people die every year due to the consequences of HBV.

It is estimated that HBV was present in the Antic times 5th before J.C. but only in year 1883 the presence of HBV in blood serum was detected by Bremen Shipyard and its colleagues (Lok, 2001). Mac Callum assigned the Hepatitis word in year 1947, and this terminology was approved by WHO in year 1973. In year 1965 Hepatitis B surface Antigen was discovered called at that time Australian antigen (Lusebrink, 2009). After this discovery many works have been done on HBV about its structure, its replication processes and its infection mechanisms. In year 1992, a world vaccination program leaded by WHO was initiated for the vaccination of the children's in the aim of reducing the infection rate of HBV. This program has been successful with an overall decrease of HBV infection prevalence (Luo, 2012).

1.3.1 Epidemiology and virology

HBV is a virus from Hepadnaviridae virus family, which infects specifically human liver cells, but it can also infect experimentally chimpanzees even though it is not infectious for them. However, there are different variants of Hepatitis specific for another animal such as woodchuck hepatitis virus or duck hepatitis virus. These hepatitis models have helped to understand their structure and their mechanism of infection liver cells (Lusebrink, 2009).

HBV is a circular partially double-stranded virus of 3.2 kb length, which the smallest genome among viruses. Up to know ten different genotypes has been discovered with a 8% genome variation (Hakami, 2013; Harkisoen, 2012). The worldwide distribution of the most dominant genotypes is given in Figure 1.10. In Turkey, the prevalent genotype was determined by a complete genome sequencing phylogenetic analysis of HBV isolates from different regions of Turkey (Bozdayi, 2005; Sunbul, 2013). Zehender and its colleagues have modeled the spatial and temporal dynamics of HBV D spreading. According to their reconstruction the origin of HBV D genotype is India, and this genotype arrived in Turkey around years 1960 (Zehender, 2012).

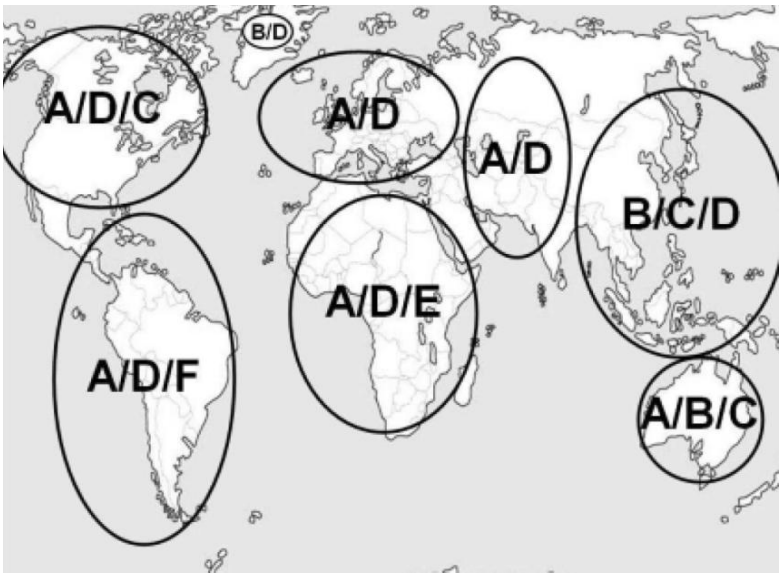

Figure 1.10 : Dominant genotypes of HBV (Harkisoen, 2012).

The HBV genome consist of a full-length strand is called negative (-) strand and a partial non-coding strand called positive strand (+) (Figure 1.11). The HBV genome contains four highly condensed and overlapping Open Reading Frames (ORF) on the minus strand. This strand encodes 7 proteins which are the surface antigens S, PreS2 and PreS1, the Hepatitis B e antigen (HBeAg), the Hepatitis B core antigen (HBcAg), the polymerase and the HBx protein (Lusebrink, 2009).

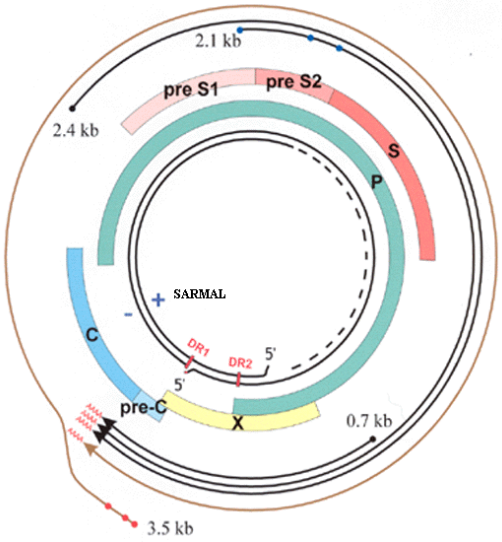

Figure 1.11 : HBV genome representation.

The polymerase protein is expressed from the longest ORF and is covalently bound to the minus strand; this polymerase is necessary for the replication of the virus. The polymerase has three functions. The first one is the primase activity at the N-

terminal. The second one is the reverse transcriptase activity for converting the pregenomic RNA into DNA and also for the generation of the + strand. It also helps the encapsidation of the pregenomic RNA in the core proteins. The last activity is the RNAse H activity which helps the degradation of the pregenomic RNA.

The core protein (183-185 aa) is essential for the formation of the nucleocapsid. The core protein is obtained by the cleavage of the peptide signal sequence (propeptide) of the precore protein. The core proteins are forming dimers then they self-assemble together for forming the HBV nucleocapsid with 90 dimers (30 nm) or 120 dimers (34 nm) the major infectious viral particle (Schadler, 2009).

The HBeAg is a clinical serum marker related with high HBV replication indicating disease severity. HBeAg, establish immune tolerance and chronic infections. HBeAg is conserved among all Hepadnaviridae family which suggests that it is evolutionary conserved. Therefore, it has an important role in HBV infections (Revill, 2010) HBeAg is produced from the same ORF as HBcAg and have a very high sequence similarity. The only sequence variation is that, instead of HBcAg, HBeAg carries the ten amino acid N-terminal propeptide and that HBeAg is deprived of the Arginine rich present in HBcAg. These two proteins have differents functional and physical properties even their sequence similarity. Recently DiMattia and his colleagues have crystallized HBeAg complexed with an HBeAg specific Fab (E6). They have discovered that HBeAg was present as a dimer and that this dimerization was due to the Cysteine residue present in the propeptide. This residue was forming a disulfide bond with the Cys 61 which is implicated in the dimerization of the HBcAg.

This conformational change was favoring the HBeAg dimerization, changing the antigenic property of the dimer drastically. This conformational change explained the functional and structural differences between the two similar antigens (Figure 1.12 and 1.13) (DiMattia, 2013).

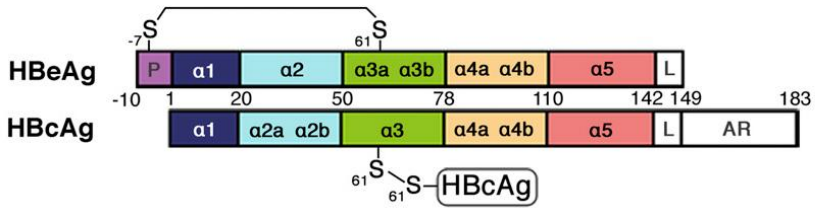

Figure 1.12 : HBcAg and HBeAg representation (DiMattia et al., 2013).

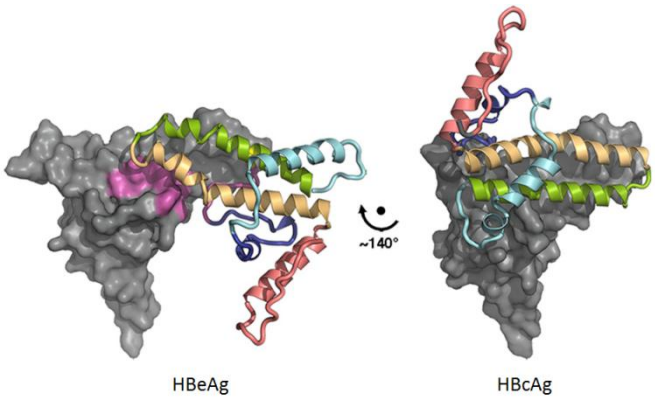

Figure 1.13 : 3D representation of HBcAg and HBeAg (DiMattia, 2013).

The X protein (17 kDa) is a highly conserved multifunctional protein acting as a transcription activator of host gene promoters required for in vivo viral replication and some proto-oncogenes such as c-jun, c-fos and c-myc. It is also regularly detected in HBV-associated HCC patients. Therefore, it is believed to be highly implicated in Hepatocellular carcinoma (HCC) (Hwang, 2003; Lucifora, 2011; Ng, 2011).

The three surface antigens constitute the virus envelope. These antigens are encoded from the same ORF with three different start codons. The small HBV surface antigen is composed by the S domain (226aa), the PreS2 antigen (334-345 aa) comprised the S domain and the PreS2 domain of 55 amino acids. The Large antigen called PreS1 (389-400aa) is expressed from the full-length ORF. Therefore, it contains the S; PreS2 and PreS1 domains (Figure 1.14).

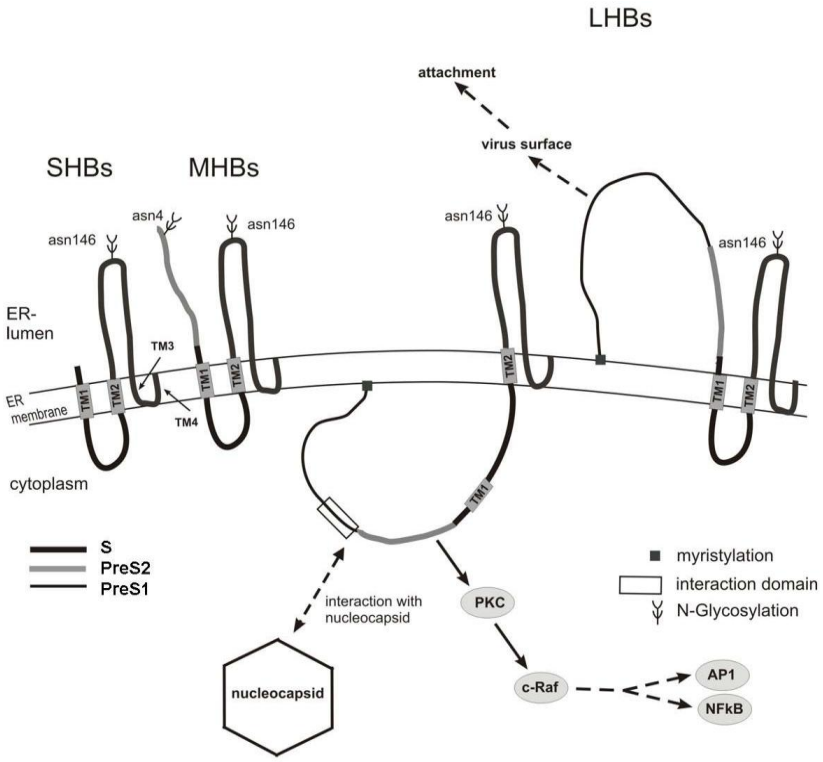

Figure 1.14 : Hepatitis B virus surface antigens (Schadler, 2009).

The position of the surface antigens on the Endoplasmic reticulum (ER) membrane is shown in Figure 1.16 where the possible glycosylation sites Asn 4 and Asn 146 are indicated. PreS1 antigen is present in two different forms due to a posttranslational translocation of the Transmembrane domain 1 (TM1). When the TM1 domain is located in the ER membrane then, the PreS1-PreS2 domains are located in the ER lumen from where there will be secreted and be found on the external part of the virions. This form of the PreS1 antigen will allow the attachment of the virions to the corresponding host cell receptor. However, if the TM1 is not translocated then the PreS1 and PreS2 domains are located at the cytoplasmic part of the host cell. Once secreted, they will be positioned in the inner part of the virions and interact with the nucleocapsid and activate intracellular signal transduction.

The expression of the HBsAg, which is higher than the required amount for the virus production, the reason is not well understood. The over-expressed HBsAg will self-assemble and form spherical or filament shaped particles of 22 nm. These non-infectious particles will then be released into the blood circulation (Figure 1.15). One hypothesis is that these non-infective particles might help to increase of the efficiency of the infection by overwhelming the host immune system. Therefore, allowing the immune escape of the infective virions (Dane particles) (Bruns, 1998).

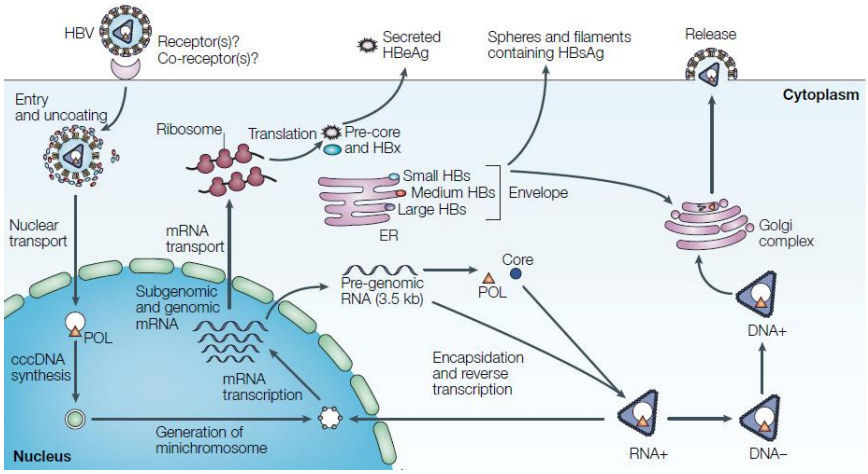

Figure 1.15 : HBV life cycle (Rehermann, 2005).

The detection of HBsAg in the blood is, therefore, a perfect indicator for HBV infection.

1.3.2 Detection of HBsAg

Molecular based detection is a very sensitive system allowing accurate detection of very low copy numbers of HBV DNA or RNA by real-time polymerase chain reaction (RT-PCR). Even different sub-genotypes of HBV can be detected and quantified by multiplex-PCR reactions making the molecular biology based detection methods (Chen, 2007). Therefore, as ELISA is the gold standard for serological tests, real time-PCR is the gold standard for all detection methods of HBV (Heiat, 2014). However, molecular-based HBV detection have several drawbacks, the systems require highly specific instrumentation, clean rooms, qualified personnel to do an experiment and to interpret it. Therefore, molecular-based systems are very sensitive but not prone to be good biosensors.

Instead, HBsAg is a very specific biomarker for HBV infection. Its detection in blood is of great importance for human health care. Therefore, many researches have been made for the development of easy, rapid, sensitive and selective HBsAg detecting immunosensing systems. The first detection systems developed which are still on the market are the serological tests such ELISA, radioimmunoassay, immunochromatographic assay and immuno-chemiluminescence (Lau, 2003). Among them radioimmunoassay (RIA) is the first detection system based on a competitive binding assay between a radiolabeled and a label-free HBsAg to an anti-HBsAg antibody. ELISA-based detection systems are the most widely used among

the commercial HBsAg detection kits especially in clinical laboratories. These intensively optimized detection kits for several generations became and are still becoming faster, more accurate and sensitive. These improvements are not due to the development of new antibodies but rather to the decrease of the environmental noise. Immunochromatography based detection systems are the most desired detection systems because of their very fast response time and their easy result interpretion. However, in a research regarding the detection of HBsAg, a comparative assay was done between immunochromatography based detection kit and a third generation ELISA kit. The authors concluded that immunochromatography based detections were still not enough for the detection of HBsAg in blood serum. The same fact was previously stated by Lin (2008), who tested commercially available 33 HBsAg rapid tests. Therefore, even if these detection methods were developed many years ago they still need some improvement to meet the requirements of FDA to be approved as a rapid test (Lin, 2008).

With the technological development many new, highly sensitive and selective devices are being investigated for the detection of HBsAg. Even so that HBsAg has been accepted as a model molecule for many biosensors in the development phase (Heiat, 2014). The detection of HBsAg was investigated with Piezoelectric immunosensors, a detection level in the range of 0,1-100ng/mL have been measured with Piezoelectric Microcantilever. A multiple piezoelectric based detection system was able to detect simultaneously HBsAg and α- feto protein, a tumor marker (Xu, 2010). HBsAg was also detected by electrochemical immunosensors using sandwich-type assays a by using gold nanoparticles and horseradish peroxidase (Nourani, 2013).

Finally, by using gold nanorods based localised SPR immunosensor, HBsAg was able to be detected in blood serum and plasma (Wang, 2010). Recently, the detection of HBsAg using plasma-treated parylene-N film on SPR chip was confirmed with a 1000 fold increase of the SPR sensitivity (Choi, 2014).

1.4 Detection probes for HBsAg

The sensitivity and the selectivity of immunosensors are increasing each day with the development of the technology. However, all the detection systems have the same goal, improving either instrumentation or the surface functionalisation methods.

The aim is to offer the most favorable environment to the bioreceptor so that it can binds specifically to its target molecules with high affinity. Even if the sensitivity of detection can be increased by using signal enhancing molecules, which might also bring some background noise, the selectivity of the immunosensor is limited to the specificity of the bioreceptor used. Therefore, the development of a better bioreceptors is one of the important and most challenging part for improving immunosensors. Many bioreceptors against HBsAg have been produced up to now. Starting with polyclonal antibodies produced by animals such as rabbit, goat, horse after several injection steps of the target antigen for which its antibody is expected. However, polyclonal antibodies are not suited for immunosensors because they give high cross reactivity with other proteins having the same epitope. Then comes the monoclonal antibodies developed by the hybridoma technology developed by Cesar Milstein, Georges J. F. Köhler in 1975 and awarded with the Nobel price in 1984. With the molecular biology techniques and the knowledge regarding antibodies, the development of genetically engineered recombinant antibody production has been boosted. Once the genetic material encoding the antibodies were obtained and combined with molecular biology techniques, the development of recombinant antibody variants was limited with the imagination. Recombination of antibodies started with a simple antibody variable region exchange. It has expanded to the modification of CDR's for increasing affinity, the modification of the frame region for increasing antibody solubility. It has also expanded to the generation of single chain variable fragment antibodies, of dimeric, trimeric, bispecific antibodies, of recombinant antibody libraries (Erdag, 2011).

New, non-proteic but nucleic acid based bioreceptor molecules are also investigated, such as aptamers, peptidic nucleic acids. Recently, an aptamer specific to HBsAg was developed for the purification of HBsAg from expression cells (Binning, 2012). However, very little is known on the structural and biochemical aspects of aptamers. Therefore, until more knowledge is acquired about these nucleic acid based recognition molecules, their use as bioreceptors for biosensor applications would add new uncertainties. Below only the hybridoma technology in its basic aspects and the phage display technology will be described. Phage display is a powerful technique, allowing the expression of proteins or antibodies on the surface of filamentous phages allowing the selection of many of recombinant antibodies against a wide range of antigens.

1.4.1 Anti-HBsAg monoclonal antibodies with Hybridoma technology

Hybridoma technology was developed by Cesar Milstein, Georges J. F. Köhler in 1975. This technology has allowed the production of large quantities of monoclonal antibodies highly specific to a single epitope of antigens. Therefore, monoclonal antibodies have found their place in the diagnostic and therapeutic arena rapidly.
The technology consists on the fusion of two differents cell lines. The B-cells, capable of producing antibodies, are isolated from the spleen of animals immunized with the target antigen. The immortal myeloma cell line, which is a B-cell cancer cell line. The fusion hybrid cells are called hybridomas. These cells will be able to multiply rapidly and indefinitely and also to produce large amounts of antibodies. The main difficulty of the hybridoma technology is a necessity to select a single hybridoma cell producing full antibody after an extensive screening procedure by limiting dilution. The major drawback of this technology is the lack of the genetic information regarding the antibody encoding genes. The discovery of polymerase chain reaction and Sanger DNA sequencing methods have opened a new area. The recombinant antibody engineering area, wherein the genetic material encoding the antibodies was isolated and then genetically modified for further antibody properties improvement suiTable for diagnostic and therapeutic applications.

1.4.2 Recombinant antibodies with phage display technology

Phage display was first introduced by Smith in year 1985. Smith has expressed a polypeptide on the surface of a lysogenic M13 filamentous phage. Since then phage display technology have found many applications such as generating recombinant antibody or cDNA libraries for diagnostic, therapeutic purposes (Rakonjac, 2011). This display technology was then expanded to cell surface display and ribosome display (Wittrup, 2001).

1.4.2.1 M13 Bacteriophage structure

M13 Filamentous phage was first isolated from wastewater in Munich 1963 (Hofschneider, 1963). It is a 900 nm long cylindrical shaped E.coli bacteriophage with 6-7nm diameter (Makowski, 1997; Webster, 1996). Wezenbeek (1980) have sequenced the single-stranded genome of M13 phages, and they have determined the

size of the genome as 6407 base pairs length (van Wezenbeek, 1980). The genome encodes 11genes, 5 of them being coat proteins (pIII, pVI, pVII, pVIII, pIX) (Figure 1.16 and 1.17) (Sambrook, 2001; Paschke, 2006).

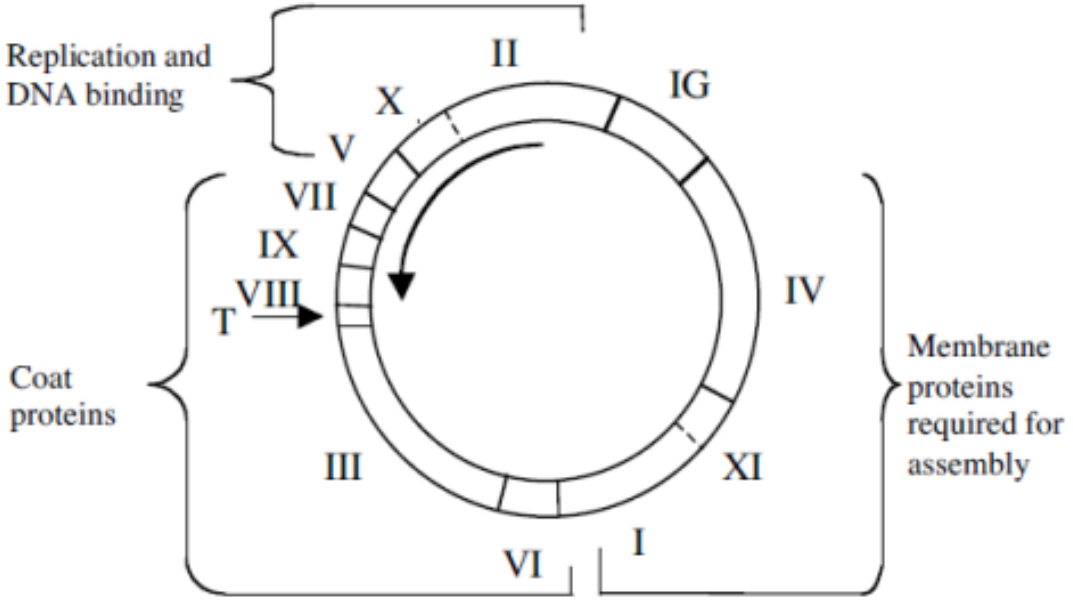

Figure 1.16 : Genetic map of the Ff phage (Sambrook, 2001).

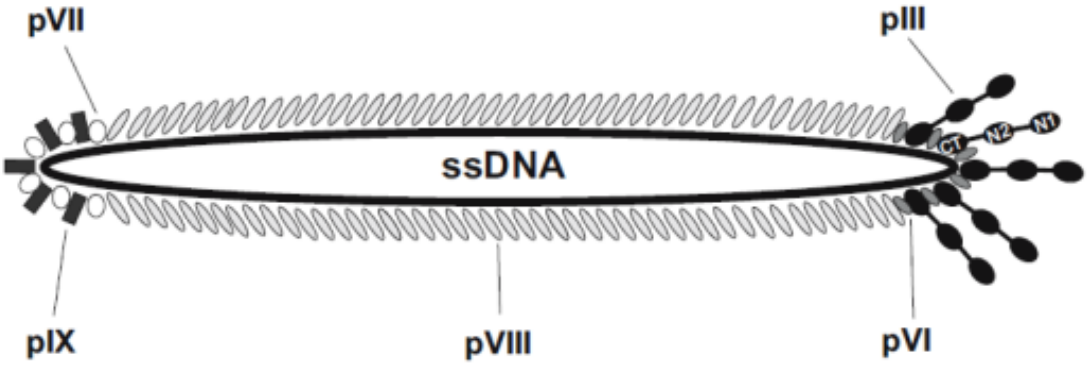

Figure 1.17 : Surface proteins of M13 phage (Paschke, 2006).

The pVIII protein (50 amino acids) is the major coat protein with 2700 copies covering approximately the whole phage responsible for the encapsulation of the DNA (Table 1.2). The pIII (406 aa) and pVI (112aa) proteins with five copies each are necessary for the phage stability and infectivity. The remaining two coat proteins pVII (33 aa) and pXI (32 aa) are implicated in phage assembly and release (Lopez, 1983; Sidhu, 2001).

Table 1.2 : M13 phages coat proteins (Sidhu, 2001).

Protein	Amino acid number	Molecular Weight (Da)	Copy number
PIII	406	42.500	~5
PVI	112	12.300	~5
PVII	33	3.600	~5
PVIII	50	5.200	~2700
PIX	32	3.600	~5

The structure of PIII has been studied more intensely because of its importance in bacteria infection (Kay, 1996). The pIII protein has three distinct domains separated with glycine-rich linkers (Figure 1.18) (Russel, 2004). The C-Terminal domain (CT) is anchored into the phage particle. Two distinct domains compose the N-terminal domain which is necessary for phage infection. These two domains are interacting with each other (N1 and N2) which shown by X-Ray Crystallography and NMR spectroscopy (Holliger, 1997; Lubkowski, 1998).

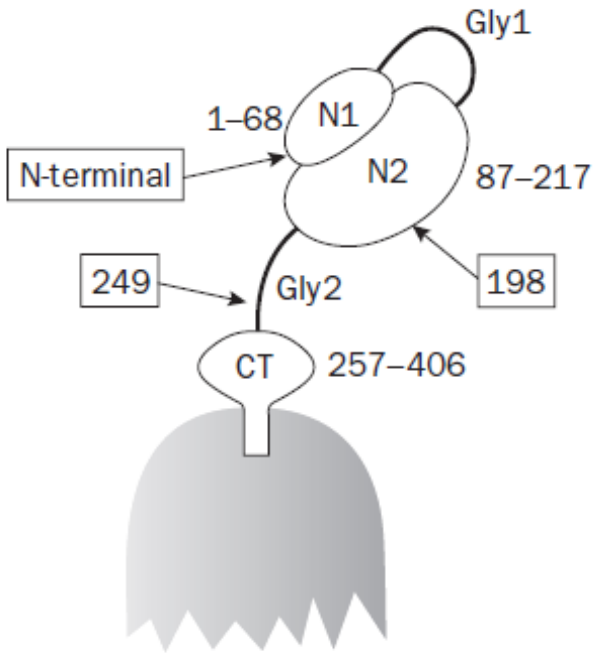

Figure 1.18 : pIII protein structure (Russel, 2004).

1.4.2.2 Infection of M13 Bacteriophage

The infection of E. coli by M13 phage is made with the strong interaction of bacterial F pili with the N2 domain of the phage (Deng, 2002). This interaction causes the

separation of the N1 domain making it accessible for interactions. With the retraction of the bacterial pilus (Jacobson, 1972; Maier, 2005; Marvin, 1969) the phage gets closer to the surface of the bacteria. This approach allows the interaction of the N1 domain of pIII protein interacts with the host TolA co-receptor (Figure 1.19).

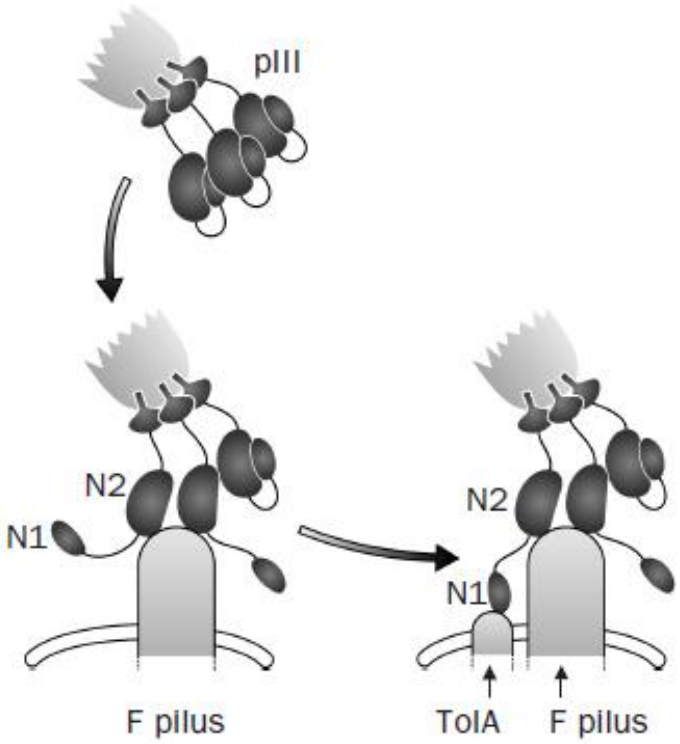

Figure 1.19 : Infection of E. Coli by Ff bacteriophage (Russel, 2004).

Even though, the interaction of the pIII proteins with the E. Coli pili is known the mechanism of phage DNA entry into the host cytoplasm is unclear. A speculative DNA entry model where the CT domain of pIII is "opened" allowing the hydrophobic helix region of CT to interact with the inner membrane of the host cell was represented (Rakonjac, 2011).

Once the phage is in contact with the host inner membrane, the phage DNA is injected in the cytoplasm, and the pVIII coat proteins are integrated into the inner membrane (Figure 1.20).

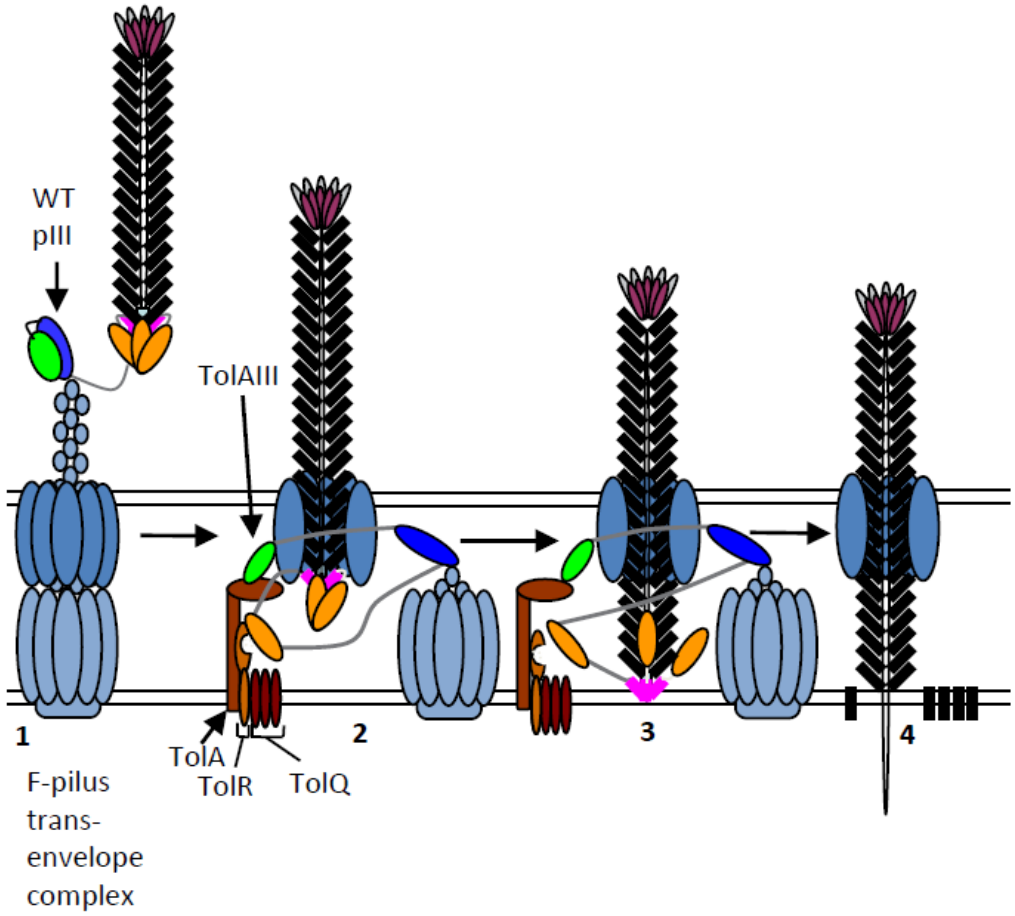

Figure 1.20 : Infection mechanism of E. Coli by Ff phage (Russel, 2004)

Once the single strand phage DNA (+ strand) is injected into the host cytoplasm, synthesis of the negative strand starts. Replication is initiated after the binding of the host RNA polymerase to the negative strand origin of replication. RNA polymerase generates an RNA primer which will be used as a template for the synthesis of the negative strand by the host polymerase III. Once the second strand is synthesized the DNA is called as double-strand (ds) DNA replicative form (RF). PII protein binds to the positive strand origin of replication of the RF and nick the + strand where after rolling circle replication of the + strand is initiated. At the initial step of the viral infection the newly synthesized + strands are used for the synthesis of – strand in the aim of increasing the copy number until about 50 copies of the RF DNA per host cell. Then phage proteins are expressed. The expressed PII, pV and pX proteins are stay in the cytoplasm for assisting to the genome replication and the virus packaging. Proteins pI, pIV and pXI form a transport complex in between the inner and the outer membrane of the host cell. The phages coat proteins pIII, pVI, pVII, pVIII and IX are transported to the inner membrane of the host cell. In the later

step of infection when the amount of pV in dimeric form got sufficient for coating the + strand DNA. The pV coated + strand DNA is brought to the cell membrane wherein the phage is packaged and exported out of the host cell (Figure 1.21) (Rakonjac, 2011; Russel, 2004).

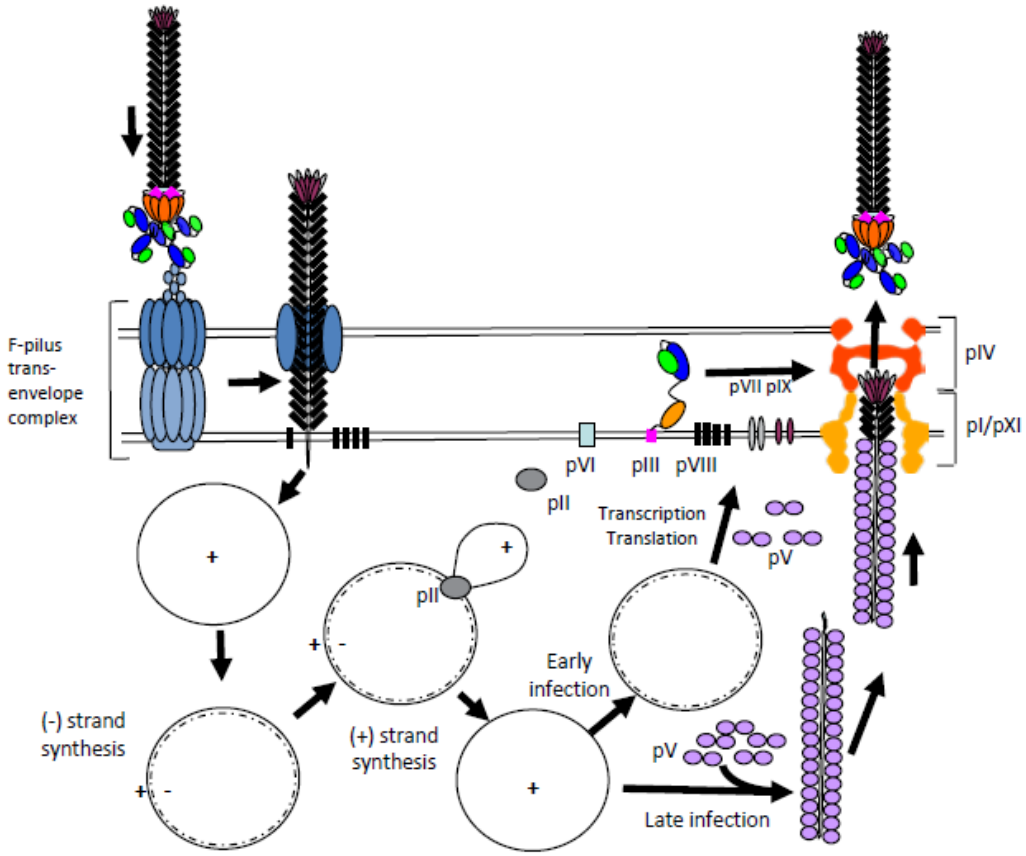

Figure 1.21 : The life cycle of the Ff phage (Rakonjac, 2011).

1.4.2.3 Displaying proteins on the phage surface

Various phages have been used for phage display such as T4 and λ phages (but filamentous bacteriophages are far more beyond because of their stability in a broad range of pH and temperature.

Different coats proteins have been used for displaying proteins and peptides. A heterodimeric protein was expressed on the surface of phage by the fusion of each monomer with either pVII or pIX (Gao, 1999). Also, pVI coat protein served as a display tool as C-terminal fusion system (Jespers, 1996). However, the major coat proteins used for phage display are the pIII and pVIII proteins. These two coat proteins, differing from their copy number, and their size have allowed to display

many peptides and proteins and had open the way for the commercialization of phage display-based systems.

For a proper display of the proteins, a signal sequence which targets the proteins to the inner membrane of the host cell is necessary. This signal sequence is cleaved by a signal peptidase allowing the release of the mature protein into the periplasm. Variable display strategies have been developed. The most commonly used one is the insertion of the protein coding region in between of the signal peptide sequence and the pIII or pVIII N-terminal region (Figure 1.22). The recombinant DNA insert has been also successfully inserted in between of the N- and C- terminal domain of pIII protein without disturbing the infectivity of the phage (Figure 1.22).

Cytosolic proteins have been also displayed on the phage surface. Because these proteins are folded in the cytoplasm, the gene encoding these proteins have been fused either at the c-terminal region of pIII or a Tat signal sequence. The c-terminal region of pIII is in the cytoplasm of host cell during phage propagation. The Tat signal sequence allowsthe translocation of folded proteins trough the inner membrane (Fuh, 2000; Velappan, 2010).

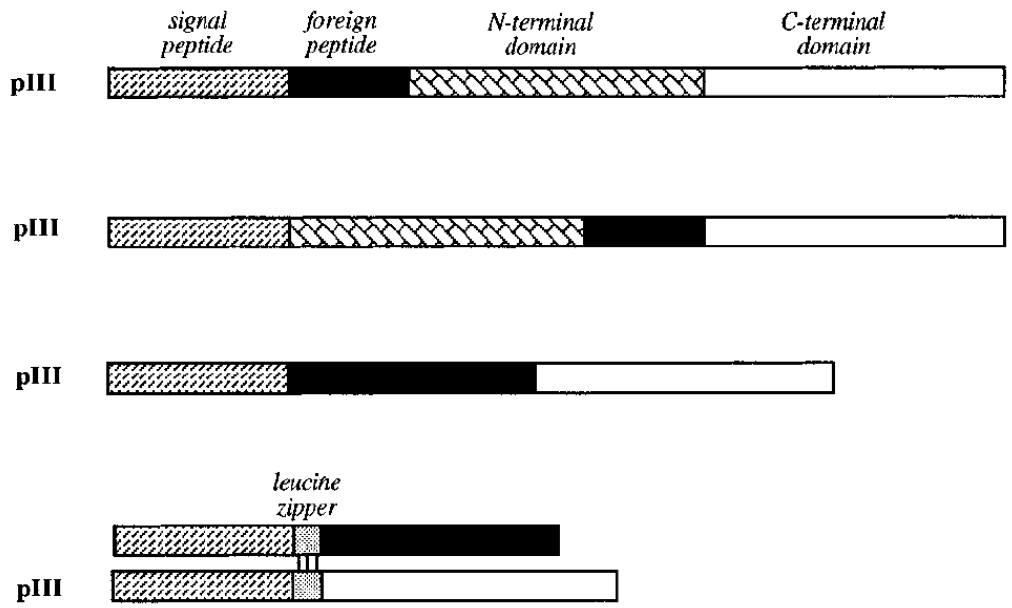

Figure 1.22 : Peptide display strategies (Smith, 1997).

1.4.2.4 Phage display systems

Since phage display technology has appeared, the display methods have changed and evolved according to the need of the protein to be displayed. The major coat proteins

used for displaying are the pIII or pVIII proteins. These two proteins have different advantages or disadvantages related to their copy number and size. The pIII coat protein having three to five copies per phage allows the selection of high-affinity molecules due to its low avidity. However, this stringency in the selection comes out during the selection steps with the loss of some proteins that might have lower binding property but better blocking ability or catalytic activity. In contrary pVIII with its high copy number allows the selection of molecules with lower affinity but increasing the chance of selecting a larger protein panel from the library. The size of the protein to be displayed is another factor to be considered. Due to the steric effects of large molecules, the latter ones cannot be displayed with pVIII proteins. Therefore, pVIII is used for displaying peptides and pIII is used for displaying larger molecules such as Fab or viral proteins such as Hepatitis B virus core antigen (Barbas, 1992; Ozdemir-Bahadir, 2011).

The way that the fusion proteins will be displayed depends according to the strategy used. One of the strategies is to insert the recombinant DNA into the phage genome. Therefore, the protein to be display is expressed theoretically in all the pIII or pVIII copies (Type 3 or type 8) (Figure 1.25) (Smith, 1993). This strategy allows maximum load of the protein to be displayed. However, the size of the filamentous phage particle depends on its genome size, Therefore, the length of the phage increases with the insertion recombinant DNA. If the insert size is too large then, it might destabilize the phage particle or even obstruct the formation of phage particles. However, even displaying peptides on all the 2700 pVIII copies might generate steric effect problem. Therefore, other strategies have been developed such as the 33 or the 88 systems (Figure 1.25). These systems consist on the insertion of a second copy of the pIII or pVIII encoding genes fused with the coding region of the protein to be displayed. The expression of wild-type coat proteins is favorited during the phage infection resulting in a fewer copy of recombinant pIII or pVIII displayed on phage particles.

The systems 3+3 and 8+8 consist of (Figure 1.23) using two copies of the pIII or pVIII genes. One of the genes, is in the wild-type phage (helper phage) genome while the recombinant one is inserted in a “phagemid” (Cesareni, 1988; Mead, 1988). Phagemid carries the origin of replication of E.coli, but also the filamentous phage replication origin allowing it to replicate either as a plasmid in or “a phage” when helper phage infects the phagemid carrying E.coli cell. Two progeny virions are

obtained after infection of helper phage. The first one is a phage particle carrying the wild-type, and the second progeny contains the phagemid both displaying a mixture of wild-type or recombinant coat proteins with a preference to wild-type pIII or pVIII.

Phagemid system, because of its smaller genetic material compared to phage genome, allows better transformation efficiency which is a great problem limiting the diversity of phage display libraries. However, this system has a major drawback due to the very low average of recombinant pIII or pVIII displayed on the phage surface, which is less than one per phage.

Therefore, to increase the copy number of recombinant proteins several modifications have been made. Oh (2007) has inserted an amber mutation into the gene III of helper phage decreasing the expression of wild-type pIII in a suppressor E.coli strains, Therefore, increasing the integration of recombinant pIII. Helper phages with complete deletion of the gene III was also done by several research groups (de Wildt, 2002; Griffiths, 1993). Moreover, recently a helper plasmid has been constructed eliminating the need of helper phage (Chasteen, 2006).

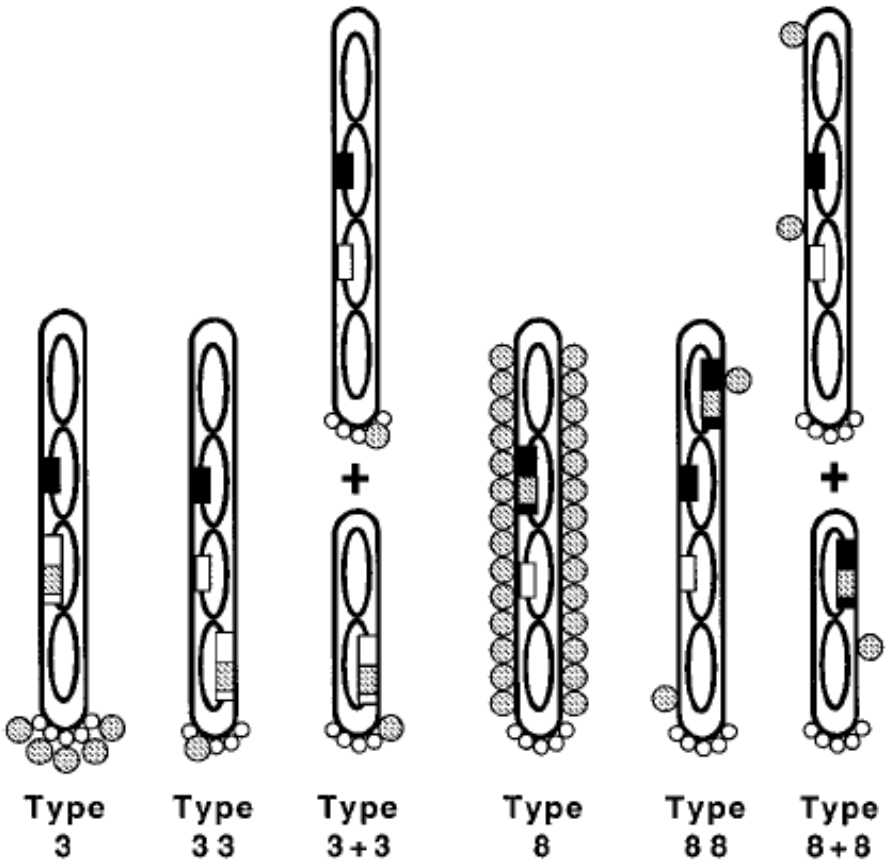

Figure 1.23 : Phage display types (Smith, 1997).

1.4.2.5 Phage display applications

Phage display has been successfully used for the display of different kind of proteins such as Enzymes (Alkaline Phosphatase (Light, 1992; McCafferty, 1991), trypsin (Wang, 1996); glutathione transferase (Widersten, 1995); hormones (human growth hormone (Lowman, 1991; Lowman, 1993); angiotensin (McConnell, 1994); inhibitors (plasminogen activator inhibitor (Pannekoek, 1993; van Meijer, 1996); receptors, (IgE receptor, T cell receptor (Onda, 1995; Scarselli, 1993); ligands, (neurokinin A 53); epitopes and antigens (epitope of malaria parasite Plasmodium falciparum, Hepatitis B virus core antigen (Greenwood, 1991; Ozdemir-Bahadir, 2011); DNA and RNA binding proteins, (zinc finger (Rebar, 1994); enzyme substrates, (protease substrates (Matthews, 1993); cytokines, (interleukin-6 (Cabibbo et al., 1995).

However, the breakthrough of phage display was the display of antibody libraries. The first antibodies displayed on the surface of phages were Fab (Barbas, 1991; Kang, 1991) and single chain Fv fragments (Clackson, 1991). These recombinant antibody structures were generated from B cell mRNA of immunized animals or volunteers and displayed as a fusion with the pIII protein. This technology has allowed the selection of different recombinant antibodies for diagnostic such as ELISA, immunostaining, in vitro and vivo imaging or for therapeutic purposes (Erdag, 2011; Melancon, 2008). Human anti-Human antibodies have been selected by using a pre-immune library (nonimmunized) and used for the development of therapeutic recombinant antibodies (Griffiths, 1993; Zhu, 1998). Human pre-immune antibody libraries have a great advantage because no immunization is necessary. Therefore, a large antigen panel such as toxins, receptors, cytokines enzymes can be screened in-vitro. However, the selected antibodies have low affinity. Various strategies have been applied for increasing the affinity of these antibodies by random mutagenesis or by shuffling variable regions of low-affinity antibodies (Schier, 1996; Thompson, 1996).

Protein-protein interactions are essential for life. Therefore, it is important to determine these interactions. Yeast two-hybrid is the most commonly used technique (Fields, 1989). Phage display technology has been used for the detection of protein-protein interactions by generating cDNA libraries. The main advantage of phage displayed cDNA libraries is the in vitro screening process whereas yeast two-hybrid

is made in vivo. Therefore, the protein panel is restricted with their toxicity to the cells.

In the last few years, phage display technology has been used for the development of vaccines. It is known that phages particles are highly immunogenic. Therefore, phages displaying viral antigens have been used for immunizing various animals wherein phages were used as haptens (Ozdemir-Bahadir, 2011; van Houten, 2010).

1.4.2.6 Random peptide libraries

Antibodies are binding specifically with high affinity to their antigens. The binding is inbetween the Complementary determining regions (CDR) of the antibody and the epitopes of the antigens. Therefore, it has been hypothesized that only few amino acids might be sufficient for binding. Since then random peptide libraries have been attracted the researchers. The greatest impact to the use of random peptide libraries was realized once these libraries have been displayed on phages or cells surfaces (Lee, 2003; Scott, 1990).

The first phage display random peptide library, generated by Scott and Smith (1990), was linear but then disulphide bond constrained peptide libraries have immerged (Vispo, 1993). Since then many different random peptide libraries with various peptide length varying from 4 to 40 amino acids have been generated (Giebel, 1995; McConnell, 1996; Rickles, 1995).

Phage or cell surface displayed random peptides libraries have been used for many different applications. Two Vascular endothelial Growth Factor (VEGF) binding 7-mer peptides with Human umbilical vein endothelial cells proliferation (HUVEC) inhibition ability have been selected from a phage display random peptide library (Erdag, 2007). Also, cancer tissue-specific peptides have been selected by in situ screening of the phage display peptides libraries for targeting the cancer drug doxorubicin to xenotransplanted human breast cancer tissue (Pasqualini, 1996). Peptides specific for cell internalization were identified for in vitro and vivo imaging (Maguire, 2013) but also for targeted gene delivery (Tannous, 2005).

Also, peptides with inorganic material binding ability have been selected from phage display and cell surface display random peptide libraries. These peptides have opened a new vision new in the bionanotechnology field.

1.5 “Self-Assembling Biosensing HBsAg Probes”

ELISA based Hepatitis B virus diagnostic kits are widely used in the world. They consist on recognizing HBsAg, HBcAg, HBeAg and the antibodies generated against these antigens from the blood by using antibodies developed against all of these protein structures. Even if ELISA is a very sensitive assay it has some disadvantages such as ELISA needs two antibodies that recognize the same antigen, but different none overlaying epitopes and in addition of these antibodies must be labeled. Therefore two different antibodies must be developed, and one of them must be labeled which increases the production cost of the kits.

Nowadays, researches are focused on the generation of faster and cheaper diagnosis systems. Studies on Surface Plasmon Resonance (SPR) based diagnosis systems are increasing and the results are getting closer and closer to ELISA results which make SPR based diagnosis systems a rival to ELISA (Elliott, 2001; Vaisocherova, 2009). The main advantages of SPR based systems are the need of developing only one antibody against the target antigen and secondly, SPR is a label-free system which decreases the production cost thus makes this system suitable for diagnosis. In addition, the other advantages are that this system is faster than ELISA, and the binding reaction can be monitored in real time.

SPR sensor technology has become as alternative to ELISA since the improvement in the last decade in terms of surface chemistry, resolution, sampling and data analysis (Homola, 2006). The most important factor to be aware for the development of SPR based biosensors is the binding of biomolecules on the surface of SPR sensor chip. Different immobilization methods for binding proteins on gold coated SPR chips, are used but binding by adsorption or chemical cross-linking for the generation of covalently bonded molecules are the most commonly used methods. Chemical binding consists on coating the gold layer of SPR chips with carboxy-terminated thiol then activating these carboxyl group by using cross-linking agents and binding proteins from their amino groups to the activated carboxyl groups. However, recently some studies have shown that carboxy-terminated thiol molecules are being oxidized which decreases their stability over time. Chemically formed covalent bonds are much stronger bonds compared to the interactions implicated in adsorption, but both methods might cause loss of biological activity of the immobilized proteins due to

unwanted bond formation or adsorption at the active site of the immobilized protein. Therefore, in both cases the orientation of the proteins to be coated can not be controlled. A system allowing the orientation of the coated proteins so that all the binding sites are accessible is, therefore, of key importance. There are some strategies for orienting antibodies like adding a cysteine residue at the very beginning or the very end of proteins in the aim of generating an active site for covalent coupling (Jung, 2007). Also, 11-mercaptoundecanoic acid monolayer coupled G-proteins was used for immobilization (Kausaite-Minkstimiene, 2010). Even tough because of the presence of other Carboxy- or amino- groups within the proteins, the immobilization of the proteins is not very effective.

Phage display (Hoess, 2001; Smith, 1985) and cell surface display (Wittrup, 2001) technologies are two powerful protein or peptide selection methods against an antigen. By using these methods polypeptides able to bind inorganic molecules have been developed. Peptides such as iron oxide (Brown, 1992), zinc oxide (Kjaergaard, 2000), silica (Naik, 2002) binding peptides or peptides binding to noble metals such as gold (Brown, 1997; Sarikaya, 2003), palladium, platinum (Sarikaya, 2004), silver (Naik, 2002) were described in previous studies.

Among noble metals, gold has great advantages for medical nanotechnology purposes. SPR chips can be easily coated with gold, and gold can be linked easily with biomolecules. Furthermore, gold has no toxic effect on cells and for the human body. Finally, gold has unique as Plasmon resonance and light scattering properties. All of these advantages make gold suitable material for *in-vitro* and *in-vivo* diagnosis and the tracking of diseases related proteins by conjugating antibodies to gold nanoparticles. Therefore, peptides binding plain gold have a great potential for being used as an immobilizing molecule on gold coated sensor chips. A peptide with gold binding ability (GBP1) was selected by cell display technology (Brown, 1997). GBP1 was composed of 14 amino acids (MHGKTQATSGTIQS) with no cysteine amino in it, which is known to make thiol bonds with gold. It was demonstrated by Brown and its co-worker in year 2000 that a polypeptide composed by the three-time repeat of GBP1 (3R-GBP1) was binding better than GBP1 itself. The binding specificity of 3R-GBP1 to gold and not to the other noble metal was demonstrated, and its binding affinity was calculated by Quartz-Crystal Microbalance (QCM) (Tamerler, 2006).

Phage display was also used as a carrier for eliciting an immune response in animal models because of their high immunogenic and their naturally immuno-stimulatory properties (Irving, 2002; Wang, 2004; Willis, 1993). In addition, it was used for the selection of recombinant antibodies such as Fab or single chain variable fragment or the selection of peptides (Benhar, 2001; Erdag, 2003; Erdag, 2007; Rosander, 2002; Smith, 1997). Recombinant antibodies, such as Fab and scFv, were developed against HBsAg in different works (Ayala, 1995; Barbas, 1991).

In this study, an accurate label-free HBsAg detecting system was foreseen. According to the information given above, an SPR based biosensor was chosen as the most appropriate device for this purpose. A recombinant antibody (scFv) developed against HBsAg was selected as the most appropriate biosensing probe because of its smaller size compared to a whole antibody and also because the genetic material encoding the scFv is easily accessible. The immobilization strategy was chosen according to three criteria; strong immobilization on gold, no need of any chemical coupling and correct orientation of the scFv on the sensor chip. Therefore, an adequate system was to use a fusion protein with a scFv as biosensing probe and a gold binding peptides as an immobilization structure (Figure 1.24).

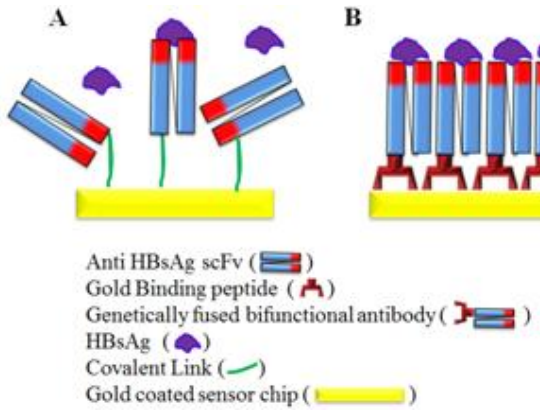

Figure 1.24 : Chemically immobilized (A) and self-assembled oriented (B) scFv.

For this purpose, a scFv against HBsAg will be developed by using phage display technology. First, a scFv library will be generated from the spleen mRNA of mice immunized with HBsAg displaying phages. The scFv with HBsAg binding ability will be selected by biopanning. Then the scFv encoding gene will be fused with GBP1 encoding gene and the fusion construct will be cloned into pQE2 expression vector. The gold binding bifunctional scFv will be expressed and tested using SPR for its potential as a biosensing probe.

2. MATERIALS AND METHODS

2.1 Materials

2.1.1 Strains

2.1.1.1 Bacterial strains genotype

- *Escherichia coli* **DH5α strain:** (F^- 80d*lac*Z M15 (*lac*ZYA-*arg*F) U169 *rec*A1 *end*A1*hsd*R17(r_k^-, m_k^+) *pho*A*sup*E44 $^-$*thi*-1 *gyr*A96 *rel*A1)
- *Escherichia coli* **TG1 strain:** K12 *Δ(lac-pro) supE thi hsdΔ5/F'* [*traD36 proAB* $LacI^q$ *lacZΔM15*], Amersham Biosciences Cat. No.
- *Escherichia coli* **HB2151 strain:** K12 *Δ(lac-pro) ara* nal^r *thi/F'* [*proAB* $lacI^q$ *lacZΔM15*], Amersham Biosciences Cat. No.
- *Escherichia coli* **BL21 Star™ (DE3) strain:** *F- ompT hsdSB (rB-mB-) gal dcm rne131* (DE3), Invitrogen Cat. No. C6010-03.
- *Escherichia coli* **M15[pREP4] strain:** , Qiagen Cat. No. 34210.

2.1.1.2 Mouse strain

BALB/cJ mice were obtained from the Animal Genetics and Reproduction Biology Laboratory of the TUBITAK Marmara Research Center, Genetic Engineering and Biotechnology Institute, Turkey. Animal studies were approved by the Ethics Committee of the Genetic Engineering and Biotechnology Institute, TUBITAK Marmara Research Center.

2.1.1.3 Mammalian cell lines

HeLa, Hek293 Trex, HepG2 and COS7 cells lines were provided from ATCC.

2.1.2 Vectors

The information regarding the vectors pCANTAB5E, pQE2 and pDUCK1 is given in appendix A.

2.1.3 Primers

The primer list is given in appendix B. The design of the primers was performed with the help of the San Diego Supercomputer Center (SDSC) Biology Workbench Internet website.

2.2 Methods

2.2.1 Development of an anti-HBsAg single chain Fv recombinant antibody

2.2.1.1 Cloning of HBsAg in phagemid vector

The plasmid construct containing the HBsAg coding gene was kindly provided by Assoc. Prof. Mehmet Yapar of the Virology Department from Gulhane Military Medical Faculty, Gulhane Military Medical Faculty (GATA) (Kubar, 1988). Hepatitis B Surface antigen gene was amplified by PCR using primers HBsAg_SfiI_For and HBsAg_NotI_Rev containing Sfi I and Not I restriction enzyme sites, respectively. The PCR reaction was prepared as following (Table 2.1):

Table 2.1 : PCR reaction for HBsAg amplification.

Reagents	**Volume**	**Final concentration**
dH_2O	34µL	
10X reaction buffer (Roche)	5 µL	1X
25 mM $MgCl_2$	3 µL	2.5mM
10 mM dNTP each	1 µL	10 pmol
10 pmol HBsAg for. primer	2 µL	20 pmol
10 pmol HBsAg rev. primer	2 µL	20 pmol
HBsAg gene containing plasmid	2 µL	100ng
1U Taq DNA polymerase (Roche)	1 µL	1U
TOTAL	50 µL	

The PCR reaction was run as following 94 ºC, 1min, 55 ºC, 2min,, 72 ºC, 2 min for 30 cycles, with an elongation step of 10 min at 72ºC in Biometra T3000

Thermocycler (Germany). The PCR products were run on 1,2 % Agarose gel at 80V. An agarose gel of 1.2% was prepared by melting 0.6 gr of agarose (Sigma, Katalog no: A5304) in 50 mL of 0.5X TAE buffer (24,2gr Tris Base, 5.7 mL Glacial Acetic acid, 5mM EDTA, pH 8.3) in the microwave and 1.3 µL of 10 mg/mL Ethidium bromide (Sigma E7637) was added in the melted Agarose. The electrophoresis was performed in 0.5X TAE Buffer for 40 minutes at 80V (BioRad, Power Pac 300). The PCR bands were visualized with the Gel Doc 2000 system under UV light. PCR products were cut from the agarose gel and purified according to the instruction manual of the agarose gel DNA extraction kit (Roche, Cat. No. 1 696 505).

The PCR products and the pCANTAB5E vector were first digested with Sfi I at 50ºC in the heat block (Techne, DB-2D) for 3 hours (Table 2.2).

Table 2.2 : SfiI digestion reaction.

Reagents	**PCR product**	**Vector**	**Final concentration**
dH_2O	16µL	16µL	-
10X reaction buffer M (Takara)	3 µL	3 µL	1X
DNA (100ng/µL)	10µL	10µL	10 µg
10U/µL Sfi I enzyme (Roche)	1 µL	1µL	10 U
TOTAL	30 µL	30µL	-

The digestion products were loaded on 1,2 % agarose gel and electrophoresis was performed at 80 V. The digestion products were extracted with the agarose gel DNA extraction kit (Roche, Cat. No. 1 696 505) according to the manufacturer instructions. The purified SfiI digestion products were then subjected to NotI digestion (Table 2.3). The NotI digestion was incubated 3 hours at 37Cº. The digestion products were agarose gel extracted (Roche, Cat. No. 1 696 505).

Table 2.3 : NotI digestion reaction.

Reagents	**PCR product**	**Vector**	**Final concentration**
dH_2O	1µL	1µL	-
10X reaction buffer H (Takara)	3 µL	3 µL	1X
Sfi I digestion product	25µL	25µL	-
10U/µL Not I enzyme (Roche)	1 µL	1µL	10U
TOTAL	30 µL	30µL	-

SfiI/NotI digested HBsAg PCR product, and the pCANTAB5E phagemid vector were ligated with T4 DNA ligase (Fermentas) at 16ºC overnight, the enzyme was heat inactivated at 72ºC for 5 minutes. The reaction mixture was prepared as mentioned below (Table 2.4).

Table 2.4 : Ligation reaction.

Reagents	**1:3 ratio**	**1:6 ratio**
dH_2O	38µL	38µL
10X ligation buffer (Fermentas)	5 µL	5 µL
Sfi I/ Not I digested PCR product	1µL (100 ng)	1µL (200 ng)
Sfi I/ Not I digested vector (200ng)	5µL	5µL
T4 DNA ligase (2,5U/µL)	1 µL	1µL
TOTAL	50 µL	50µL

The ligation product was transferred by Calcium chloride method into chemically competent *E.coli* TG1 cells (Pharmacia, The Netherlands). The transformation reaction was performed according to Maniatis (1982). Ligation product completed to 50 µL with 50mM Tris pH 7.2 was mixed with 300 µL of *E.coli* TG1 competent cells in glass culture tube and incubated for 1 hour on ice. Then the mixture was incubated for 3 minutes at 42ºC followed by 10 minutes of incubation at room temperature. LB medium (1mL) was added to the transformation product and bacteria were incubated at 37ºC for 1 hour at 220 rpm in an incubator shaker (Innova, 4230 Refrigerated incubator shaker). After that time, 200µL of the transformation product was taken and spread on LB/Agar/Ampicillin (100µg/mL) plate. The plate was incubated overnight at 37ºC (Innova). The remaining transformation product was poured in 50 mL of LB containing Ampicillin (100µg/mL) and incubated overnight at 37ºC at 220 rpm (Innova, 4230 Refrigerated incubator shaker).

The presence of HBsAg coding gene in bacteria colonies was controlled by colony PCR. Cells picked from colonies were suspended in 15 µl distilled water. Tubes were incubated at 95°C for 3 minutes and centrifuged; the upper fluid was used as a template for polymerase chain reaction. Primers specific to the cloning region of pCANTAB5E vector were used as forward and reverse primers. The PCR reaction was prepared as following (Table 2.5).

Table 2.5 : Colony PCR reaction for HBsAg.

Reagents	Volume	Final concentration
dH_2O	34µL	
10X reaction buffer (Roche)	5 µL	1X
25 mM $MgCl_2$	3 µL	2.5mM
10 mM dNTP each	1 µL	10 pmol
10 pmol pCANTAB5E For	2 µL	20 pmol
10 pmol pCANTAB5E Rev	2 µL	20 pmol
Supernatant of bacterial lysates	2 µL	-
1U Taq DNA polymerase (Roche)	1 µL	1U
TOTAL	50 µL	

The PCR reaction was run as following 94ºC, 1min, 55ºC, 2min, 72ºC, 2 min for 30 cycles, with an elongation step of 10 min at 72ºC in Biometra T3000 Thermocycler (Germany). The PCR products were run on 1.2% Agarose gel at 80V.

One *E.coli* colony containing the plasmid of interest was selected for further DNA sequencing. For this purpose the selected colony was inoculated in 5 mL LB medium containing 100 µg/mL Ampicillin and incubated overnight at 37ºC, then plasmid isolation was performed by using Roche High pure plasmid isolation kit (Cat. No. 11754777 001). The purified plasmids were used as a template for DNA sequencing. Sequencing reactions were done according to the Beckman coulter Genome Lab DTCS quick start kit protocol (Beckman Coulter, Cat. No. 608120). Primers HBsAg sequencing primer For and HBsAg sequencing primer Rev were used respectively for forward and reverse sequencing. The reactions were prepared in thin wall 0,2mL tubes as mentioned in Table 2.6.

Table 2.6 : DNA sequencing reaction.

Reagents	PCR product
DTCS	8 µL
Template (400ng)	4 µL
Primer (1,6pmol/µL)	2 µL
Distilled water	6 µL
TOTAL	20 µL

The 30 cycles DNA sequencing PCR reaction was run as following 96°C for 20 sec, 50°C for 2 min and 60°C for 4 min in Biometra T3000 Thermocycler (Germany). The reactions were terminated by adding 5 µL of stop solution (2 µL of 3M Sodium

Acetate (pH 5.2), 2 µL of 100 mM Na2-EDTA (pH 8.0) and 1 µL of 20 mg/mL of glycogen) to each reaction tubes. The sequencing reaction products were then purified by alcohol precipitation. The air dried pellets were dissolved in 40 µL of Sample Loading Solution (Beckman Coulter) and loaded to Dye Terminator cycle sequencing automated sequencing system CEQ8800. The reaction program used for sequencing was lfr-a program (Capillary: 50ºC, Denaturation: 90ºC for 2 minutes, Injection: 2.0 kV for 15 seconds, Separation: 4.0 kV for 110 minutes). The DNA sequences were then uploaded to the SDCD Biology Workbench Internet website (Url-2), where multiple alignments, database searches and protein translations were conducted.

2.2.1.2 Production of HBsAg displaying phages and phage ELISA

Wild-type phages and phage-displayed HBsAg were produced by M13K07 helper phage infection. For this purpose a single transformant *E. Coli* TG1 colony containing the wild-type phagemid or the correct HBsAg gene insertion were selected and were cultured overnight at 37°C at 220 rpm in 2xTY (16.0 gr bacto-tryptone, 10.0 gr yeast extract, 5.0 gr NaCl) containing 100 µg/mL ampicillin and 2% glucose. The next day overnight cultures were inoculated in 50 mL of 2xTY containing 100 µg/mL ampicillin and 2% glucose and cells were grown at 37°C at 220 rpm until the OD_{600} reached 0.5. Then 10 mL of the culture was added into 50 mL fresh 2xTY medium containing 100 µg/mL ampicillin and 2% glucose, and finally 10^{10} M13KO7 helper phages were added to the culture. After 45 min of incubation at 37°C without agitation and 45 min at 37°C with agitation (220rpm), cells were harvested for 10 min at 3,000×g. The cells were resuspended in the same volume of 2xTY containing 100 µg/mL ampicillin and 50 µg/mL kanamycin and grown at 30°C overnight with agitation (220 rpm). The next day cells were harvested at 8,000g and the supernatants containing either the recombinant or the wild-type infective phages were precipitated at 4°C by adding ¼ of the supernatant volume of polyethylene glycol-6000 (1M PEG 6000, 2.5M NaCl). After 2 hours of incubation on ice phages were centrifuged at 12000 rpm for 40 minutes. The pellet containing phage particles were resuspended in 1 mL of phosphate buffer saline (PBS; 3.2 mM $Na_2HPO_4 \times 2H_2O$, 1.4 mM KH_2PO_4, 2.7 mM KCl and 137 mM NaCl) and the suspension was centrifuged for 10 minutes at 4000 rpm for pelleting residual cells.

The supernatant containing the phages was transferred into a new tube. The purified phage particles were then filter sterilized with Millex-HV (Millipore) for further experiments. The number of infective phages produced was determined by the phage plaque counting assay. A single colony of *E. coli* TG1 was inoculated into 5mL of 2xTY and grown overnight at 37°C at 220 rpm. The next day overnight culture was inoculated (50µL) in 5mL of 2xTY and bacteria were grown at 37°C until mid-log phase (OD_{600} of 0.5-0.8). Then 100 µL of culture was infected with 10µL of serial phage dilutions (10^{-6}, 10^{-8} and 10^{-10}) for 30 min at 37°C. Infected bacteria were spread on 2xTY agar plates containing 100µg/mL Ampicillin and incubated overnight at 37°C. The next day colonies were counted and translated to colony forming units (CFU) per mL.

The binding property of HBsAg displayed on the phage surface was tested by Phage ELISA. Two different ELISA methods have been used to detect the HBsAg displayed on phage particles. Each assay was conducted in triplicate. In the first method, ELISA well plates were coated overnight at +4°C with either 10^{10} HBsAg displaying or wild-type phage particles. The next, day the wells were washed 6 times with TPBS (PBS containing 0.1% Tween 20) and then blocked for 2 hours at room temperature with TPBS containing 1% BSA. The wells were washed 6 times with TPBS. Polyclonal anti-HBsAg rabbit antibody (1/200), as primary antibody, was incubated for 1 hour at room temperature. The wells were then washed again 6 times with TPBS and goat anti-rabbit alkaline phosphatase (Thermo Scientific) conjugate (1/1000) was used as secondary antibody. After one hour of incubation at room temperature the wells were washed 6 times with TPBS and *para*-nitrophenyl phosphate substrate (PNPP) solution (1 mg/mL of pNPP in substrate buffer (0,1 M glycine, 1mM ZnCl2, 1mM MgCl2, pH: 10,4) was used as a chromogen. The absorbance was measured one hour later at 405 nm using an ELISA reader (Bio-Rad) after stopping the reaction with 1 M NaOH.

In the second method, ELISA well plates were coated overnight at 4ºC with anti-HBsAg polyclonal antibody (1/200). The next day wells were washed 6 times with TPBS and then blocked with TPBS containing %1 BSA. Wells were washed 6 times with TPBS, phage particles (10^{10}) displaying HBsAg, or wild-type phage was then added to each well. After one hour of incubation at room temperature wells were washed 6 times with TPBS and mouse anti-M13 horseradish peroxidase (GE Healthcare) conjugate (1/1000) was used as secondary antibody. The absorbance was

measured at 410nm using a microplate reader (Bio-Rad) after a 2,2'- azino-bis (3-ethylbenzothiazoline-6-sulphonic acid) (ABTS) substrate solution (1 mg ABTS in 4.5 mL 50mM citric acid (pH=4) containing %0.05 H_2O_2).

2.2.1.3 Mouse Immunization and ELISA from immunized mice sera

Immunization assays were conducted with 8-week-old male immunocompetent BALB/cJ mice. Six different mice groups containing 3 mice each were subjected to different injections without any adjuvant. The first 3 groups received 300 µL of different concentrations of phage displaying HBsAg (10^{10}, 10^{11} and 10^{12} phage particles diluted in PBS). The fourth and fifth groups received 10^{11} or 10^{12} phage particles without HBsAg in 300 µL of PBS. The mice in group 6 received 300 µL of PBS as control. Each group was constituted of 2 mice except group five and six where only one mouse was used. All the immunizations were performed in triplicate at 3-week intervals. Intradermal injections were conducted using 50 µL under each front leg and 100 µL under each back leg pit). Blood samples were collected from the tail of each mouse before each injection; the last bleed was performed 4 days after the last injection. Blood samples were centrifuged, and the supernatants were used for ELISA assays.

ELISA plates were coated overnight with 200 ng of HBsAg (Ad/Ay, 100 ng each) (Fitzgerald Industries International) in coating solution (0.1N NaHCO3). Wells were washed 6 times with TPBS (0,1 % PBS-Tween 20) and then blocked with TPBS containing %1 BSA. The wells were washed 6 times with TPBS, mice sera (1/50) were then incubated for 1 hour at room temperature. Wells were washed 6 times with TPBS and goat anti-mouse HRP conjugate (1/1000) (Thermo Scientific) was added and incubated for 1 hour at room temperature. Following 6 times of washing with TPBS, ABTS substrate solution was added then the absorbance was measured at 410 nm after 1 hour of incubation with an ELISA Reader (Bio-rad).

2.2.1.4 Statistical analysis

The IBM SPSS Statistics (SPSS), version 17 for Windows was used for statistical analysis. The differences in BALB/cJ mice humoral immune response between groups were analyzed using mixed model ANOVA with Tukey post hoc test. A significant difference between groups and within groups at different injection periods

was analyzed using univariate General Linear Model with Tukey post hoc test. P values of <0.05 were considered statistically significant.

2.2.1.5 Construction of a recombinant antibody library

The construction of a single chain variable fragment (ScFv) recombinant antibody library necessitate B cells mRNA extracted the spleen of immunized mouse. Therefore, the spleen of mice immunized with HBsAg were collected and were homogenized (Janke & Kunkel Ika Werk RW20) according to the EZ-RNA Total RNA Isolation Kit (Biological Industries, Israel) protocol. The purified total RNA was dissolved in 100µL of DEPC treated dH_2O at 55°C for 15 min. The RNA quality was controlled according to the OD_{260} / OD_{280} ratio.

After the isolation of total RNA, Hexamer primer based standard method (Samsbrook, Cold Spring Harbor Laboratory Press 1989, second edition) was used to generate a cDNA library from mRNA. The cDNA library was used as a template for the amplification of immunoglobulin heavy and light chain variable regions by PCR.

Heavy chain variable region (V_H) amplification was performed in a total volume of 50µL containing 5 µL Taq polymerase buffer (10X); 3 µL $MgCl_2$ (25 mM); 1 µl dNTP/10 mM of each, 2 µl of each heavy chain primers (primer 701 and 702), 2 µl of template cDNA, 1 µL of Taq polymerase enzyme (1U /µl) (Fermentas). A similar PCR reaction was made for the amplification of the Light chain variable region (V_L) and the linker region except that the primers used were different, primers 703 and 704 for V_L and primers 422 and 423 for the linker region. The PCR program for the amplifications was set to 5 minutes of incubation at 94°C and 30 cycles, each cycle corresponding to 1 min at 94°C, 2 minutes at 55°C and 2 minutes at 72°C with an elongation step at 72°C for 10 minutes. PCR products were controlled on 1.5% agarose gel then extracted from the gel with the agarose gel DNA extraction kit (Roche, Cat. No. 1 696 505) according to the manufacturer instructions.

The construction of the scFv library was carried out with two successive PCR reactions. The first stage consisted of the assembly of variable light and heavy chain PCR products via the linker coding region. The 50 µL reaction was set up with 5 µL of Taq polymerase buffer (10X); 3 µL of $MgCl_2$ (25 mM); 1 µl of dNTP/10 mM from each, 3 µl V_H PCR product (100ng/µl), 3 µl V_L PCR product (100 ng/µl), 1 µl linker PCR product (100ng/µL) , 1 µL of Taq polymerase enzyme (1U/µl)

(Fermentas). The reaction was performed as follows: 1 min at 94 °C, 4 min at 63 °C for a total of 7 cycles. The second PCR reaction was run as soon as the first reaction was terminated by adding to the first reaction tube 50 µl of mixture containing 5 µl Taq polymerase buffer (10X), 3 µl $MgCl_2$ (25 mM), 1 µl dNTP/10 mM from each , 2 µl of primers 702 and 704, 1 µL of Taq polymerase enzyme (1U /µl) (Fermentas). The second reaction was set up to 25 cycles of 1 min at 94°C, 2 min at 55°C, 2min at 72 °C with an elongation step of 10 min at 72°C. The scFv library was controlled on 1.2 % agarose gel.

Once the scFv library was obtained, SfiI and NotI restriction enzymes sites were integrated respectively at the 5' and 3' ends of the scFv library by PCR. The integration reaction was performed in 50µL total volume containing 5 µL Taq polymerase buffer (10X); 3 µL $MgCl_2$ (25 mM); 1 µl of dNTP/10 mM of each, 2 µl of 702 primer with SfiI restriction enzyme site and 704 primer with NotI restriction enzyme site, 2 µl of template cDNA, 1 µL of Taq polymerase enzyme (1U /µl) (Fermentas). Then the reaction was set up to 30 cycles of 1 min. at 94°C, 2 min at 55°C, 2 min at 72°C with an elongation step of 10 min at 72°C. The PCR products were controlled on 1.2 % agarose gel.

The scFv library cloning procedure was the same as the cloning of HBsAg described previously. The PCR product and the pDUCK1 phagemid vector were first digested with Sfi I and NotI, the digestion products were extracted from agarose gel with the agarose gel DNA extraction kit (Roche, Cat.No. 1 696 505) then ligated to each other with T4 DNA ligase (Fermentas). The ligation products were transferred into chemically competent *E.coli* TG1 cells (Pharmacia, The Netherlands) by calcium chloride transformation (Maniatis et al., 1982). The presence of scFv library was controlled by colony PCR using the same primers as pCANTAB5E vector.

2.2.1.6 Selection of an anti-HBsAg scFv from the library

The scFv phage library was produced as mentioned in section 2.2.1.2. Briefly, the scFv library containing cell mixture was grown overnight at 37°C at 220 rpm in 2xTY (16.0 gr bacto-tryptone, 10.0 gr yeast extract, 5.0 gr NaCl) containing 100 µg/mL ampicillin and 2% glucose. The next day overnight cultures were inoculated in 50 mL of 2xTY containing 100 µg/mL ampicillin and 2% glucose and cells were grown at 37°C at 220 rpm until the OD600 reached 0.5. Then 10 mL of the culture

was added into 50 mL fresh 2xTY medium containing 100 μg/mL ampicillin and 2% glucose and finally 10^{10} M13KO7 helper phages (New England Biolabs) were added to the culture. After 45 min of incubation at 37°C without agitation and 45 min at 37°C with agitation (220rpm), cells were harvested for 10 min at 3,000×g. The cells were resuspended in the same volume of 2xTY containing 100 μg/mL ampicillin and 50 μg/mL kanamycin and grown at 30°C overnight with agitation (220 rpm). The next day cells were harvested at 8,000g and the supernatants containing either the recombinant or the wild-type infective phages were precipitated at 4°C by adding ¼ of the supernatant volume of polyethylene glycol-6000 (1M PEG 6000, 2.5M NaCl). After 2 hours of incubation on ice phages were centrifuged at 12000 rpm for 40 minutes. The pellet containing phage particles were resuspended in 1 mL of phosphate buffer saline (PBS; 3.2 mM Na2HPO4 × 2H2O, 1.4 mM KH2PO4, 2.7 mM KCl and 137 mM NaCl) and the suspension was centrifuged for 10 minutes at 4000 rpm for pelleting residual cells. The supernatant containing the phages was transferred into a new tube. The purified phage particles were then filter sterilized with Millex-HV (Millipore) for further experiments. The concentration of phage particles in the developed phage-displayed library was determined by the phage plaque counting assay. A single colony of E. coli TG1 was inoculated into 5mL of 2xTY and grown overnight at 37°C at 220 rpm. The next day overnight culture was inoculate (50μL) in 5mL of 2xTY and bacteria were grown at 37°C until mid-log phase (OD600 of 0.5-0.8). Then 100 μL of culture was infected with 10μL of serial phage dilutions (10-6, 10-8 and 10-10) for 30 min at 37°C. Infected bacteria were spread on 2xTY agar plates containing 100μg/mL Ampicillin and incubated overnight at 37°C. The next day colonies were counted and translated to colony forming units (CFU) per mL.

The selection of anti-HBsAg antibody from the phage-displayed library was done by Biopanning. Immunomaxisorb tube was coated with 500 ng of HBsAg (Ad/Ay, 250 ng each, Fitzgerald Industries International) in coating solution (0.1N NaHCO3) overnight at 4°C. The next day the tube was washed 3 times with PBS containing 0.1% Tween (TPBS) then blocked with TPBS containing 1%BSA for 2 hours at room temperature. The tube was then washed 3 times with TPBS. The phage-displayed library (500μl containing 10^{11} phage particles) was added to the tube and incubated 2 hours at room temperature. After the incubation, the tube was washed 30 times with PBS then 30 times with TPBS. The phages bound to the tube were then

incubated for 30 min at 37°C with 500 µl of *E.coli* TG1 cells (OD_{600} 0.5) for infection. The infected cells (100µl) were spread on LB agar plates containing ampicillin (100 µg/mL) and incubated overnight at 37°C. The next day all the colonies were counted then collected in one tube with a scrapper. The cell mixture was used for the generation of a new phage library enriched against HBsAg by the same phage amplification procedure as mentioned at the beginning of this section. The new phage-displayed titer was calculated then used for a second round of biopanning. After 2 biopanning rounds, each colony from the infection plate were separately subjected to phage amplification then their titer was calculated.

The binding property of each clone to HBsAg was tested by Phage ELISA. ELISA well plates were coated overnight at 4ºC with HBsAg (Ad/Ay, 100 ng each, Fitzgerald Industries International). The next day wells were washed 6 times with TPBS and then blocked with TPBS containing %1 BSA. Wells were washed 6 times with TPBS, phage particles (10^{10}) were then added to each well. After one hour of incubation at room temperature wells were washed 6 times with TPBS and mouse anti-M13 horseradish peroxidase (GE Healthcare) conjugate (1/1000) was used as secondary antibody. The absorbance was measured at 410nm using a microplate reader (Bio-Rad) after a 2,2'- azino-bis (3-ethylbenzothiazoline-6-sulphonic acid) (ABTS) substrate solution (1 mg ABTS in 4.5 mL 50mM citric acid (pH=4) containing %0.05 H_2O_2).

2.2.2 Development and characterization of an anti-HBsAg gold binding recombinant antibody

The strategy selected for cloning experiments are as indicated in Figure 2.1. The pQE2 multiple cloning site is indicated in Figure 2.1 A, the Lig7 scFv will be first cloned into the pQE2 vector (Figure 2.1 B) then the GBP-1 and the GBP-1 and the repeated GBP-1 sequences will be cloned into the Lig7/pQE2 vector (Figure 2.1 C).

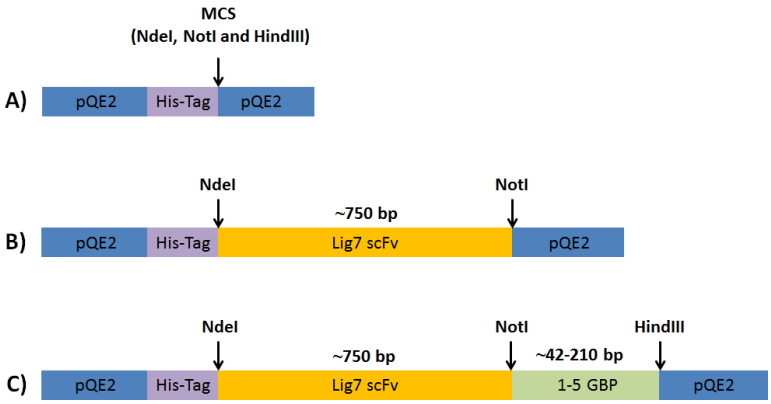

Figure 2.1 : Cloning strategy.

2.2.2.1 Cloning of the anti-HBsAg Lig7 recombinant antibody into pQE2 vector

The anti-HBsAg Lig7 scFv present in the pDUCK1 phagemid vector was recloned into the pQE2 (Qiagen) vector. For this purpose, the Lig7 scFv was amplified by PCR using Lig7_Forw_NdeI and Lig7_Rev_NotI primers including the NdeI and NotI restriction enzyme sites. The reaction was set up as following (Table 2.7);

Table 2.7 : Lig7 PCR amplification reaction.

Reagents	**Volume**	**Final concentration**
dH_2O	34µL	
10X reaction buffer (Roche)	5 µL	1X
25 mM $MgCl_2$	3 µL	2.5mM
10 mM dNTP each	1 µL	10 pmol
10 pmol Lig7_Forw_NdeI	2 µL	20 pmol
10 pmol Lig7_Rev_NotI	2 µL	20 pmol
plasmid 100ng/µL	2 µL	200 ng
1U Taq DNA polymerase (Roche)	1 µL	1U
TOTAL	50 µL	

The PCR reaction was run as following 94 ºC, 1min, 55 ºC, 2min, 72 ºC, 2 min for 30 cycles, with an elongation step of 10 min at 72ºC in Biometra T3000 Thermocycler (Germany). The PCR products were run on 1,2 % Agarose gel at 80V. The amplified PCR fragments and the pQE2 vector were first digested with NotI (Fermentas) then extracted from agarose gel (1.2%). The digestion products were

then digested with NdeI (Fermentas) enzyme. Both digestions were run for 3 hours at 37ºC, the digestion reactions are indicated below (Table 2.8 and Table 2.9):

Table 2.8 : NotI digestion of Lig7.

Reagents for NotI digestion	**PCR product**	**Vector**	**Final concentration**
dH_2O	16µL	16µL	-
10X reaction buffer	3 µL	3 µL	1X
DNA (100ng/µL)	10µL	10µL	10µg
10U/µL NotI	1 µL	1µL	10U
TOTAL	30 µL	30µL	-

Table 2.9 : NdeI digestion of Lig7.

Reagents for NdeI digestion	**Digested PCR product**	**Digested Vector**	**Final concentration**
dH_2O	-	-	-
10X reaction buffer	3 µL	3 µL	1X
DNA (100ng/µL)	26µL	26µL	-
10U/µL NdeI	1 µL	1µL	10U
TOTAL	30 µL	30µL	-

The agarose gel extracted NotI and NdeI double digested products were ligated with T4 DNA ligase (Fermentas, Sweden), the 50 µL reaction was prepared (Table 2.10) and the reaction mixture was incubated overnight at 16ºC. The ligase was inactivated by treating the mixture at 72ºC for 5 minutes.

Table 2.10 : Ligation of Lig7 into pQE2.

Reagents	**1:3 ratio**	**1:6 ratio**
dH_2O	38µL	37µL
10X ligation buffer (Fermentas)	5 µL	5 µL
Sfi I/ Not I digested PCR product	1µL (100 ng)	2µL (200 ng)
Sfi I/ Not I digested vector (200ng)	5µL	5µL
T4 DNA ligase (2,5U/µL)	1 µL	1µL
TOTAL	50 µL	50µL

The ligation products were transferred into chemically competent *E.coli* DH5α cells by calcium chloride method according Maniatis et al. (1982). The transformed cells were spread on LB/Agar/Ampicillin (100μg/mL) plates and incubated overnight at 37ºC (Innova). The remaining transformation product was poured in 50 mL of LB containing Ampicillin (100μg/mL) and incubated overnight at 37ºC at 220 rpm (Innova, 4230 Refrigerated incubator shaker). The presence of the Lig7 scFv encoding gene was controlled by colony PCR. The reaction was set up as mentioned before. Plasmid isolation was made from the colony PCR positive clones by using Roche High pure plasmid isolation kit (Cat. No. 11 754 777 001) according the manufacturer instructions. The presence of Lig7 scFv in the pQE2 vector was confirmed with DNA sequence analysis by using Beckman coulter Genome Lab DTCS quick kit.

2.2.2.2 Insertion of gold binding peptide coding region in the Lig7/pQE2 vector

The amplification of the gold binding peptide encoding gene was made PCR using specific primers with NotI and HindIII restriction enzyme sites (Table 2.11). For this purpose GBP_forward_NotI_with tail and GBP_reverse_HindIII_ with tail primers were used. The reaction was set up as following;

Table 2.11 : PCR reaction for the amplification of GBP.

Reagents	**Volume**	**Final concentration**
dH_2O	34μL	
10X reaction buffer (Qiagen)	5 μL	1X
10 mM dNTP each	1 μL	10 pmol
10 pmol GBP_forward_NotI_with_tail	2 μL	20 pmol
10 pmol GBP_reverse_HindIII_with_tail	2 μL	20 pmol
plasmid (Lig7/pQE2) 100ng/μL	2 μL	200 ng
1U HotStart Taq DNA polymerase (Qiagen)	1 μL	1U
TOTAL	50 μL	

The PCR reaction was run as following 94 ºC, 1min, 55 ºC, 2min, 72 ºC, 2 min for 30 cycles, with an elongation step of 10 min at 72ºC in Biometra T3000 Thermocycler (Germany). The PCR products were run on 2 % Agarose gel at 80V.

The half of the PCR product was purified with QIAquick PCR purification kit (Qiagen, Cat.No. 28106) according to the manufacturer instructions. Briefly, the PCR product was mixed with 5 volume of PB buffer, then the mixture was poured into the QIAquick column. The column was centrifuged for 1 min. The column was then washed with 750µL of PE buffer and centrifuged for 1 min. The flow-through was removed, and the column was centrifuged for 1 min for drying the columns membrane. The DNA was eluted with 50 µL of Buffer EB (10 mM Tris·Cl, pH 8.5). The other half was extracted from agarose gel with the agarose gel DNA extraction kit (Roche, Cat.No. 1 696 505). The purified PCR products were quantified with nanodrop (Thermo scientific). The PCR products were then double digested with NotI and HindIII (Thermo Scientific) for 3 hours at 37ºC (Table 2.12).

Table 2.12 : NotI and HindIII digestions.

Reagents for NotI and HindIII digestion	**PCR product**	**Vector**
dH_2O	16µL	16µL
10X FastDigest Buffer	3 µL	3 µL
DNA (100ng/µL)	10µL	10µL
10U/µL FastDigest NotI	1 µL	1µL
10U/µL FastDigest HindIII	1 µL	1µL
TOTAL	30 µL	30µL

The digestion products were controlled on 1.5% agarose gel and then extracted with agarose gel DNA extraction kit (Roche, Cat.No. 1 696 505). The purified DNA products were quantified with nanodrop then ligated with T4 DNA ligase (Fermentas, Sweden). The 50 µL ligation reaction (Table 2.13) was incubated overnight at 16ºC. The ligase was then inactivated by treating the mixture at 72ºC for 5 minutes.

Table 2.13 : Ligation reaction of Lig7 and pQE2.

Reagents	**1:3 ratio**	**1:6 ratio**
dH_2O	38µL	37µL
10X ligation buffer (Fermentas)	5 µL	5 µL
NotI/ HindIII digested PCR product	1µL (100 ng)	2µL (200 ng)
NotI/ HindIII digested vector (200ng)	5µL	5µL
T4 DNA ligase (2,5U/µL)	1 µL	1µL
TOTAL	50 µL	50µL

The ligation products were transferred into chemically competent *E.coli* DH5α cells by calcium chloride method according Maniatis et al. (1982). The transformed cells were spread on LB/Agar/Ampicillin (100μg/mL) plates and incubated overnight at 37ºC (Innova). The remaining transformation product was poured in 50 mL of LB containing Ampicillin (100μg/mL) and incubated overnight at 37ºC at 220 rpm (Innova, 4230 Refrigerated incubator shaker). The presence of the Lig7-GBP fusion encoding gene was controlled by colony PCR using 3 sets of primer pairs. The first set was GBP_forward_NotI_with_tail and GBP_reverse_HindIII_with_tail primers; the second set was primers specific to Lig7 scFv, Lig7_Forw_NdeI and Lig7_Rev_NotI primers. The last set was pQE2 promoter and reverse primers specific to the cloning site of the pQE2 vector. The reactions were set up as mentioned in Table 2.14.

Table 2.14 : Colony PCR reaction.

Reagents	**Volume**
dH_2O	34μL
10X reaction buffer (Roche)	5 μL
25 mM $MgCl_2$	3 μL
10 mM dNTP each	1 μL
10 pmol Forward primer	2 μL
10 pmol Reverse primer	2 μL
Supernatant of bacterial Lysate	2 μL
1U Taq DNA polymerase (Roche)	1 μL
TOTAL	50 μL

Plasmid isolation was made from the colony PCR positive clones by using Roche High pure plasmid isolation kit (Cat. No. 11 754 777 001) according the manufacturer instructions. The presence of the gold binding peptide encoding sequence scFv in the Lig7/pQE2 vector was confirmed with DNA sequence analysis by using Beckman coulter Genome Lab DTCS quick kit.

2.2.2.3 Expression of the bifunctional recombinant antibodies

To express the bifunctional antibodies first plasmids containing either Lig7 itself or Lig7-GBP encoding gene was isolated with QIAprep Spin Miniprep Kit (Qiagen, Cat.No. 27106) according to the manufacturer instructions. The plasmids were then

transferred into either chemically competent *E.coli* BL21(DE3) strain or *E. coli* M15[pREP4] strain by calcium chloride transformation as mentioned in section 2.2.1.1. Transformant cells were selected on selective medium containing ampicillin (100 µg/mL) for *E.coli* BL21(DE3) strain, containing ampicillin (100 µg/mL) and kanamycin (50 µg/mL) for *E. coli* M15[pREP4]. One clone for each bifunctional construct was selected for protein expression studies.

The protein expression experiment was started by inoculating 5 mL of LB medium containing the appropriate selection agent regarding the cell strain used, and cells were grown overnight at 37 °C and 220 rpm. The next, 5 mL of LB medium containing the appropriate selection agent were inoculated with the overnight cultures. The cells were grown at 37 °C and 220 rpm until OD_{600} reached 0.5, and an aliquot was taken as a time 0 (T0) sample. Then IPTG was added into the culture flasks to a final concentration of 1mM. An aliquot was taken after 4 hours as T4 induction sample. The remaining cells were harvested at 4000 rpm for 10 min and the pellet was stored at -20 °C.

The T0 and T4 pellet samples were prepared by resuspending the pellets with 30 µL of sample buffer (1 % Glycerol, 1 % SDS, 0.1% 2-β-mercaptoethanol, 0.05 % bromophenol blue in 0.5M Tris-HCl, pH:6.8) and denatured at 95 °C for 3 min. The samples were loaded (5 µL) on a 12% acrylamide gel and run at 100 V for 10 min than at 120 V for 1.5 hours with Miniprotean II system (Bio-Rad). After the electrophoresis one gel was stained with Coomassie staining solution (50% Methanol, 10% Acetic acid and 0.1% Coomassie Blue R) for 40 min and destained with destaining solution (10% Methanol and 7% Acetic acid). The twin gel was subjected to western blot by electro-blotting the proteins on nitrocellulose membrane using a semi-dry blotting system (Bio-Rad). The nitrocellulose membrane was then blocked for 1.5 hours with a blocking solution (PBS containing 0.1% Tween-20 and 1% BSA). The membrane was washed 3 times for 5 min. with washing buffer (PBS containing 0.1% Tween-20). Mouse monoclonal anti-His HRP conjugate (Sigma) diluted in blocking buffer (1/16000) was incubated for 1 hour. The membrane was washed 3 times with washing buffer then a 4-Chloro-1-Naphthol substrate solution was used as chromogen (2 mL of 4-Chloro-1-Naphthol solution (30 mg of 4-Chloro-1-Naphthol in 10 mL of methanol), 50 µL of 3% H_2O_2 in 10 mL of triethanolamine buffer (128 mM NaCl, 0.28 % triethanolamine, pH 7.5).

2.2.2.4 Purification of bifunctional antibodies from large scale culture and removal of His-Tag

Large scale production of the bifunctional recombinant antibody was made using clones in M15[pREP4] cells. Cells were grown overnight in 50 mL LB medium containing ampicillin (100 µg/mL) and kanamycin (50 µg/mL) at 37 °C and 220 rpm. The next day all the 50 mL of the overnight culture was poured into 500 mL of LB medium containing ampicillin (100 µg/mL) and kanamycin (50 µg/mL). The cells were grown at 37 °C and 220 rpm until OD_{600} reached 0.5 and IPTG was added into the culture flasks to a final concentration of 0.1 mM. Cells were then harvested at 4000 rpm for 10 min and the pellet was resuspended with 20 mL of B-PER bacterial protein extraction reagent (Thermo Scientific, Cat. No. 78243) and incubated at room temperature and 200 rpm for 10 min. The suspension was centrifuged for 15 min at 27000 g and the supernatant was stored. The inclusion body pellet was solubilized with inclusion body solubilization reagent (Thermo scientific, Cat. No: 78115) according to the manufacturer instructions indicating that 8 mL of reagent must be used for 1 g of wet inclusion body pellet. After 2 hours of solubilization at room temperature, the suspension was centrifuged for 15 min at 27000 g and room temperature. The supernatant was collected for metal affinity purification step.

The metal affinity purification was done by mixing the solubilized inclusion body solution with HisPur Cobalt resin (Thermo Scientific, cat. No. 89965) (1/4 volume of solubilized inclusion bodies) and incubated for 80 min at 37 °C and 200 rpm. The suspension was then centrifuged for 1 min at room temperature and 700 g. The supernatant was collected. The resin was washed by shaking for 10 min (37 °C and 200 rpm) with 8 mL of Buffer C (100 mM NaH_2PO_4, 10 mM Tris-Cl, 8M urea, pH 7.0) then centrifuged for 1 min at 700 rpm. The supernatant was collected, and the pellet was washed 2 times with 4 mL of Buffer C (pH 7.0). The supernatants were collected after 1 min of centrifugation at 700 rpm. The elution was made 2 times by resuspending the resin with 4 mL of Buffer E (100 mM NaH_2PO_4, 10 mM Tris-Cl, 8M urea, pH 4.5) and incubating for 10 min at 37 °C and 200 rpm. The purification steps were controlled on 12% SDS-PAGE. The percentage of the purity of the antibodies was determined by the 2001 Bioanalyzer instrument (Agilent).

The affinity column purified denatured recombinant antibodies were then subjected to refolding process by successive 1/2 dilutions (Yang et al., 2011). For this purpose successive dilutions of the solubilized recombinant antibodies was done with dilution Buffer (100mM NaH2PO4, 10mM Tris.Cl) until Urea concentration reached 2 M Then, for a correct disulphide bonds formation within the antibody structure a red-ox environment was generated with reduced and oxidized glutathione (GSH 2mM, GSSG 0,4mM). The prevention of recombinant antibody precipitation was planned by adding L-Arginine for a final concentration of 400 mM. The same red-ox and L-Arginine conditions were followed until the Urea concentration was decreased to 0.5 M. Finally all the additives were removed from the recombinant antibody solution by dialysis against Dilution Buffer for 2 days at +4°C.

Histidine tag removal experiments were done with DAPase enzyme according to the manufacturer instructions. Briefly 50 µg of recombinant antibody in 50 µl of buffer was digested with 10.5 µL of activated enzyme mixture (2.5 mU of DAPase enzyme, 5 µL of 2 mM of Cysteamine-HCl and 150 mU of Q-cyclase) for 15, 30 and 45 min. at 37 °C. The digestion products, for each time period, were controlled on 12% Acrylamide gel.

2.2.3 The use of the recombinant antibodies as a biosensing probe

2.2.3.1 Binding studies using Surface Plasmon Resonance spectroscopy (SPR)

The SPR spectroscopy and SPR slides were obtained from Reichert Instruments (Reichert Technologies, Depew, NY, USA).

Immobilization of gold binding bifunctional antibodies studies was made by adsorbing the antibodies to gold coated SPR chips. First the gold coated chips were cleaned by UV/Ozon treatment for 15 min. Then the chips were placed on the SPR spectrometer and washed for 10 min with dilution buffer (100mM NaH2PO4, 10mM Tris.Cl) at 100µL/min rate and 25°C. Once baseline was stabilized, different concentrations (200 nM, 300 nM, 400 nM and 600 nM) of Lig7-GBP, Lig7-3GBP and Lig7-5GBP were flown on the sensor chip for 5 min at 100µL/min rate and 25°C. After each injections the chips were washed with dilution buffer until the stabilization of the chips surface.

The binding of HBsAg to the immobilized bifunctional antibodies was monitored first immobilizing 300 nM of antibodies on the chip surface. Then various concentrations of HBsAg (100 nM, 150 nM and 200 nM) were flown over the chip with immobilized recombinant antibodies at 100µL/min rate and 25°C. After each injections the chips were washed with dilution buffer until the stabilization of the chips surface.

For chemically immobilization of Lig7 on SPR chips, the SPR chip surfaces were functionalized overnight with mercaptoundecanoic acid (Sigma) to form self-assembled monolayers (SAMs) of COOH-terminated thiols. The functionalized SPR surface was activated by injecting 1:1 volume ratio of N-hydroxysulfosuccinimide (NHS) and 1-ethyl-3-(-3-dimethiyaminopropyl) carbodiimide (EDC) in a flow cell. Lig7 scFv solution was passed across the activated SAM surface at a constant flow rate (2 µL/Min) at 25◦C. After immobilization of Lig7 scFv on the surface, loosely bound and unbound receptors were removed by extensive washing of the chip surface with buffer solution. Ethanolamine was passed across the Lig7 scFv decorated SPR chip surface in the aim of blocking the amine-coupling end of SAM. Interaction of the Lig7 scFv with HBsAg was monitored by passing HBsAg over the chip surface at 50, 100, and 200 nM.

All the measurements were analyzed with the BIAevaluation Software 4.1 (Biacore). The maximum uptake and adsorption values were plotted on graphs. The adsorption kinetics were calculated using 1:1 Langmuir association model represented by the equation given below:

$$R(t) = R_{eq}[1 - \exp(-(k_a * C + k_d)(t - t_0))] + RI \qquad \textbf{(2.1)}$$

where

$$R_{eq} = k_a * C / (k_a * C + k_d) * R\max \qquad \textbf{(2.2)}$$

R(t) correspond to the SPR signal (µRIU) at time t. The injection start time is t_0. The association rate ($M^{-1}s^{-1}$) constant is represented by (ka) and the dissociation rate (s^{-1}) constant is represented by (kd). The analyte concentration is C. Rmax corresponds to maximum analyte binding capacity (µRIU) and RI corresponds to the bulk refractive index contribution (µRIU).

The equilibrium dissociation constant (K_D) was deduced from adsorption (ka) and desorption (kd) rates according to equation 2.3.

$$K_D = \frac{k_d}{k_a} \qquad \textbf{(2.3)}$$

2.2.3.2 Monitoring HBsAg in *in-vitro* cell model

For monitoring HBsAg presence in mammalian cells first HBsAg was cloned into mammalian expression vector and transfected into mammalian cells and the expression of HBsAg was controlled by ELISA and microscopic observations. The cloning experiments were done according to the cloning protocol given in section 2.2.1.1. Briefly, HBsAg gene was amplified with PCR by using HBsAg_Forward_BamHI and HBsAg_Reverse_BamHI primers containing BamHI restriction site. The PCR product was extracted from 1.2 % agarose gel by using agarose gel DNA extraction kit (Roche, Cat. No. 1 696 505). Then the pCEP4 vector and PCR product were digested with BamHI enzyme. The digestion products were purified and then ligated with T4 DNA ligase (Fermentas). The ligation product was transferred into chemically competent DH5α cells by calcıum chloride transformation method. The presence of HBsAg in pCEP4 was confirmed by colony PCR and then by DNA sequence analysis (Beckman coulter Genome Lab DTCS quick kit). One position clone was selected and plasmid was isolated from it with Roche High pure plasmid isolation kit (Cat. No. 11754777001).

High purity HBsAg-pCEP4 plasmid was then transfected into different mammalian cell lines such as HeLa, Hek293 Trex, HepG2 and COS7. For this purpose, 1day before transfection, 0.5 x 10^5 cells in 1 mL of DMEM-F12 growth medium (containing %10 FBS) were poured in wells. The next day 8 µg HBsAg-pCEP4 plasmid was gently mixed in 500 µl of DMEM-F12 without serum. In another tube, 20 µL of Lipofectamine 2000 was gently mixed with 500 µl of DMEM-F12 medium and incubate for 4 min. at room temperature. After incubation, the Lipofectamine mixture and the diluted plasmid solution were mixed together and incubate for 20 min. at room temperature. Then, 50 µl of mixture was added to each cell culture well. The cell culture plate was then mixed gently by rocking. The cells were left to grow at 37°C in a CO_2 incubator. Twenty-four hours after transfection the growth medium was replaced with fresh medium containing 200 µg Hygromycin B. The

medium was then collected 7 days after transfection for testing the presence of HBsAg in the culture media by ELISA.

ELISA well plates were coated overnight at 4ºC with the 7 days cell culture medium. The next day wells were washed 6 times with TPBS (0,1 % PBS-Tween 20) and then blocked with TPBS containing %1 BSA for 2 hours. Wells were washed 6 times with TPBS and polyclonal anti-HBsAg rabbit antibody (1/200) was used as primary antibody. After 1 hour of incubation at room temperature, wells were washed 6 times with TPBS. Then, goat anti-rabbit alkaline phosphatase (Thermo Scientific) conjugate (1/1000) was used as secondary antibody. After 1 hour of incubation at room temperature, wells were washed 6 times with TPBS.

The absorbance was measured at 405 nm using a microplate reader (Bio-Rad) 1 hour after the addition of *para*-nitrophenyl phosphate substrate (PNPP) solution (1 mg/mL of pNPP in substrate buffer (0,1 M glycine, 1mM ZnCl2, 1mM MgCl2, pH: 10,4). The color reaction was stopped with 1 M NaOH.

For monitoring the expression of HBsAg directly in HeLa cells. A new transfection was done as mentioned above, but instead of growing cell directly in the wells, the cells were grown on steril 12 mm coverslips. Twenty-four hours after transfection the growth medium was replaced with fresh medium containing 200 µg Hygromycin B. Then previously expressed Lig7 scFv, mcherry (fluorescent protein) or Lig7-mcherry fusion construct were added to the wells and cells were incubated for 24 hours. Then cells were fixed with ice-cold 100% methanol after aspirating the growth medium. Cells were incubated for 20 minutes at -20 C° for fixation. Then the fixative was aspirated and the coverslips were rinsed three times with PBS for 5 min. The nucleus of the cells were stained with a drop of mounting medium (%50 Glycerol + %50 PBS) containing Hoechst dye. Coverslips were turned up site down on a lamel and cells were analysed with a fluorescence microscope.

3. RESULTS AND DISCUSSION

3.1 Development of an anti-HBsAg single chain Fv recombinant antibody

The first scope of the thesis was the development of a recombinant antibody against Hepatitis B surface antigen by using phage display technology. For this purpose mice immunized with HBsAg was necessary. Commercial HBsAg is available on the market but the production and purification processes for HBsAg are expensive and time-consuming which is reflected into the price of HBsAg. HBsAg was first purified from human plasma in 1980. It was then produced in a recombinant yeast system (Valenzuela, 1982), followed by expression in mammalian cells. Several years ago, a lower-cost method using phage display for the expression of HBsAg for immunization purposes was demonstrated. Tan (2005) fused the 111 - 156 amino acid coding DNA region of HBsAg, including the dominant neutralizing epitope “a”, with T7 phage capsid proteins. T7 phages expressing the 45 amino acid-length partial HBsAg on their surfaces were used as immunization agents in rabbits. Until now, a full-length HBsAg was not displayed on the phage surface and hence it was not used for immunization of mice with the aim of developing an anti-HBsAg recombinant antibody. This approach is facilitated by our group for the first time. This section describes the expression of the entire small HBsAg on phage surfaces as a pIII fusion protein and use of these recombinant phage nanoparticles as immunization agents in immunocompetent BALB/cJ mouse strain based on the paper published in 2014 (Balcioglu, 2014).

3.1.1 Cloning of HBsAg in phagemid vector

In the purpose of cloning the HBsAg gene in the phagemid vector, the gene was first amplified by PCR with flanking primer containing appropriate restriction enzyme cutting sites. Then restriction enzyme digested gene was inserted into the phagemid clone by classical ligation procedure and the transformant vector was transferred into competent *E. coli* cells. The experiments are described below in more details.

The HBsAg gene provided by GATA was amplified by polymerase chain reaction using primers flanked with SfiI or NotI restriction enzyme sites, the single ~700 bp PCR amplified product was confirmed by 1.2% Agarose gel (Figure 3.1).

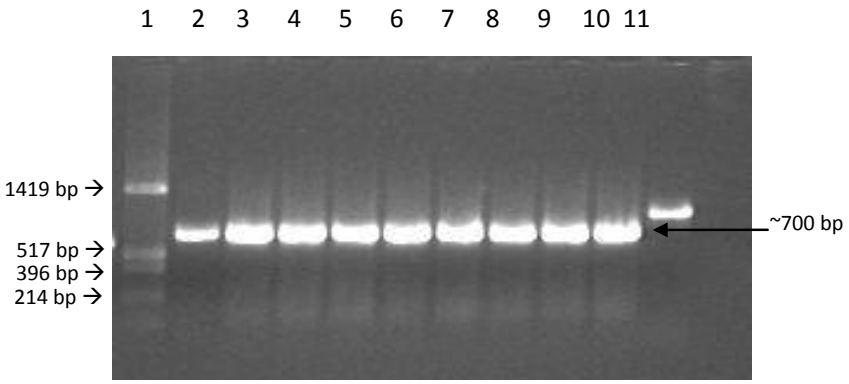

Figure 3.1 : PCR amplification of HBsAg gene with Sfi I ve Not I restriction enzyme site containing primers. Lane 1. M4 marker, Lane 2. ScFv marker, Lane 3-10., Lane 11. Control PCR product.

Multiple PCR reactions were prepared for increasing the amount of amplified HBsAg gene after Agarose gel extraction. The purified PCR products were controlled by 1.2% Agarose gel electrophoresis (Figure 3.2) and were quantified by nanodrop measurements.

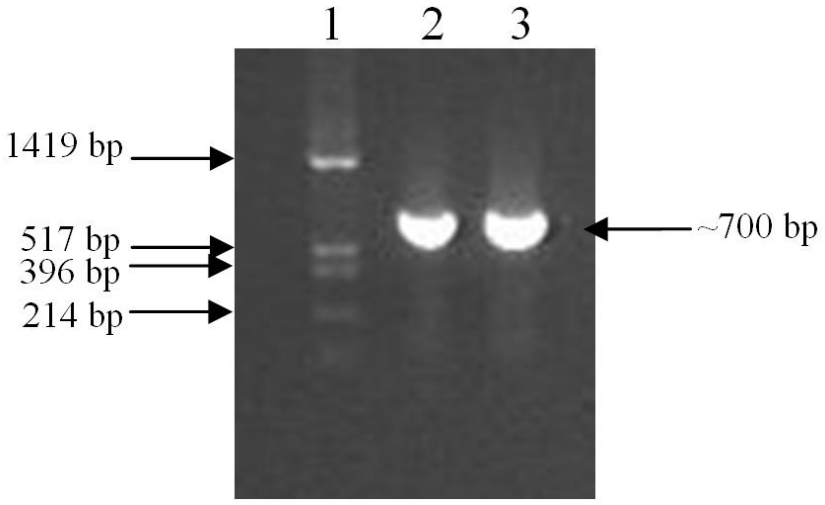

Figure 3.2 : Purification of Sfi I and Not I restriction enzyme site containing PCR products from agarose gel. Lane 1; M4 Marker, Lane 2-3; Agarose gel extracted PCR product.

The Agarose gel extracted PCR products, and the phagemid pCANTAB5E vector were digested first with SfiI I then with NotI restriction enzymes (Figure 3.3) then extracted from Agarose gel after each digestion steps.

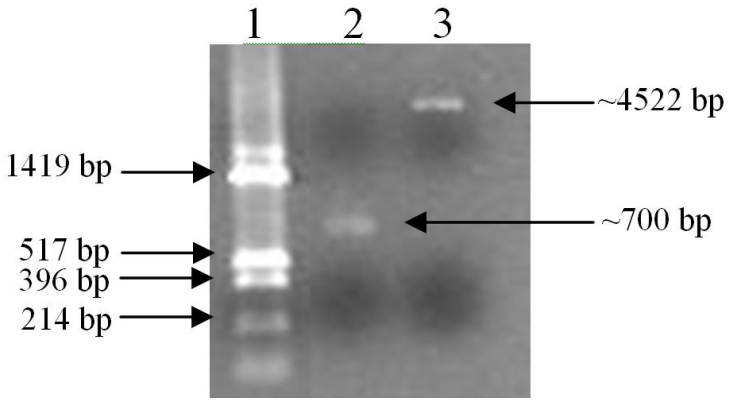

Figure 3.3 : Control of pCANTAB5E phagemid vector and PCR products after Sfi I and Not I digestion. Lane 1; M4 marker, Lane 2; HBsAg, Lane 3; pCANTAB5E. The DNA band size was deduced from semi-log plotting.

Double digested products of PCR amplified HBsAg gene (~700 bp) and the pCANTAB5E phagemid vector (~4522 bp) were ligated with T4 ligase overnight at 16ºC. The ligation product was transferred into chemically competent TG1 *E.coli* cells with Calcium Chloride transformation method (Maniatis). Transformant colonies were picked randomly for control with colony PCR reaction method (Figure 3.4).

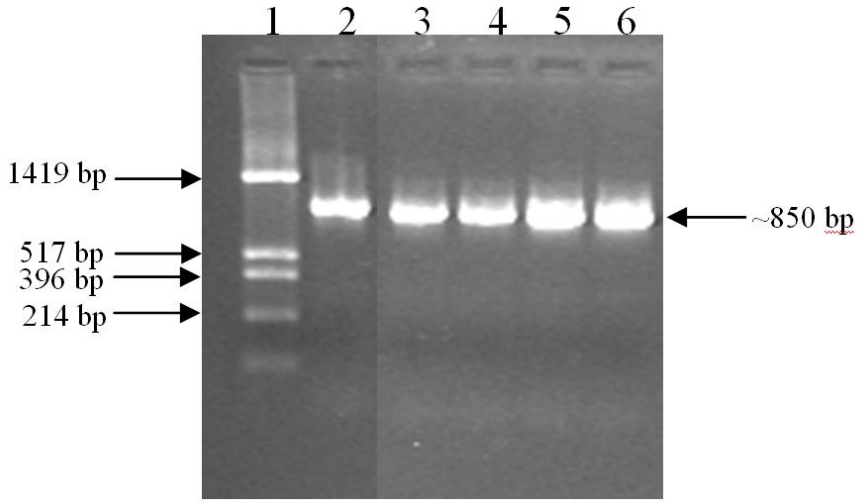

Figure 3.4 : Colony PCR results of transformation colonies. Lane 1; M4 Marker, Lane 2; ScFv marker, Lane 3-6; Colony PCR products.

A Single band of ~850 bp containing the HBsAg encoding gene and the flanking regions of the pCANTAB5E gene as drawn in (Figure 3.5) was observed.

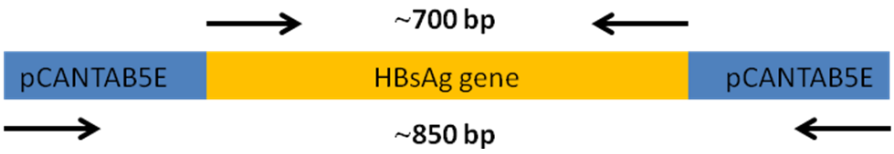

Figure 3.5 : A schematic representation of the emplacement of the HBsAg and the pCANTAB5E primers resulting of a PCR amplification.band of ~700 bp and ~850 bp, respectively.

Plasmids bearing the HBsAg gene were isolated with the Roche High pure plasmid isolation kit from PCR confirmed transformation colonies. The plasmids were controlled on 1% Agarose gel and quantified with nanodrop. According to the Beckman Coulter Genome Lab DTCS kit 400 ng of plasmids was used for DNA sequencing. The DNA sequences obtained from duplicated sequencing (Figure 3.6). were converted into a protein sequence and the protein sequence was searched in the reference sequence viral protein database by using BlastP compared from the San Diego Supercomputer Center (SDSC) Biology Workbench Internet website (Url-2).

```
      E  T  V  I  M  K  Y  L  L  P  T  A  A  A  G  L  L  L  L  A
3     gagacagtcataatgaaatacctattgcctacggcagccgctggattgttattactcgcg  62
      A  Q  P  A  M  E  N  I  T  S  G  F  L  G  P  L  L  V  L  Q
63    gcccagccggccatggagaacatcacatcaggattcctaggacccctgctcgtgttacag  122
      A  G  F  F  L  L  T  R  I  L  T  I  P  Q  S  L  D  S  W  W
123   gcggggtttttcttgttgacaagaatcctcacaataccgcagagtctagactcgtggtgg  182
      T  S  L  N  F  L  G  G  S  P  V  C  L  G  Q  N  S  Q  S  P
183   acttctctcaattttctagggggatcacccgtgtgtcttggccaaaattcgcagtcccca  242
      T  S  N  H  S  P  T  S  C  P  P  I  C  P  G  Y  R  W  M  C
243   acctccaatcactcaccaacctcctgtcctccaatttgtcctggttatcgctggatgtgt  302
      L  R  R  F  I  I  F  L  F  I  V  L  L  C  L  I  F  L  L  G
303   ctgcggcgttttatcatattcctcttcatcgtgctgctatgcctcatcttcttgttgggt  362
      L  L  D  Y  Q  G  M  L  P  V  C  P  L  I  P  G  T  T  T  T
363   cttctggattatcaaggtatgttgcccgtttgtcctctaattccaggaacaacaacaacc  422
      S  T  G  P  C  K  T  C  T  T  P  A  Q  G  N  S  M  F  P  S
423   agtacgggaccatgcaaaacctgcacgactcctgctcaaggcaactctatgtttccctca  482
      C  C  C  T  K  P  S  D  G  N  C  T  C  I  P  I  P  S  S  W
483   tgttgctgtacaaaaccttcggatggaaattgcacctgtattcccatcccatcgtcttgg  542
      A  F  A  K  Y  L  W  E  W  A  S  V  R  F  S  W  L  S  L  L
543   gctttcgcaaaatacctatgggagtgggcctcagtccgtttctcttggctcagtttacta  602
      V  P  F  V  Q  W  F  V  G  L  S  P  T  V  W  L  S  A  I  W
603   gtgccatttgttcagtggttcgtagggctttcccccactgtttggctttcagctatatgg  662
      M  M  W  Y  W  G  P  S  L  Y  S  I  V  S  P  F  I  P  L  L
663   atgatgtggtattgggggccaagtctgtacagcatcgtgagtccctttataccgctgtta  722
      P  I  F  F  C  L  W  V  Y  I  *
723   ccaattttcttttgtctctgggtatacatttaa
```

Figure 3.6 : DNA and protein sequences of the HBsAg gene region cloned into the pCANTAB5E vector. The yellow region indicates the vector sequence, the underlined sequence correspond to SfiI restriction enzyme site and the red star indicates the end of translation.

The protein sequence showing the highest homology HBsAg (Hepatitis B virus isolate 4436-97 HBsAg protein (S) gene, complete) with the cloned HBsAg was compared by CLUSTALW multiple sequence alignment compared from the San Diego Supercomputer Center (SDSC) Biology Workbench Internet website (Figure 3.7). The cloned HBsAg showed ~97% of homology with the HBsAg from the database, sufficient to accept that HBsAg was cloned into a phagemid vector.

```
56417967_56417968               : Hepatitis B virus isolate 4436-97 HBsAg protein (S) gene,
complete
56417967_56417968               ----------MENITSGFLGPLLVLQAGFFLLTRILTIPQ
HbsAg_faj_full_17_II_Transla    MKYLLPTAAAGLLLLAAQPAMENITSGFLGPLLVLQAGFFLLTRILTIPQ
                                          ******************************

56417967_56417968               SLDSWWTSLNFLGGSPVCLGQNSQSPTSNHSPTSCPPICPGYRWMCLRRF
HbsAg_faj_full_17_II_Transla    SLDSWWTSLNFLGGSPVCLGQNSQSPTSNHSPTSCPPICPGYRWMCLRRF
                                **************************************************

56417967_56417968               IIFLFILLLCLIFLLVLLDYQGMLPVCPLIPGSTATSTGPCKTCTTPAQG
HbsAg_faj_full_17_II_Transla    IIFLFIVLLCLIFLLGLLDYQGMLPVCPLIPGTTTTSTGPCKTCTTPAQG
                                ******:******** ***************:*:***************

56417967_56417968               NSMFPSCCCTKPTDGNCTCIPIPSSWAFAKYLWEWASVRFSWLSLLVPFV
HbsAg_faj_full_17_II_Transla    NSMFPSCCCTKPSDGNCTCIPIPSSWAFAKYLWEWASVRFSWLSLLVPFV
                                ************:*************************************

56417967_56417968               QWFVGLSPTVWLSAIWMMWYWGPSLYSIVSPFIPLLPIFFCLWVYI
HbsAg_faj_full_17_II_Transla    QWFVGLSPTVWLSAIWMMWYWGPSLYSIVSPFIPLLPIFFCLWVYI
                                ***********************************************
```

Figure 3.7 : Sequence alignment of the cloned HBsAg and the HBsAg sequence selected from the reference sequence viral protein database (Hepatitis B virus isolate 4436-97 HBsAg protein (S) gene, complete) by CLUSTALW multiple sequence alignment. The blue color indicates total homology; green color indicates similar amino acids.

3.1.2 Production of HBsAg displaying phages and phage ELISA

Once HBsAg cloning was confirmed, cells containing the phagemid vector were grown for the production of infective phages displaying HBsAg protein on their surface as a fusion protein with the PIII minor phage surface protein. For this purpose cells containing the recombined pCANTAB5E were mixed with M13K07 helper phages and incubated for the production of infective phages. Phages were purified by PEG precipitations and the titer was calculated by phage titration protocol.

Then two different ELISA methods were used to verify the HBsAg display on the phage particles (Figure 3.8).

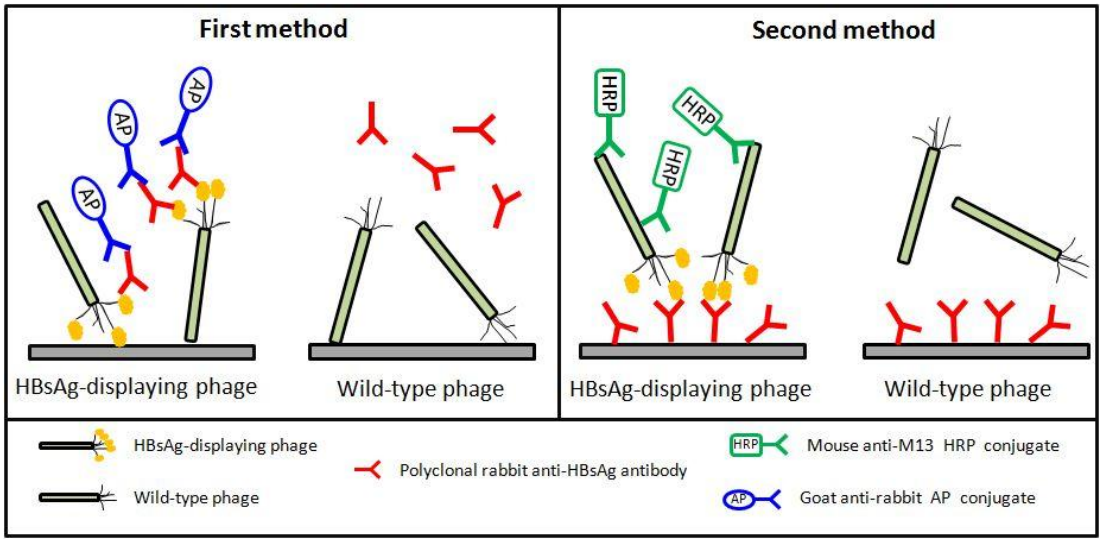

Figure 3.8 : Detection methods of M13 phages displaying HBsAg based on ELISA.

In the first method, ELISA plate wells were coated either with phage particles displaying HBsAg or wild-type phages. Then, a rabbit anti-HBsAg polyclonal antibody was used as a primary antibody, and goat anti-rabbit AP conjugate was used as the secondary antibody. The ELISA results had a 9-fold higher binding signal for HBsAg-displaying phages relative to the wild-type phages (Figure 3.9). In the second method, polyclonal rabbit anti-HBsAg antibody was used to coat the wells. In this assay, either phage particles displaying HBsAg or wild-type phages were used as the primary antibody, and a mouse anti-M13/HRP conjugate was used as the secondary antibody. The binding signal for HBsAg-displaying phages was 7.7 times higher than the binding signal for the wild-type phages (Figure 3.9).

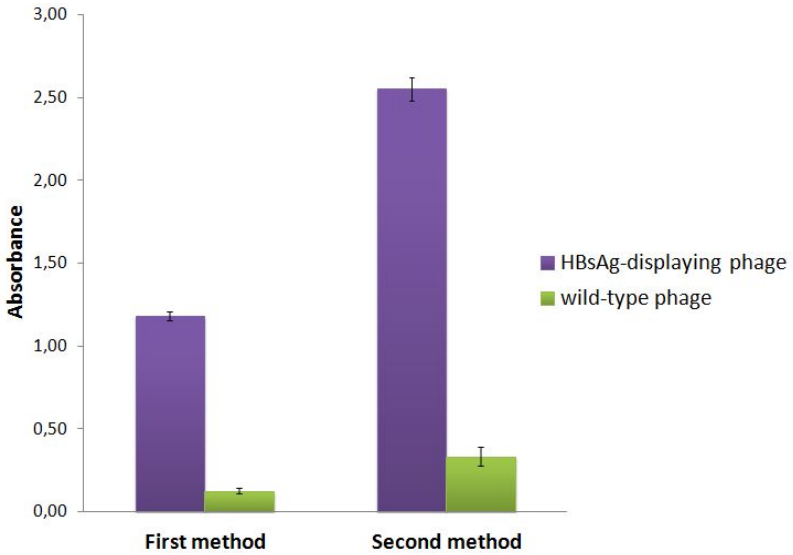

Figure 3.9 : Phage ELISA results of the first and second ELISA strategies.

The goal of this present study was to express the full-length small HBsAg on the surface of an M13 filamentous phage as a PIII fusion protein. The gene coding the full-length HBsAg was cloned into a pCANTAB5E phagemid vector for this purpose. After the gene insertion was confirmed by DNA sequence analysis, infective phages displaying HBsAg were obtained. Small HBsAg expression was confirmed by two different ELISA methods as illustrated in Figure 3.8. In both methods, a binding signal was expected if HBsAg was displayed on phage surfaces, and if no HBsAg was displayed (wild-type phages), then no signal was expected. The ELISA results from both methods clearly showed a specific binding between phages displaying HBsAg and polyclonal anti-HBsAg antibodies. In contrast, no binding for the wild-type phages to the polyclonal anti-HBsAg antibodies was detected proving the expression of HBsAg on the phage surfaces.

3.1.3 Mouse immunization and ELISA from immunized mice sera

Immunizations of 8-week-old male BALB/cJ mice were performed by intradermal injections of the phage nanoparticles at different concentrations (10^{10}, 10^{11} or 10^{12} phage particles). The immunizations used either HBsAg-displaying recombinant phage nanoparticles, wild-type phage nanoparticles or PBS. Three injections were performed at three-week intervals, and mouse blood was collected prior to each injection. For determining the immune response developed against HBsAg, an ELISA test against anti-HBsAg antibodies in mice sera was conducted. The injections gave no signal for mice immunized with 10^{10} and 10^{11} phage particles. However, a three-fold increase in absorbance was observed in the sera of mice immunized with 10^{12} recombinant phage nanoparticles displaying HBsAg. A mixed model ANOVA with Tukey post hoc test was conducted to assess the immune response difference between different treatment groups (phage particles displaying HBsAg, phage particles without HBsAg and PBS) across different injection periods (Before injection, first injection, second injection and third injection). There was a statistically significant interaction between the treatment groups and the injections on the immune response, $F(6,18) = 80.208$, $p < 0.0005$, partial eta squared = 0.964. Then univariate General Linear Model with Tukey post hoc analysis were conducted to determine the differences of immune responses be-tween groups at each level of injection periods. Their immune response was statistically lower in the PBS group

(M = 0.39, SE = 0.017, p < 0.0005) and the phage particles without HBsAg group (M = 0.38, SE = 0.017, p < 0.0005) compared to the phage particles displaying HBsAg group (Figure 3.10).

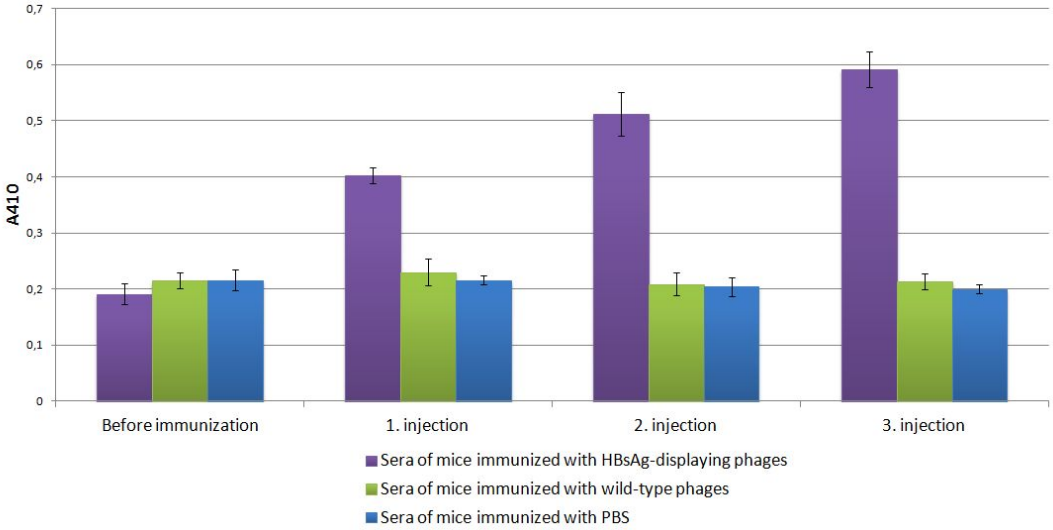

Figure 3.10 : Immune response results of mice before the injection of phages and after each injection of 10^{12} phages.

The goal of this present study was to express the full-length small HBsAg on the surface of an M13 filamentous phage as a PIII fusion protein. The gene coding the full-length HBsAg was cloned into a pCANTAB5E phagemid vector for this purpose. After the gene insertion had been confirmed by DNA sequence analysis, infective phages displaying HBsAg were obtained. Small HBsAg expression was confirmed by two different ELISA methods. In both methods, a binding signal was expected if HBsAg was displayed on phage surfaces, and if no HBsAg was displayed (wild-type phages), then no signal was expected. The ELISA results from both methods clearly showed a specific binding between phages displaying HBsAg and polyclonal anti-HBsAg antibodies. In contrast, no binding for the wild-type phages to the polyclonal anti-HBsAg antibodies was detected as expected. Therefore, the expression of HBsAg on the phage surfaces was confirmed.

The HBsAg-displaying phage nanoparticles were then used for immunization assays. The results showed that injections of 10^{10} and 10^{11} phage nanoparticles were not sufficient to generate an immune response against HBsAg but were sufficient for generating an immune response against an M13 phage (data not shown). A significant ($p< 0.05$) anti-HBsAg immune response was observed in mice immunized with 10^{12} recombinant phage nanoparticles after the third immunization. Therefore,

our results demonstrated that at least 10^{12} recombinant phage nano-particles are necessary to generate an immune response against HBsAg. The present results support the concept that M13 phages are good antigen carriers built upon the inexpensive and easy phage display method to express HBsAg for immunization. Further, the results demonstrate that full-length HBV small surface antigen displayed on M13 phage minor pIII coat proteins can activate an anti-HBsAg immune response in BALB/cJ mice, even at a very low pIII copy number.

3.1.4 Construction of a recombinant antibody library

ScFv antibodies are recombinant antibodies generated from the genetic fusion of the light and heavy chain of variable region. Therefore, scFvs' are six times smaller than IgG type antibodies (Figure 3.11).

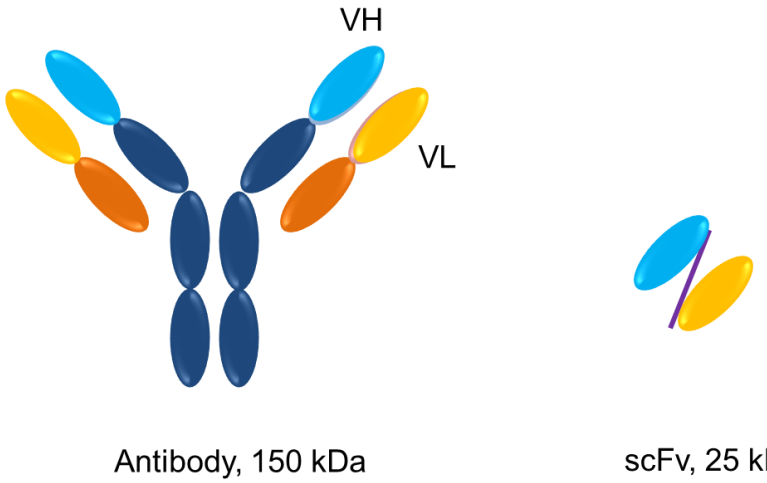

Figure 3.11 : Schematic representation of an antibody and a single chain Fv. Orange color represent the light chain, and the blue color represent the heavy chain. Dark color represents the constant region, and light color represent the variable region.

The scFv recombinant antibody is generated by the fusion of the antibody variable regions via a linker. The 15 amino acids linker peptide is the optimized amino acid number which gives the exact antibody recognition conformation to the scFv. The linker sequence may vary for each laboratories but the most commonly used linker is the 3 times repeat of the Gly-Gly-Gly-Gly-Ser (Gly for Glycin and Ser for serine) Pentapeptide flanked with short VH and VL homologue sequence necessary for the genetic fusion process to generate the scFv (Figure 3.12).

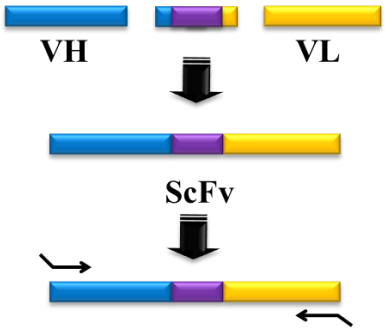

Figure 3.12 : Schematic representation of the construction of a single chain Fv from variable domains of light (VL) and heavy (VH) chains and a linker. Orange color represent the light chain, and the blue color represent the heavy chain variable domain. The linker is represented by purple color flanked with short homologue sequences to VL or VH.

The construction of the scFv library was, Therefore, initiated with a total RNA extraction from the spleen of mice immunized with 10^{12} phage particles displaying HBsAg. For this purpose total, RNA was extracted from homogenized immunized mice spleen with the EZ-RNA Total RNA isolation kit. The RNA quality was controlled according to OD_{260} / OD_{280} ratio. The RNA was then converted to a cDNA library by using random primers (Froussard, 1992). The cDNA library was used as a template for the PCR amplification of VH and VL regions (Figure 3.13).

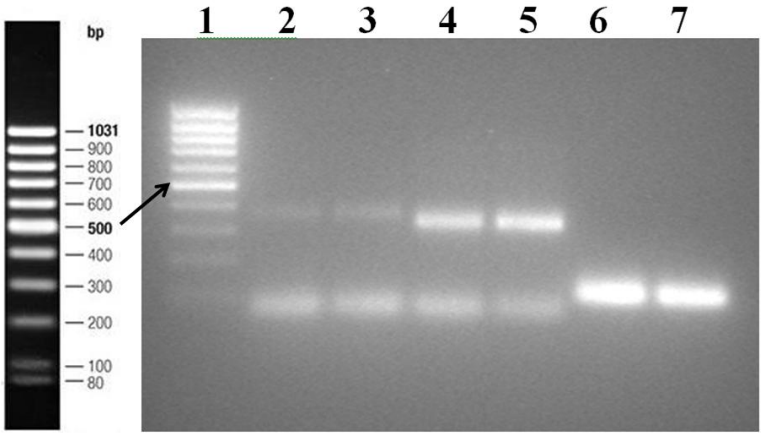

Figure 3.13 : PCR amplification results of VH and VL on 1.5% agarose gel. Lane 1; Thermo scientific Mass ruler Low Range DNA ladder (SM0383), Lane 2-3; Variable Heavy chain PCR, Lane 4-5; Variable Heavy chain PCR, Lane 6-7; Linker PCR.PCR amplification bands of ~350 bp for VH and ~320 bp for VL were obtained (Figure 3.13). Also, a single band of ~100 bp was also observed for the PCR amplification of the linker. These results confirmed the presence of a VH and a VL library. Primers dimers in the PCR product were purified with an agarose gel DNA extraction kit (Roche, Cat. No. 1 696 505) according to the manufacturer instructions and controlled on 1.5% agarose gel (Figure 3.14).

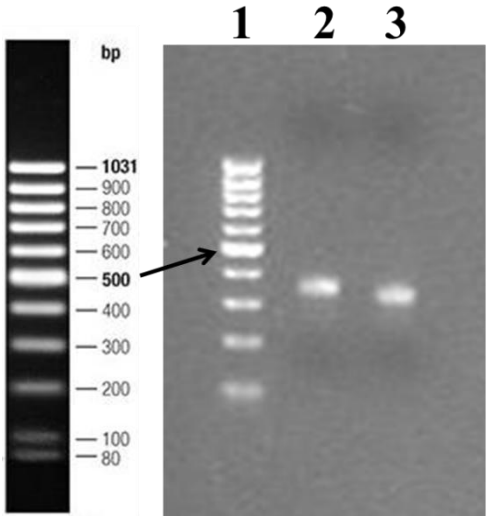

Figure 3.14 : Agarose gel purification results of VH and VL on 1.5% agarose gel electrophoresis. Lane 1; Thermo scientific Mass ruler Low Range DNA ladder (SM0383), Lane 2; Heavy chain variable region, Lane 3; Light chain variable region.

The VH and VL library was quantified then used as a template for the generation of the scFv encoding gene. The genetical fusion reaction was made by mixing the VH library, the VL library and the $(Gly\text{-}Gly\text{-}Gly\text{-}Gly\text{-}Ser)_3$ linker in an equimolar quantity. The fusion product was then amplified by PCR using primers 702 and 704 specific for scFv (Figure 3.15).

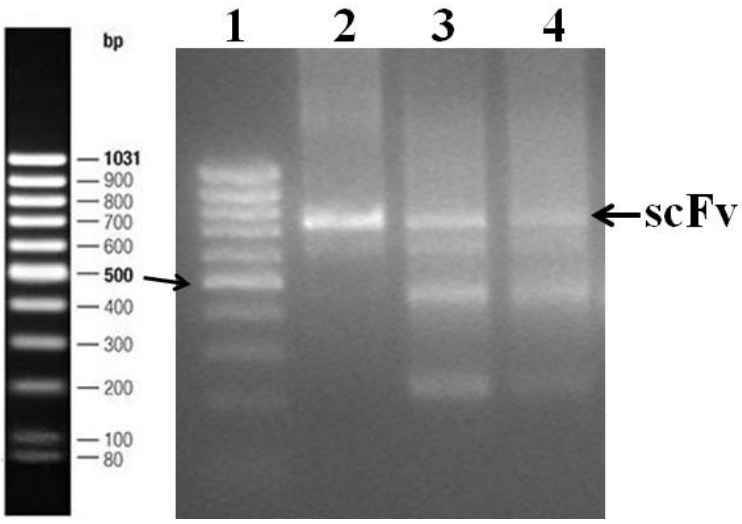

Figure 3.15 : The PCR amplification results after the fusion of the VH and VL libraries with the $(Gly\text{-}Gly\text{-}Gly\text{-}Gly\text{-}Ser)_3$ linker on a 1.2% agarose gel. Lane 1; Thermo scientific Mass ruler Low Range DNA ladder (SM0383), Lane 2-4; scFv fusion products.

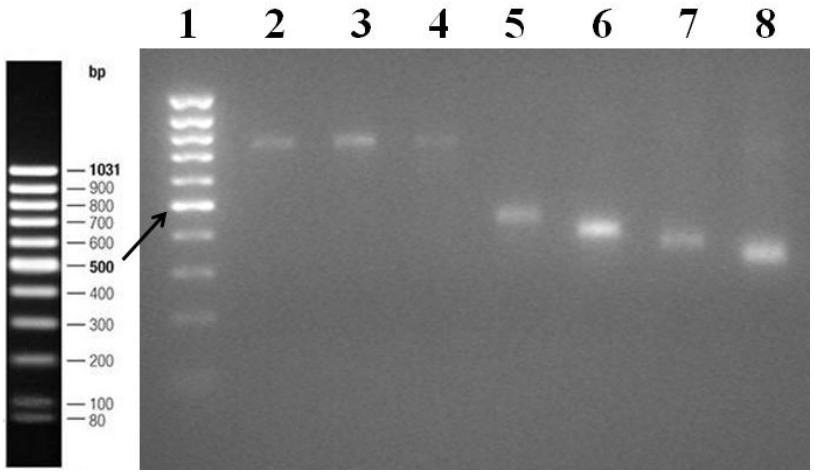

Figure 3.16 : The scFv PCR amplification products after agarose gel extraction. Lane 1; Thermo scientific Mass ruler Low Range DNA ladder (SM0383), Lane 2-4; Purified scFv fusion products, Lane 5; Purified VH-Linker fragment, Lane 6; Purified VL-Linker fragment, Lane 7; Purified VH fragment, Lane 8; Purified VL fragment.

VH and VL fragments and their linker fusion versions and finally, the scFv was monitored on 1.2% agarose gel. The scFv library was then amplified with scFv specific primers containing SfiI and NotI restriction enzyme sites necessary for the cloning of the library into the pDUCK1 phagemid vector. The library PCR amplified product, and the pDUCK1 phagemid vector were digested with SfiI then with NotI restriction enzymes. The digestion products were then ligated with T4 DNA ligase. The ligation product was transferred into *E.coli* TG1 cells by calcium chloride method. The transformant cells were then pooled into one tube, and phage-displayed scFv library was produced by phage amplification method. The titration of the library was done, and a titer of 3.10^{12} phage particles per mL was calculated.

3.1.5 Selection of an anti-HBsAg scFv from the library

The scFv library was then screened against 500ng of HBsAg (Ad/Ay, 100 ng each, Fitzgerald Industries International) coated in a maxisorb immunotube. The biopanning process was initiated with an equivalent number of the phage particle so that the eluted phage particle number could be measured.

The enrichment of the phage-displayed scFv library, specific to HBsAg after two rounds of biopanning is given in Table 3.1.

Table 3.1 : Enrichment of HBsAg specific scFv phage-displayed library.

Biopanning round	Starting phage particle number	Eluted phage particle number	Amplification rate	Phage particle concentration after amplification (pfu/ml)
First	10^{11}	3.3×10^{4}	-	10^{13}
Second	10^{11}	8.9×10^{5}	26,97	-

After the second round of biopanning, a ~ 27 fold enrichment against HBsAg was observed. Randomly selected 95 differents scFv-displaying phage particles were amplified and tested the display of HBsAg on phages surface (Figure 3.17).

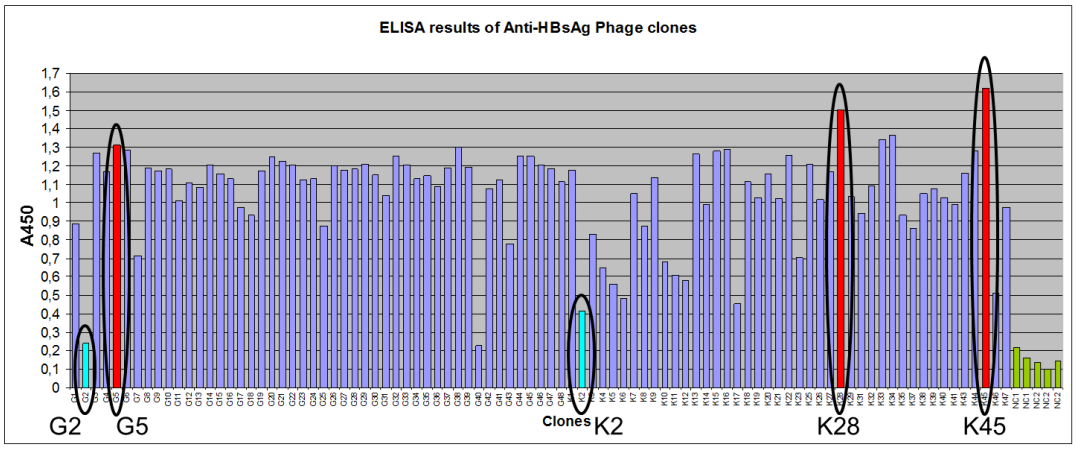

Figure 3.17 : ELISA results of HBsAg binding phage particles after two rounds of biopanning. The clones indicated in red (G5, K28 and K54) correspond to high HBsAg binding and the clones indicated in blue (G2, K2) correspond to low HBsAg binding phages. The green color correspond to negative control clones.

Three clones (G5, K28 and K54) with high binding signal (A450>1.3) and two clones (G2 and K2) with low binding signal (A450<0.4) were selected for a second ELISA experiment for checking cross-reactivity.

No cross reactivity for clones G5, K28 and K45 were found. Therefore, these clones were specific to HBsAg (Figure 3.18).

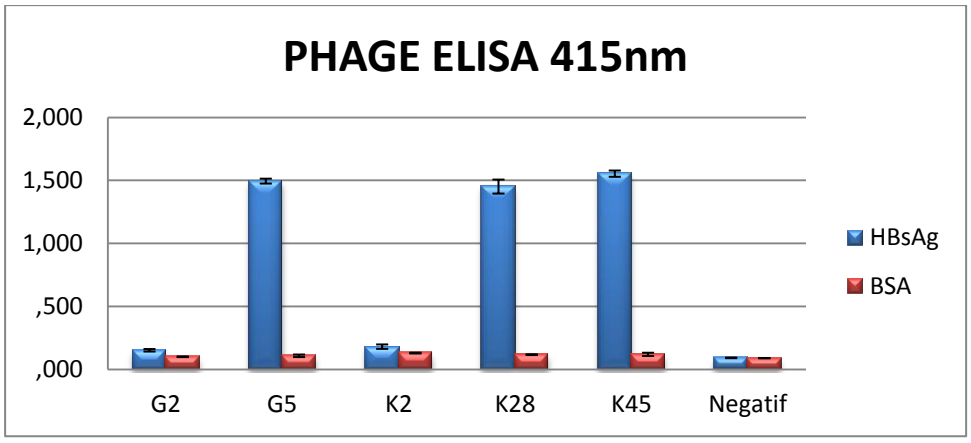

Figure 3.18 : ELISA results of the selected clones for HBsAg and BSA.

3.2 Development and characterisation of an anti-HBsAg gold binding recombinant antibody

3.2.1 Cloning of the anti-HBsAg Lig7 recombinant antibody into pQE2 vector

An anti-HBsAg scFv recombinant antibody (Lig7), developed and characterized by Dr. Berrin Erdağ and her group was used as a template. Because the Lig7 scFv was inserted into a pDUCK1 phagemid vector, the Lig7 scFv encoding gene was recloned into the pQE2 expression vector (Figure A.2). The pQE2 expression vector is a vector allowing the cleavage of the His-tag, which might interfere with the binding of the bifunctional antibody to the gold surface.

Primers specific to Lig7 were designed according to the DNA and protein sequences given in the Qiagen TAGzyme handbook by taking care of not leading a frameshift error (Figure 3.19). Also the C-terminal region of Lig7 was modified by adding glutamine (Q) between the first methionine (M1) and the alanine (A2) so that the cleavage of the His-tag with the TAGzyme enzyme stops after the "HM" amino acid sequence (Figure 3.20). Finally, the NdeI and NotI restriction enzyme sites, necessary for the recloning of Lig7 scFv into the pQE2 vector were inserted to the primers (Lig7_Forw_NdeI and Lig7_Rev_NotI).

```
                                NdeI      SphI          SacI  NotI      SacII     KpnI  PmlI  SalI          PstI      HindIII
                                CAT ATG   CAT GCG GGA   GCT CAT GCG   GCC GCG   GGT ACC   CAC GTG TCG   ACC   TGC AGC   CAA GCT T
M K   H H   H H   H H   H  M    H  A    G  A    H  A    A  A    G  T    H  V    S  T    C  S    Q  A
```

Figure 3.19 : The multiple cloning sites of the pQE2 expression vector (Qiagen).

```
Lig7 sequence in pDUCK1 vector          M - A Q V Q L Q E S G G A
Lig7 sequence adapted for pQE2 vector   M Q A Q V Q L Q E S G G A
```

Figure 3.20 : Modification of the Lig7 C-terminal region. Glutamine (Q) indicated in red was added to the Lig7 sequence to stop the cleavage of the Tagzyme enzyme.

The lig7 scFv was amplified by PCR with the designed primers. The agarose gel purified PCR amplification purified products and the pQE2 vector were then successively digested with NdeI and NotI enzymes. The digestion products were ligated and transferred into chemically competent *E.coli* DH5α cells with calcium chloride method. The next day colony PCR was made from randomly selected 14 transformant colonies (Figure 3.21).

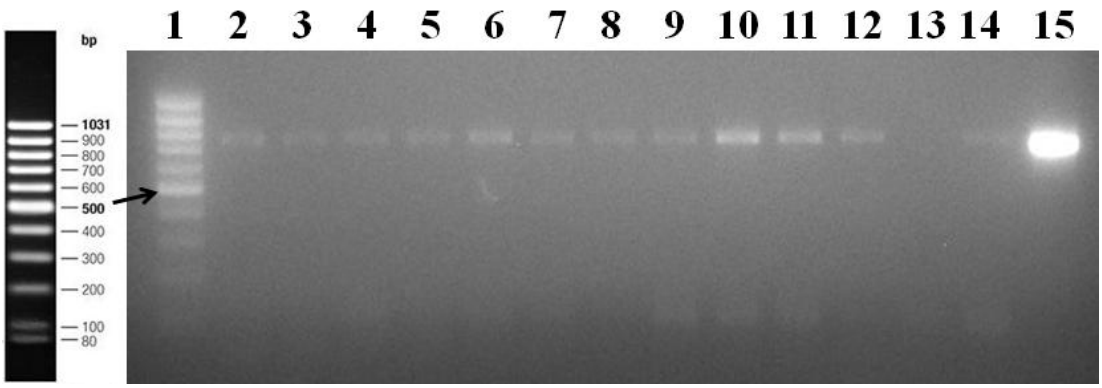

Figure 3.21 : Colony PCR results from 14 randomly selected transformant colonies. Lane 1; Thermo scientific Mass ruler Low Range DNA ladder (SM0383), Lane 2-14; different transformation colonies, Lane 15; Control PCR of Lig7 scFv from the original Lig7/pDUCK1 vector.

One clone containing the ~750 bp PCR amplification band was randomly selected and was subjected to DNA sequence analysis. Forward and reverse sequencing primers specific to the pQE2 vector was used for the dye terminator cycle sequence analysis. The resulting sequences were translated using the San Diego Supercomputer Center (SDSC) Biology Workbench Internet website. No frameshift within the sequence was observed, and the presence of the inserted Glutamine (Q) amino necessary for the excision of the His tag was confirmed (Figure 3.22).

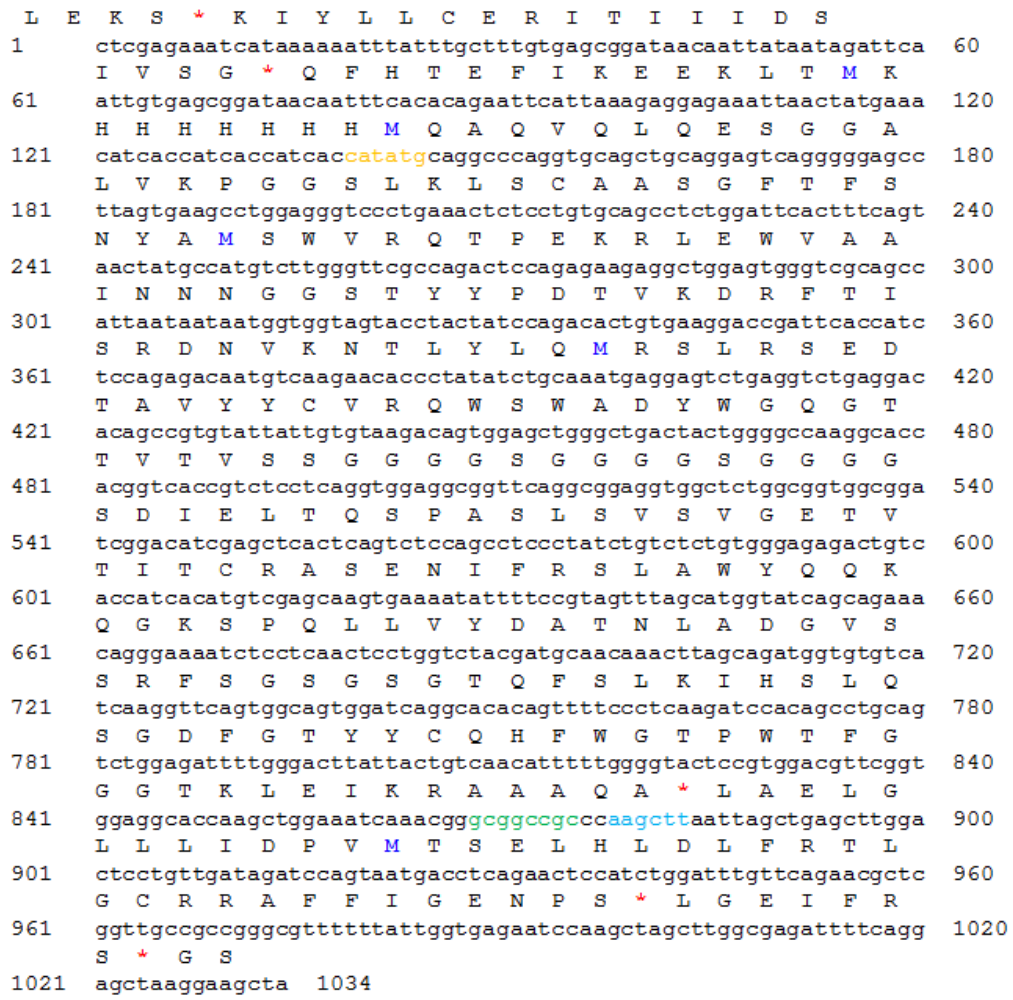

Figure 3.22 : DNA and protein sequence results retrieved from the San Diego Supercomputer Center (SDSC) Biology Workbench Internet website. Color code for restriction enzyme site; orange; NdeI, green; NotI, blue; HindIII.

3.2.2 Insertion of gold binding peptide coding region in the Lig7/pQE2 vector

Following the confirmation of the insertion of the Lig7 scFv, the cloning of the GBP1 encoding region at the C-terminal of Lig7 was initiated. The 14 mer GBP1 is encoded from a 42bp DNA sequence. Primers specific to the 5' and 3' end of GBP1 containing NotI and HindIII restriction enzyme sites, respectively, GBP1_Not_F and GBP1_HindIII_R were designed using the San Diego Supercomputer Center (SDSC) Biology Workbench Internet website. The PCR reaction was realized by using the pDrive cloning vector containing the 5-time repeats of GBP1 (5GBP) as template, which was kindly provided from Candan Tamerler's research group. To

increase the resolution of the electrophoretic pattern of the small PCR amplification bands an Agarose gel of 2,5% was used (Figure 3.23).

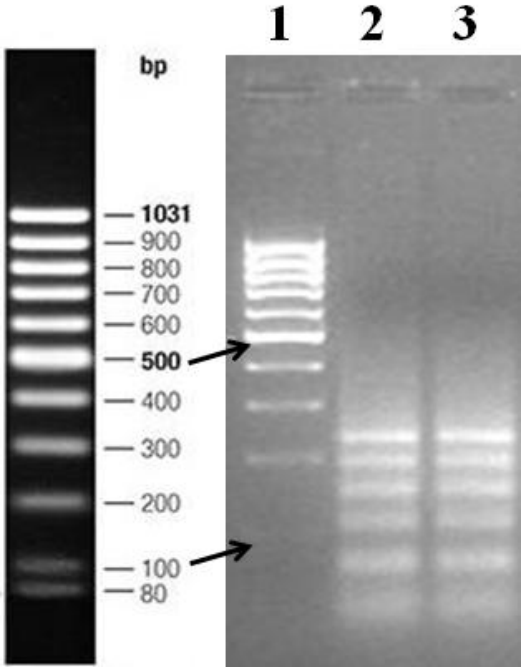

Figure 3.23 : Results of PCR amplification from the pDrive-5GBP vector using primers containing NotI and HindIII restriction enzyme sites. Lane 1; Thermo scientific Mass ruler Low Range DNA ladder (SM0383), Lane 2-3; PCR products.

Five PCR bands with sizes, ~66 bp, ~108 bp, ~150 bp, ~192 bp and ~234 bp were observed. These five bands are corresponding to the amplification of GBP1 repeats. Each band were ~ 24 bp higher than the GBP1 nucleotide itself because of the integration of NotI and HindIII restriction enzyme sites. The bands were individually extracted from the agarose gel for further cloning experiments. But due to the low recovery of the bands after NotI and HindIII digestions the cloning experiments were unsuccessful. After several assays with the same results, the cloning strategy was changed.

New primers including the BamHI and EcoRI restriction enzyme from the pDrive-5GBP vector were designed in the aim of obtaining a single PCR amplification band (GBP_forward_NotI_with tail, GBP_reverse_HindIII_ with tail) flanked with NotI and HindIII restriction enzyme sites (Figure 3.24).

Figure 3.24 : Schematic representation of the GBP_forward_NotI_with_tail and GBP_reverse_HindIII_with_tail primers annealing emplacement on pDrive-5GBP vector.

PCR amplification of 5GBP was done with the new "GBP_forward_NotI_with_tail" and "GBP_reverse_HindIII_with_tail" primers using the pDrive-5GBP vector as template. Also, a higher quality of Taq polymerase with high proofreading was used for cloning experiments (Qiagen, HotStart Taq DNA polymerase). The PCR results are shown in Figure 3.25.

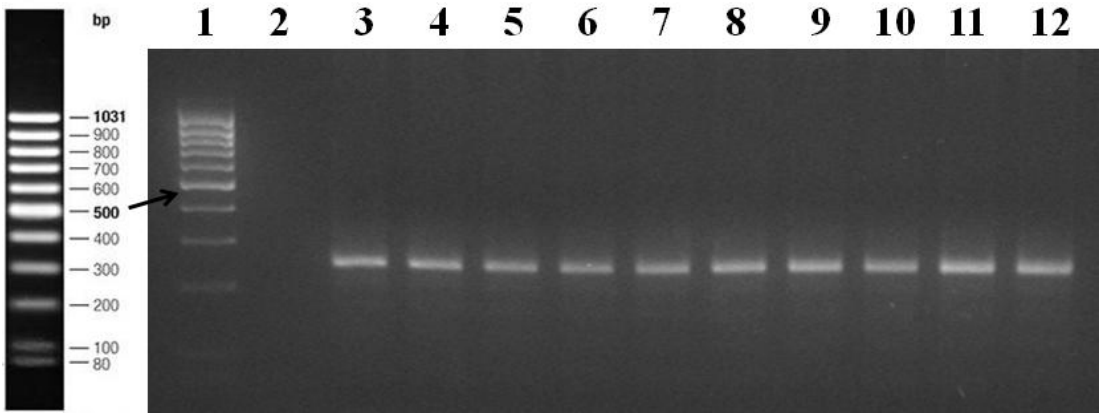

Figure 3.25 : PCR amplification results of 5GBP by using the "GBP_forward_NotI_with_tail" and "GBP_reverse_HindIII_with_tail" primers. Lane 1; Thermo scientific Mass ruler Low Range DNA ladder (SM0383), Lane 2; empty well, Lane 3-12; PCR amplifications.

A major band which is ~ 260 bp was obtained from the PCR amplifications. The new primers set allowed the amplification of 5GBP encoding region in a higher amount. All the PCR amplification reactions were pooled together. Half of the PCR amplified products were purified with QIAquick PCR purification kit (Qiagen), and the remaining PCR products were extracted as a single band from agarose gel. The purified PCR products were quantified with nanodrop. The DNA concentration obtained from the agarose gel extraction was 10ng/mL whereas a better yield was obtained with eluted DNA from the PCR purification kit was 36ng/mL.

The purified 5GBP PCR product and the Lig7- pQE2 vector were then double digested with NotI and HindIII restriction enzymes for 3 hours. The digestion products were controlled on 1.5 % agarose gel (Figure 3.26).

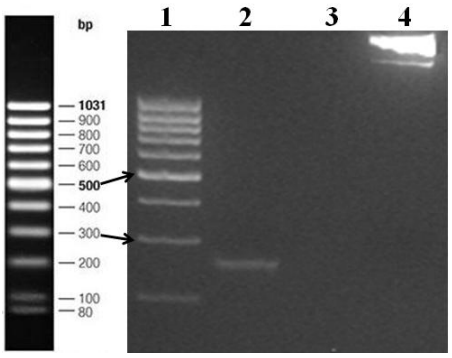

Figure 3.26 : PCR amplification results of 5GBP by using the "GBP_forward_NotI_with_tail" and "GBP_reverse_HindIII_with_tail" primers. Lane 1; Thermo scientific Mass ruler Low Range DNA ladder (SM0383), Lane 2; empty well, Lane 3-12; PCR amplifications.

The digestion products were quantified with nanodrop after agarose extraction. A final concentration of 22.4 ng/µL and 42.5 ng/µL was obtained for the digestion of Lig7-pQE2 vector and the 5GBP PCR product, respectively. Ligation ratio selected for insertion was 3:1, insert: vector, the ligation reaction was limited to 10 minutes at 22°C. The recombinant vector was transfered into chemically competent *E.coli* DH5α cells with calciun chloride method. The next day, 16 colonies were randomly selected for the colony PCR reaction made with GBP1 specific primers (GBP_forward_NotI_with_tail and GBP_reverse_HindIII_with_tail) (Figure 3.27).

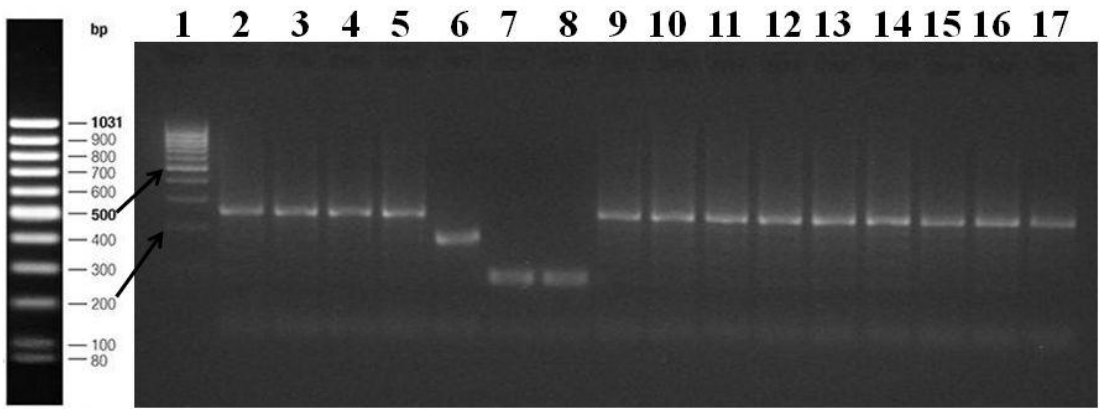

Figure 3.27 : Agarose gel image of the colony PCR made with GBP1 specific primers set. Lane 1; Thermo scientific Mass ruler Low Range DNA ladder (SM0383), Lane 2-17; transformation colonies from 1 to 16.

A major band of ~ 260 bp was observed for the colonies from 1 to 4 and 8 to 16 corresponding to 5GBP amplification. However, the PCR bands obtained for colonies 5; 6 and 7 were unexpected. Because that GBP1 specific primer were used for colony PCR, these PCR products suggested that some different GBP1 repeats were also cloned individually. To verify this hypothesis, plasmids were isolated from clones 1, 5, 6 and 7 and used as a template for PCR amplifications. Three different PCR amplifications with different primer set were done for each clone. The first primer set contained the GBP_forward_NotI_with_tail and GBP_reverse_HindIII_with_tail primers specific to GBP1. The second primer set contained primers specific for Lig7 (Lig7_Forw_NdeI and Lig7_Rev_NotI). The last primer set contained primers specific for the pQE2 vector, i.e. pQE2 promoter and reverse primers.

The PCR products were controlled on 1.5% agarose gel (Figure 3.28) and the size of the PCR bands are given in Table 3.2.

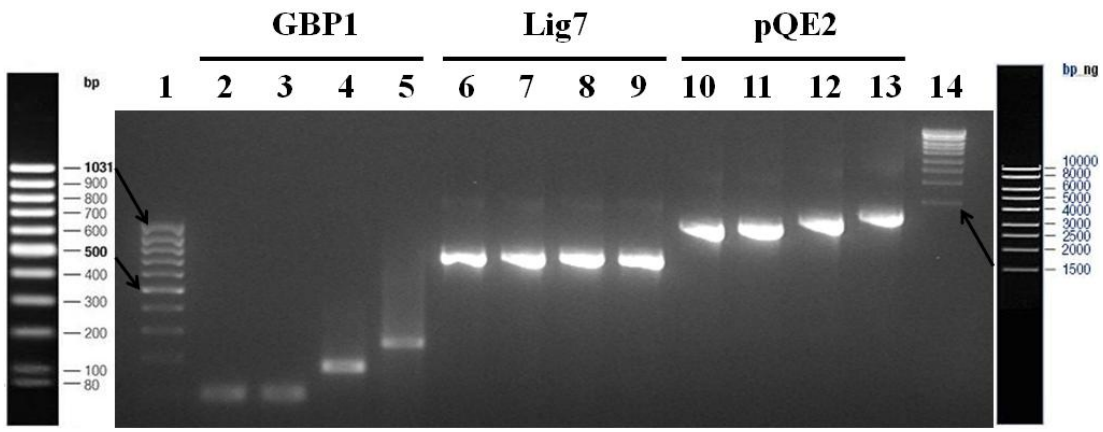

Figure 3.28 : Agarose gel image of the PCR amplification products. Lane 1; Thermo scientific Mass ruler Low Range DNA ladder (SM0383), Lane 2, 6, 11; clone 7, Lane 3, 7, 11; clone 6, Lane 4, 8, 12; clone 5, Lane 5, 9, 13; clone 1, Lane 14; Thermo scientific Mass ruler High Range DNA ladder (SM0393).

Table 3.2 : PCR amplification band size of each clone.

	GBP primer set	**ScFv primer set**	**Vector primer set**
Clone 1	~260 bp	~750 bp	~1150 bp
Clone 5	~180 bp	~750 bp	~1050 bp
Clone 6	~100 bp	~750 bp	~950 bp
Clone 7	~100 bp	~750 bp	~950 bp

The Lig7 PCR bands and the GBP bands present for each clone confirmed the presence of Lig7 encoding gene (~750 bp) and of the GBP1 sequence. But regarding the different sizes of the amplification product specific to GBP1, clone 1, clone 5 and clone 6 (or clone 7) were integrating different repeat number of GBP1 encoding region. The PCR amplification with the pQE2 primers set shows that Lig7 and the GBP1 sequences are within the vectors cloning site, therefore, the fusion of the Lig7 scFv with the different GBP1 sequences is confirmed. According to an approximation regarding the size of bands, clone 6 and 7 were a fusion of Lig7 with one GPB1 (Lig7-GBP), clone 5 was the fusion of Lig7 with 3 GBP1 repeats (Lig7-3GBP) and the clone 1 was the fusion of lig7 with 5 GBP1 repeats (Lig7-5GBP).

The DNA sequences obtained from the Beckman Coulter CQE8800 instrument were analysed using the San Diego Supercomputer Center (SDSC) Biology Workbench Internet website. The DNA and protein sequences of the clones were compared to each other (Figure 3.29 and 3.30).

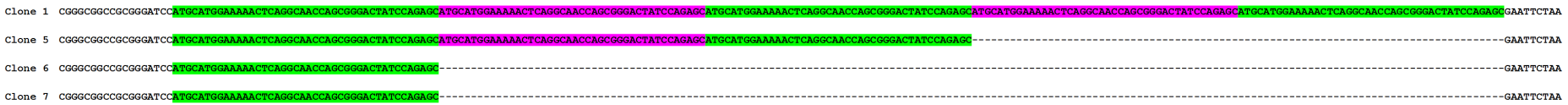

Figure 3.29 : DNA sequence alignment of the four clones at the 3’ end. The green and purple colors indicate the GBP1 peptide encoding region.

Figure 3.30 : Protein sequence alignment of the four clones. The green and purple colors indicate the GBP1 encoding region. The stars correspond to 100% amino acid homology for each clone at the same amino acid emplacement.

The protein and DNA sequences showed that clone 6 and 7 were identical and that the other clones were as hypothesis above. No frameshift regarding the protein sequences were observed, therefore, clones were suiTable for further protein expression works.

3.2.3 Expression of the bifunctional recombinant antibodies

Once the DNA sequence was confirmed the Lig7-GBP, Lig7-3GBP and the Lig7-5GBP containing pQE2 vectors were transferred into chemically competent *E.coli* BL21(DE3) strain by calcium chloride transformation. The transformation colonies were picked and small-scale expression (5 mL of LB medium) of the bifunctional gold binding Lig7 recombinant antibodies was done by using 1mM IPTG for 4 hours. The cells subjected to protein expression were directly loaded on 12% SDS-PAGE. The expression profile was observed by Coomassie staining (Figure 3.31) and western blot (Figure 3.32).

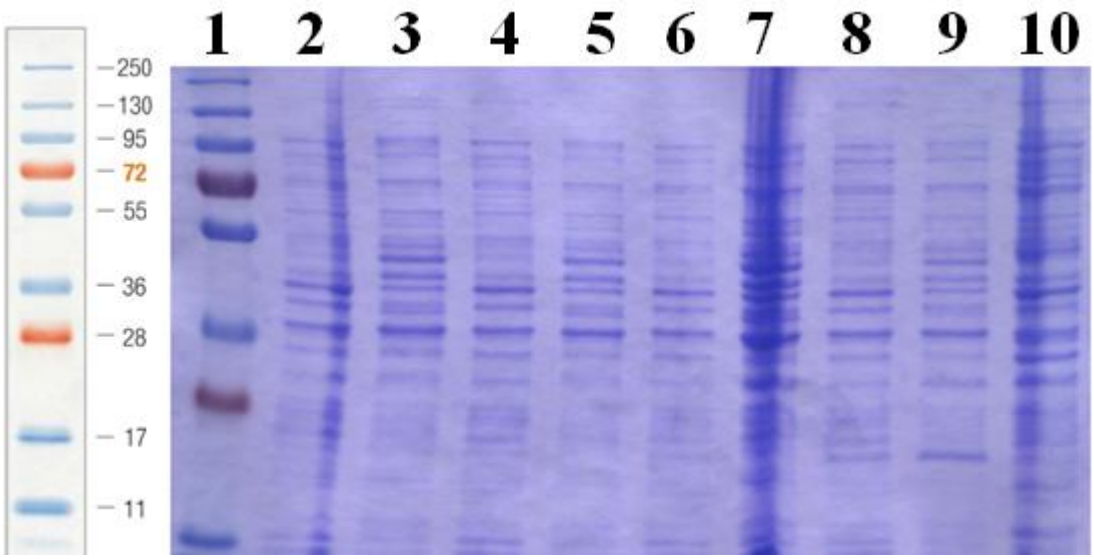

Figure 3.31 : Coomassie staining for bifunctional Lig7 antibodies expression in BL21(DE3) cells. T0: before expression, T4: 4 hours of induction. Lane 1; Fermentas PageRulerTM plus Prestained protein Ladder (SM1811), Lane 2; Lig7-5GBP T0, Lane 3, Lig7-5GBP T4, Lane 4; Lig7-3GBP T0, Lane 5; Lig7-3GBP T4, Lane 6; Lig7-GBP T0 (clone 6), Lane 7; Lig7-GBP T4 (clone 6), Lane 8; Lig7-GBP T0 (clone 7), Lane 9; Lig7-GBP T4 (clone 7), Lane 10; control scFv T4.

Figure 3.32 : Western blot image for bifunctional Lig7 antibodies expression in BL21(DE3) cells. T0: before expression, T4: 4 hours of induction. Lane 1; Fermentas PageRulerTM plus Prestained protein Ladder (SM1811), Lane 2; Lig7-5GBP T0, Lane 3, Lig7-5GBP T4, Lane 4; Lig7-3GBP T0, Lane 5; Lig7-3GBP T4, Lane 6; Lig7-GBP T0 (clone 6), Lane 7; Lig7-GBP T4 (clone 6), Lane 8; Lig7-GBP T0 (clone 7), Lane 9; Lig7-GBP T4 (clone 7), Lane 10; control scFv T4.

No significant protein expression profile was visualized with Coomassie staining, but protein bands were seen with western blot by using mouse anti-His tag HRP conjugate. The bands for Lig7-5GBP and Lig7-3GBP were not as visible as for Lig7-GBP. The expression bands were ~35 kDa, ~33 kDa and ~30 kDa for Lig7 5GBP, Lig7 3GBP and Lig7 GBP clone. The protein expression was not as high as expected, therefore, a new bacterial strain was selected for the expression of the bifunctional antibody. The *E. coli* M15[pREP4] strain which have a strong expression control was selected according to Qiagen, Qiaexpressionist protocol. The plasmid encoding the bifunctional antibodies were transferred into chemically competent *E. coli* M15[pREP4] cell with calcium chloride method. Transformant cells were used for protein expression studies in 5 mL of LB medium. The expression was made at the same conditions than for the BL21(DE3) cells in the aim of comparing expression profiles. The cells were run on 12% SDS-PAGE.

The expression profile was observed by Coomassie staining (Figure 3.33) and western blot (Figure 3.34).

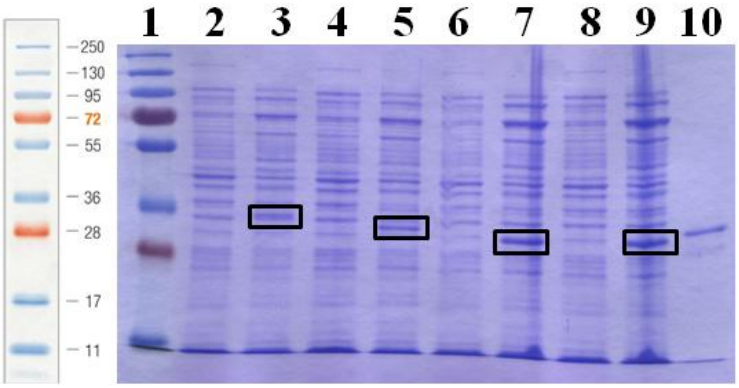

Figure 3.33 : Coomassie staining results for the bifunctional Lig7 antibodies expression in M15[pREP4] cells. T0: before expression, T4: 4 hours of induction. Lane 1; Fermentas PageRulerTM plus Prestained protein Ladder (SM1811), Lane 2; Lig7-5GBP T0, Lane 3, Lig7-5GBP T4, Lane 4; Lig7-3GBP T0, Lane 5; Lig7-3GBP T4, Lane 6; Lig7-GBP T0 (clone 6), Lane 7; Lig7-GBP T4 (clone 6), Lane 8; Lig7-GBP T0 (clone 7), Lane 9; Lig7-GBP T4 (clone 7), Lane 10; control scFv T4. The bands entoured with a black rectangle correspond to protein expression.

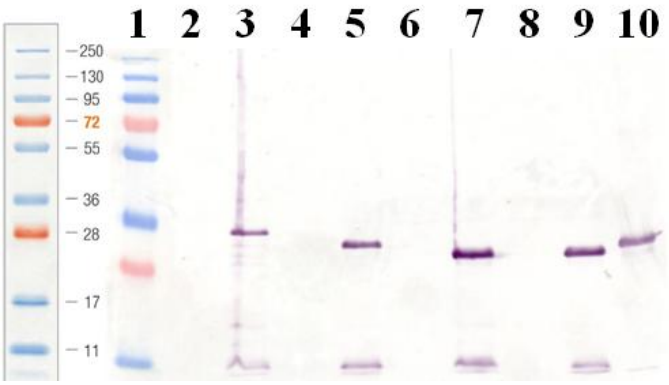

Figure 3.34 : Western blot image for the bifunctional Lig7 antibodies expression in M15[pREP4] cells. T0: before expression, T4: 4 hours of induction. Lane 1; Fermentas PageRulerTM plus Prestained protein Ladder (SM1811), Lane 2; Lig7-5GBP T0, Lane 3, Lig7-5GBP T4, Lane 4; Lig7-3GBP T0, Lane 5; Lig7-3GBP T4, Lane 6; Lig7-GBP T0 (clone 6), Lane 7; Lig7-GBP T4 (clone 6), Lane 8; Lig7-GBP T0 (clone 7), Lane 9; Lig7-GBP T4 (clone 7), Lane 10; control scFv T4.

The expression of the bifunctional antibodies was stronger with M15[pREP4] than BL21(DE3) cells. Even in Coomassie staining the expression bands were visible when compared with the control cells with no expression. Therefore, expression studies were continued with M15[pREP4] cells. According to the western blot results the bigger is the expression protein the lesser its expression. Therefore, the expression of Lig7-5GBP is lesser than Lig7-GBP and Lig7-3GBP.

Since antibody expression was confirmed, the expression was scaled-up to 50 mL than to 500mL LB medium. The scale-up was successful and higher protein

expression was observed from SDS-PAGE Coomassie staining and western blot analysis (Figure 3.35 and 3.36).

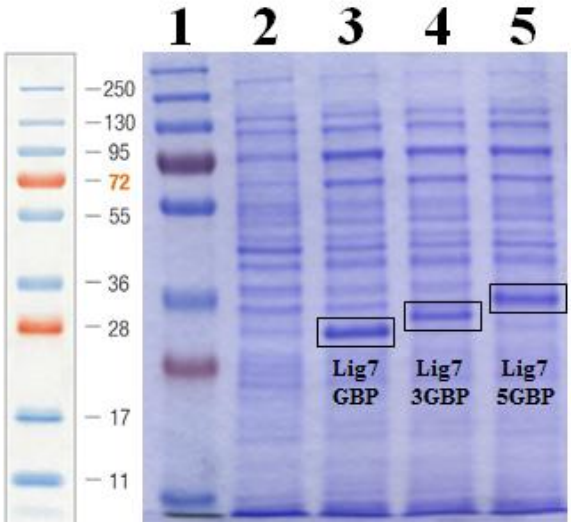

Figure 3.35 : Coomassie staining results for the large scale production of the bifunctional Lig7 antibodies in M15[pREP4] cells. T0: before expression, T4: 4 hours of induction. Lane 1; Fermentas PageRulerTM plus Prestained protein Ladder (SM1811), Lane 2; M15[pREP4] T0, Lane 3, Lig7-GBP T4, Lane 4; Lig7-3GBP T0, Lane 5; Lig7-5GBP T4.

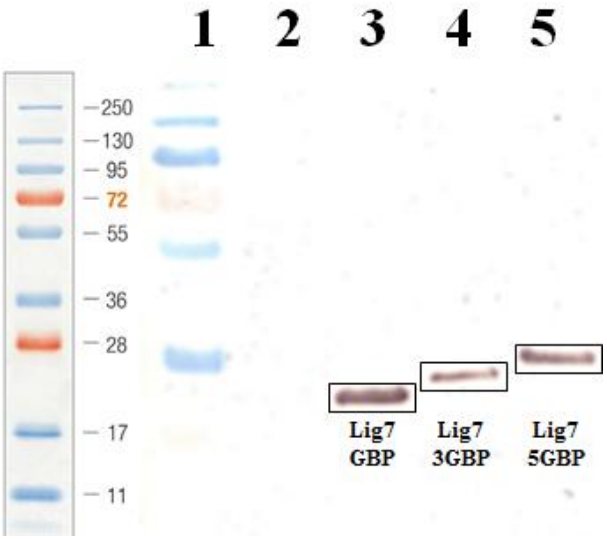

Figure 3.36 : Western blot results for the large scale production of the bifunctional Lig7 antibodies in M15[pREP4] cells. T0: before expression, T4: 4 hours of induction. Lane 1; Fermentas PageRulerTM plus Prestained protein Ladder (SM1811), Lane 2; M15[pREP4] T0, Lane 3, Lig7-GBP T4, Lane 4; Lig7-3GBP T0, Lane 5; Lig7-5GBP T4.

The expression of the bifunctional Lig7-GBP, Lig7-3GBP and Lig7-5GBP antibodies were, therefore, confirmed by SDS-PAGE and western blot analysis.

Different expression conditions were tested for increasing the protein expression. Two parameters, the amount of IPTG (0.1 mM, 0.5 mM and 1 mM) and the induction temperature (20°C, 30°C and 37°C) were modified. But no significant differences were observed for Lig7 expression. Only, a decrease of protein expression was observed for the expression at 20°C with 0,1mM IPTG (data not shown). The bacterial pellets from different expression conditions were treated with lysis buffer (50mM Tris-Cl pH 8.0, 200mM NaCl, 1mM EDTA) and the supernatants (15 min at 12000 rpm) were controlled with 12% SDS-PAGE and western blot (data not shown). The Lig7 extraction profile after lysis buffer treatment showed that the best extraction was performed from the pellets induced at 37°C and the best result was obtained from the cells induced at 0.1 mM IPTG.

3.2.4 Purification of bifunctional antibodies from large scale culture and removal of His-Tag.

The bifunctional antibodies were expressed at large scale using the optimum established conditions (37°C and 0.1 mM IPTG). After four hours of induction the cells were harvested and the pellets were treated with lysis buffer (50mM Tris-Cl pH 8.0, 200mM NaCl, 1mM EDTA). After centrifugation the supernatants were run on 12% SDS-PAGE and controlled with Coomassie Blue and western blot (Figure 3.37).

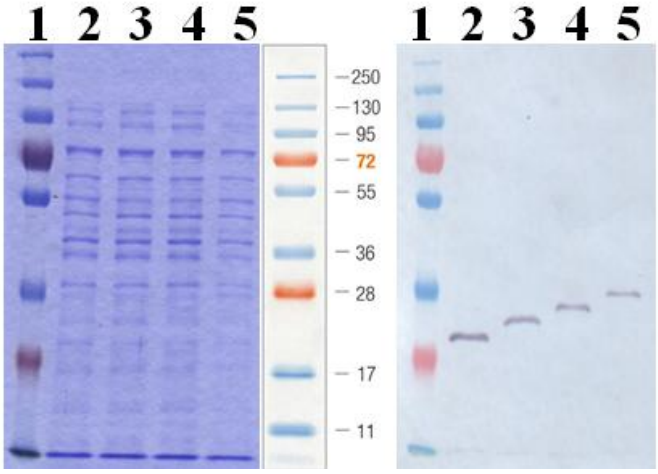

Figure 3.37 : Coomassie staining and western blot results of periplasmic extraction from large-scale production of the bifunctional antibodies in M15[pREP4] cells. Lane 1; Fermentas PageRulerTM plus Prestained protein Ladder (SM1811), Lane 2; Lig7 scFv, Lane 3; Lig7-GBP, Lane 4; Lig7-3GBP, Lane 5; Lig7-5GBP.

Single western blot band was observed for each recombinant antibodies. Therefore, a non-denaturing Cobalt affinity purification was applied to the lysed cell supernatant after a dialysis step against refolding buffer (100mM NaH_2PO_4, 10mM Tris.Cl). But no recovery was obtained (Figure 3.38, Lanes 2 to 5). The remaining pellets containing the inclusion bodies were solubilized with the inclusion body solubilization reagent (Thermo Scientific, Cat.No. 78115) and the elution products are shown in Figure 3.38, Lanes 6 to 9.

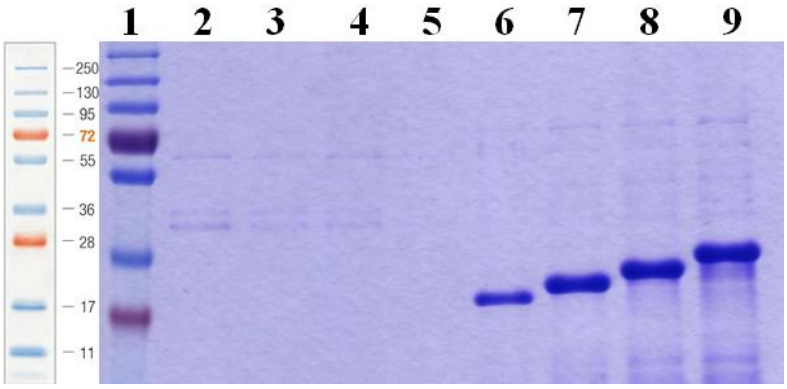

Figure 3.38 : Coomassie staining of Cobalt affinity purified periplasmic extraction (lane 2-5) and solubilized inclusion bodies (lane 6-9) from large scale production of the bifunctional antibodies. Lane 1; Fermentas PageRulerTM plus Prestained protein Ladder (SM1811), Lane 2; Lig7 scFv, Lane 3; Lig7-GBP, Lane 4; Lig7-3GBP, Lane 5; Lig7-5GBP, Lane 6; Lig7 scFv, Lane 7; Lig7-GBP, Lane 8; Lig7-3GBP, Lane 9; Lig7-5GBP.

High amount of recombinant antibody having ~90% purity, determined by the bioanalyzer instrument, was obtained from the inclusion body solubilization, therefore, this method was chosen for further experiments.

The affinity column purified denatured recombinant antibodies were then subjected to refolding process by successive 1/2 dilutions (Yang et al., 2011). For this purpose successive dilutions of the solubilized recombinant antibodies was done with dilution buffer (DB) (100 mM NaH_2PO_4, 10 mM Tris-Cl) until Urea concentration reached 2 M Then, for a correct disulphide bonds formation within the antibody structure a red-ox environment was generated with reduced and oxidized glutathione (GSH 2 mM, GSSG 0.4 mM). The prevention of recombinant antibody precipitation was planned by adding L-Arginine for a final concentration of 400 mM. The same red-ox and L-Arginine conditions were followed until the Urea concentration was decreased to 0.5M. Finally all the additives were removed from the recombinant antibody solution

by dialysis against Tagzyme Buffer (20 mM sodium phosphate, pH 7.0; 150 mM NaCl) necessary for the TAGZyme digestion (His tag removal). But at that step the recombinant antibodies tended to aggregate. Therefore, to prevent aggregation several different dialysis conditions were tested. The different conditions are indicated in Table 3.3.

Table 3.3 : Refolding parameters of Lig7-GBP.

Buffers	Original Buffer pH	Buffers Final pH	Precipitation	Volume before dialysis (µL)	Volume after dialysis (µL)
Dilution Buffer (DB)	5.65	10.0	No	400	465
DB + 400 mM L-Arg	10.0	10.0	No	400	395
DB + 0.5 M Urea	5.9	10.0	No	400	425
DB+400 mM L-Arg + 0.4% Triton X100	10.0	10.0	No	400	475
DB +0.5 M Urea,+ 0.4% Triton X100	5.9	10.0	No	400	525
DB+0.5 M Urea+ 400 mM L-Arg	5.95	8.0	No	400	480
DB+ 0.5 M Urea+ 400 mM L-Arg	5.95	6.3	No	400	440
Tagzyme Buffer	4.17	10	Yes	400	-

Because the recombinant antibodies were tending to aggregate in TAGZyme Buffer. It was decided to finish first the refolding process in DB than dialysing against TAGZyme buffer just before the His-Tag removal process.

It is known that L-Arginine, when provided at 400 mM concentration is protecting proteins from aggregation. Another reason for aggregation is having lower pH value. Therefore, the pH value of the recombinant antibody solution (DB + 0.5 M urea + 400 mM L-Arg) just before dialysis was measured and a pH of 10.0 was determined. According to this measurement, the pH of the different DBs were set at pH 10.0. The effect of 0.5 M urea, 400 mM L-Arginine and 0.4% Triton X100. The recombinant antibody solution was also dialyzed against the initial DB containing 0.5 M urea, 400 mM L-Arg but at different pH such as pH 8.0 and pH 6.3.

After dialysis, no visible aggregation particles were observed for all the dialysis except for the TAGZyme buffer. The dialysis tubes were centrifuged for harvesting

the aggregate and the supernatant was loaded on 12% Acrylamide gel to control the soluble recombinant antibodies. The gel was then stained with Coomassie (Figure 3.39).

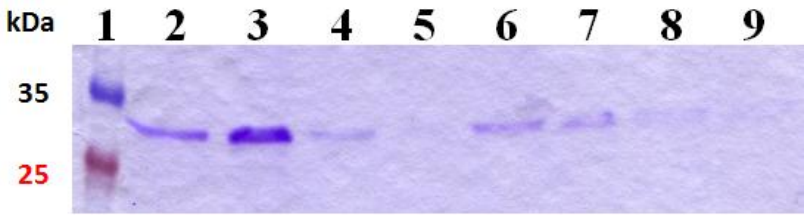

Figure 3.39 : Coomassie staining results of Lig7-GBP after different dialysis conditions. Lane 1; Marker, Thermo Scientific 26619, Lane 2; DB + 0.5 M Urea + 400 mM L-Arg, pH10.0, Lane 3; DB alone, pH10.0, Lane 4; DB + 400 mM L-Arg, pH10.0, Lane 5; DB + 0.5 M urea, pH10.0, Lane 6; DB + 400 mM L-Arg + 0.4% Triton X100, pH10.0, Lane 7; DB + 0.5 M Urea + 0.4% Triton X100, pH10.0, Lane 8; DB + 0.5 M Urea + 400 mM L-Arg, pH8.0, Lane 9; DB + 0.5 M Urea + 400 mM L-Arg, pH6.3.

The Coomassie staining results showed that the decrease of pH value to pH8.0 and pH6.3 in DB caused also aggregation even if it was not visible with bare eyes. Interestingly, the dialysis against DB at pH10.0 showed higher solubilized recombinant antibody amount. Therefore, a higher volume of recombinant antibody was dialyzed (3 mL) against DB at pH10.0. But this time the precipitation was visible. This might be because the amount of protein present in the mediım was higher. Even though, the solution was filtered through a 0,22µm filter and controlled with SDS-PAGE for determining if soluble recombinant antibodies were present is the solution. Unfortunately, no protein was seen on the gel. Then the solution was 74 fold concentrated and loaded on SDS-PAGE (Figure 3.40).

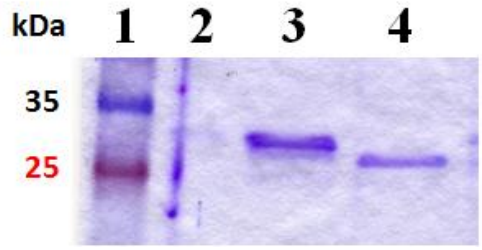

Figure 3.40 : Coomassie staining of concentrated soluble Lig7 and Lig7-GBP, Lane 1; Ladder, Thermo scientific, Cat.No. 26619, Lane 2; empty, Lane 3; Lig7-GBP, Lane 4; Lig7 scFv.

After the concentration process, soluble Lig7 and Lig7 GBP bands were visible on SDS-PAGE. A part of the remaining soluble recombinant antibodies was dialyzed against TAGZyme buffer but presipitation occurred again. Therefore, the remaining solution was used for His-tag removal, as it is. The pH of the DB containing the recombinant proteins was brought to pH6.0-7.0, the optimum pH value for the DAPase enzyme according to the manufacturer instructions (TAGZyme handbook, Qiagen). Then His-tag digestion was initiated and aliquots were taken after 15, 30 and 45 minutes. The digestions were controlled on SDS-PAGE (Figure 3.41).

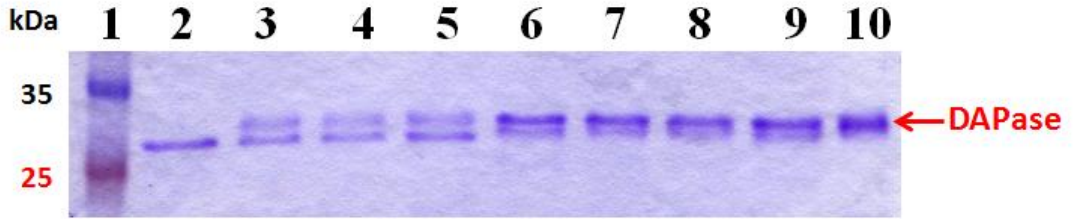

Figure 3.41 : Coomassie staining of DAPase digestion products, 1; Ladder, Thermo scientific, Cat.No. 26619, Lane 2; Lig7 scFv, Digestion time: Lane 3; 15 min, Lane 4; 30 min, Lane 5; 45 min, Lane 6; Lig7-GBP, Digestion time: Lane 7; 15 min, Lane 8; 30 min, Lane 9; 45 min, Lane 10; DAPase enzyme.

Unfortunately, not any digestion products were observed with the Coomassie staining. This is probably because of the very high sensitivity of DAPase enzyme to its environment and a very narrow optimum pH value. Therefore, the use of DB buffer instead of the TAGzyme buffer even if the composition was similar was not sufficient to provide the optimum environment to the enzyme or maybe the enzyme itself was not properly working.

The cause of stability of the recombinant antibodies was researched, because Lig7 scFv was expressed and easily purified from the periplasmic region of the HB2151 *E.coli* strain by using the pDUCK1 phagemid vector. But the His-Tag present on Lig7 scFv expressed from pDUCK1 was at the C-terminal of the scFv. In contrary because of the TAGZyme system requirement the His-tag was fused at the N-terminal of Lig7 scFv which might have unstabilized the scFv.

Even if the His-tag was not been able to cut from the recombinant antibodies. Their use as biosensing probe was tested.

3.3 The use of the recombinant antibodies as a biosensing probe

3.3.1 Binding studies using Surface Plasmon Resonance spectroscopy

HBV infects human hepatocytes. HBV infection results in the release of infectious virions and excessive hepatitis B surface antigens (HBsAg) from host cells to the blood-stream. Therefore, the presence of HBsAg in circulating blood is an indicator of HBV infection. ELISA kits are widely used throughout the world to detect HBsAg, but it takes approximately 3 hours to have the results and labeled antibodies are necessary with these systems. Therefore, the development of new fast diagnosis systems are of great interest. Surface plasmon resonance spectroscopy is a method allowing a label-free, real-time monitoring of protein-protein interactions (Gopinath et al., 2014; J. Homola, 2008; Ladd, Taylor, Piliarik, Homola, & Jiang, 2009). This method can be used as diagnostic is also faster compared to ELISA. With all these advantages, this method has great potential to be the successor of ELISA-based diagnostic methods.

For the purpose of developing a new biosensor system, the gold binding anti-HBsAg recombinant antibody was tested as a biosensing probe on the SPR instrument. The binding of the bifunctional antibodies to gold coated sensor chip was monitored at various antibody concentrations (0.2 µM, 0.3 µM, 0.4 µM and 0.6 µM) with the Reichert SPR instrument. The measurements for all three antibodies were analyzed with BIAevaluation Software 4.1 (Biacore) and plotted on graphs (Figure 3.42, Figure 3.43 and 3.44).

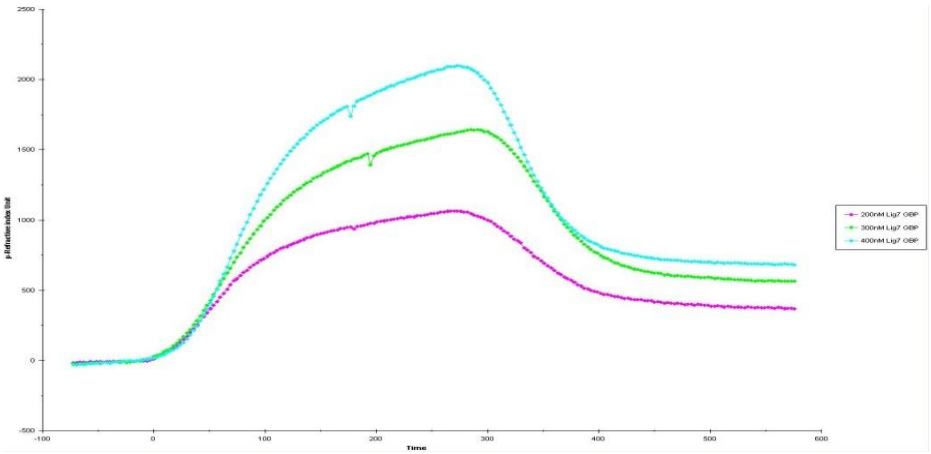

Figure 3.42 : SPR binding sensograms of Lig7-GBP on gold coated sensor chip. Cyan; 0.4 µM, Green; 0.3 µM, Purple; 0.2 µM.

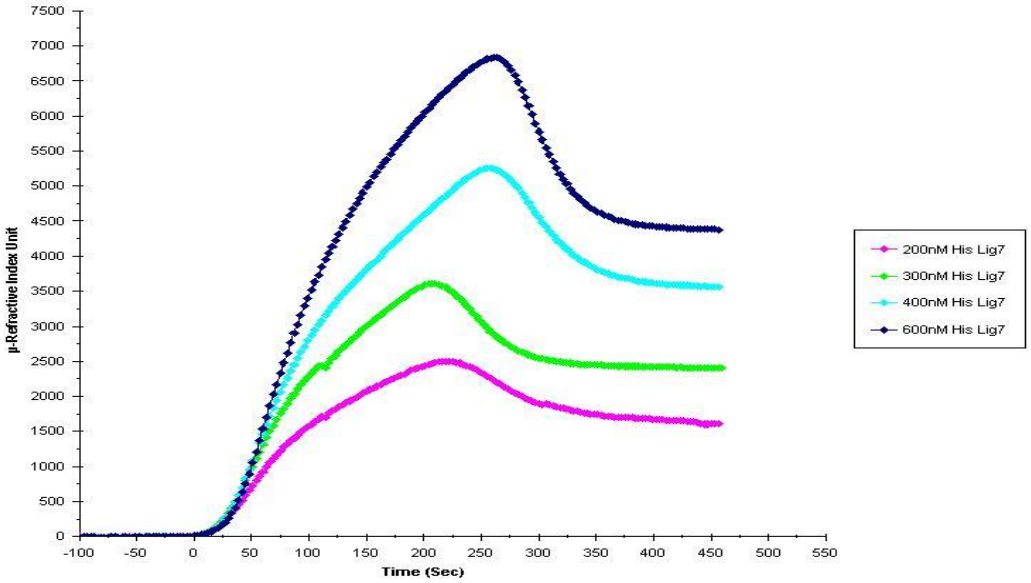

Figure 3.43 : SPR binding sensorgrams of Lig7-3GBP on gold coated sensor chip. Dark Blue; 0.6 μM, Cyan; 0.4 μM, Green; 0.3 μM, Purple; 0.2 μM.

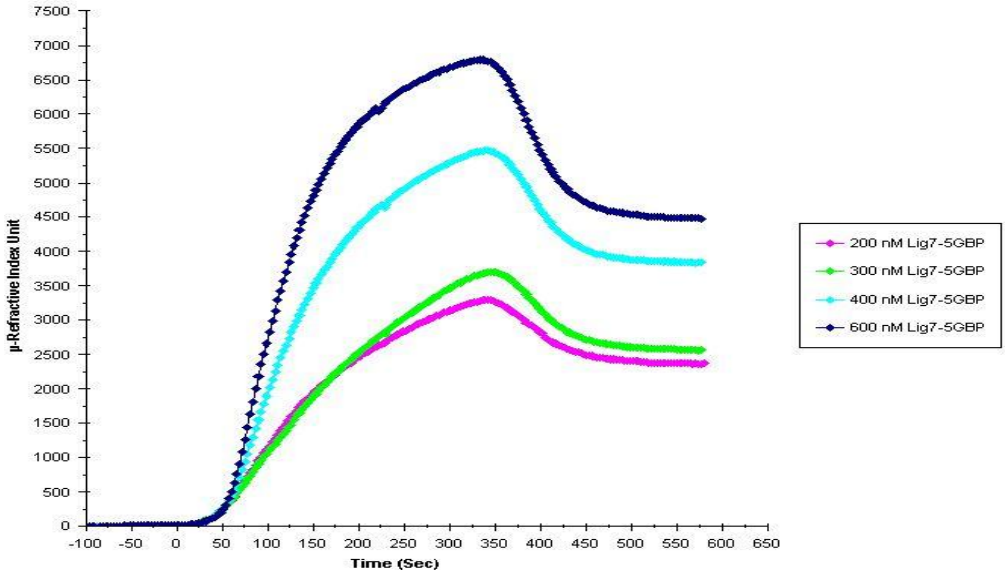

Figure 3.44 : SPR binding sensorgrams of Lig7-5GBP on gold coated sensor chip. Dark Blue; 0.6 μM, Cyan; 0.4 μM, Green; 0.3 μM, Purple; 0.2 μM.

The sensograms show that all the bifunctional antibodies were adsorption to the gold coated SPR sensor chip. But also a strong desorption is observed for higher concentration. This desorption might be due to the presence of misfolded or unfolded antibodies generated during the antibody purification and refolding step. The refractive index unit of the uptake (the maximum μRIU observed during the loading of the antibodies) and the adsorption (the lower μRIU observed after the washing of the antibody loaded sensor chip) were deduced from the sensograms as indicated in

Figure 3.45. The uptake and adsorption values are given in Figure 3.46 and Figure 3.47.

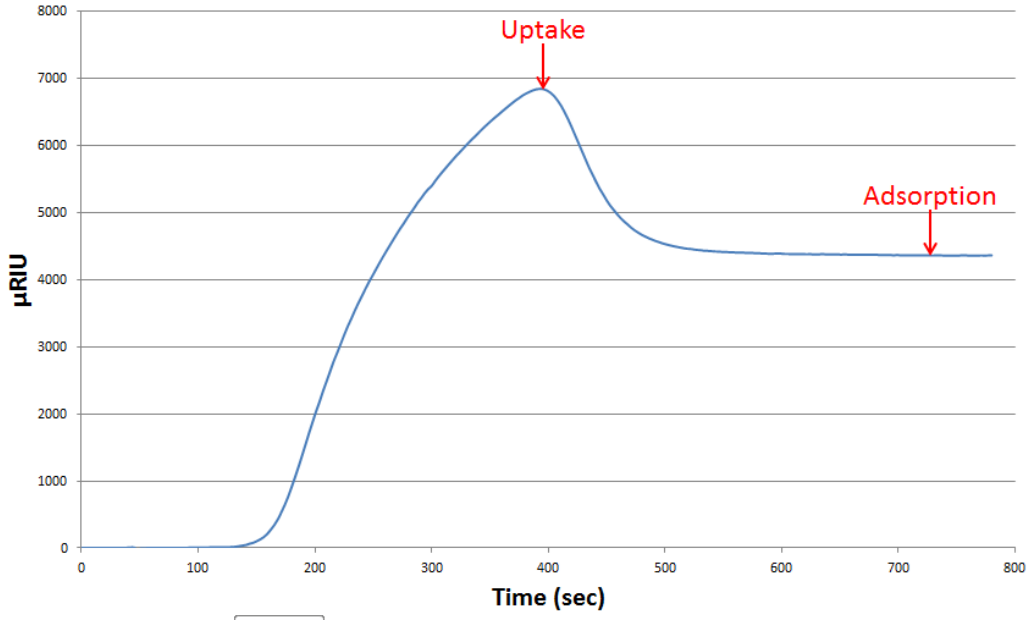

Figure 3.45 : Figure describing the uptake and the adsorption values of the bifunctional antibodies flown on the gold-coated SPR sensor chip.

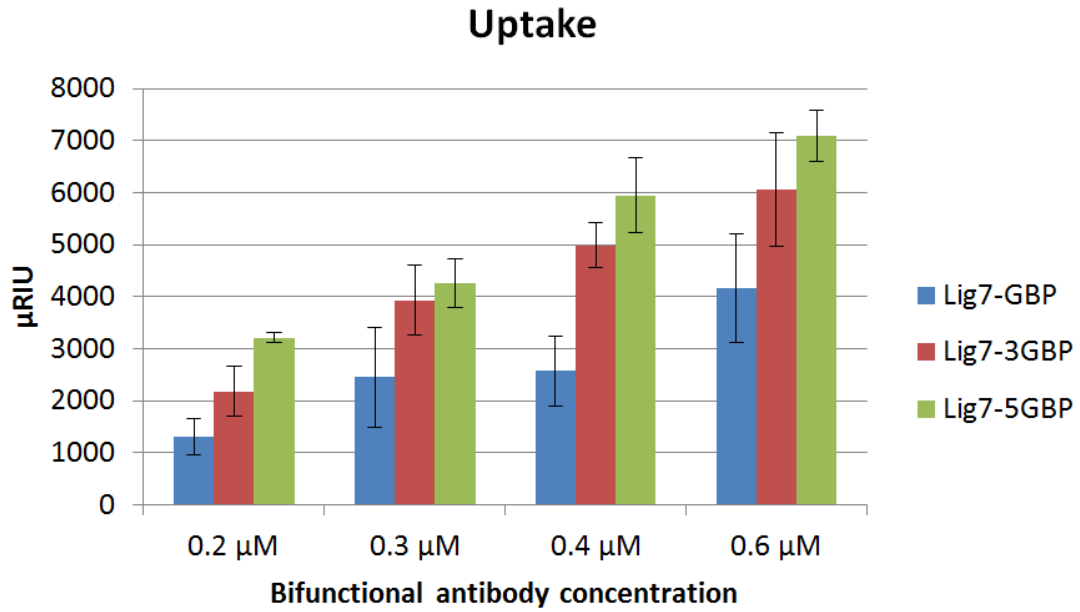

Figure 3.46 : The uptake of the fusion recombinant antibodies on gold coated SPR sensor chip in refractive index unit.

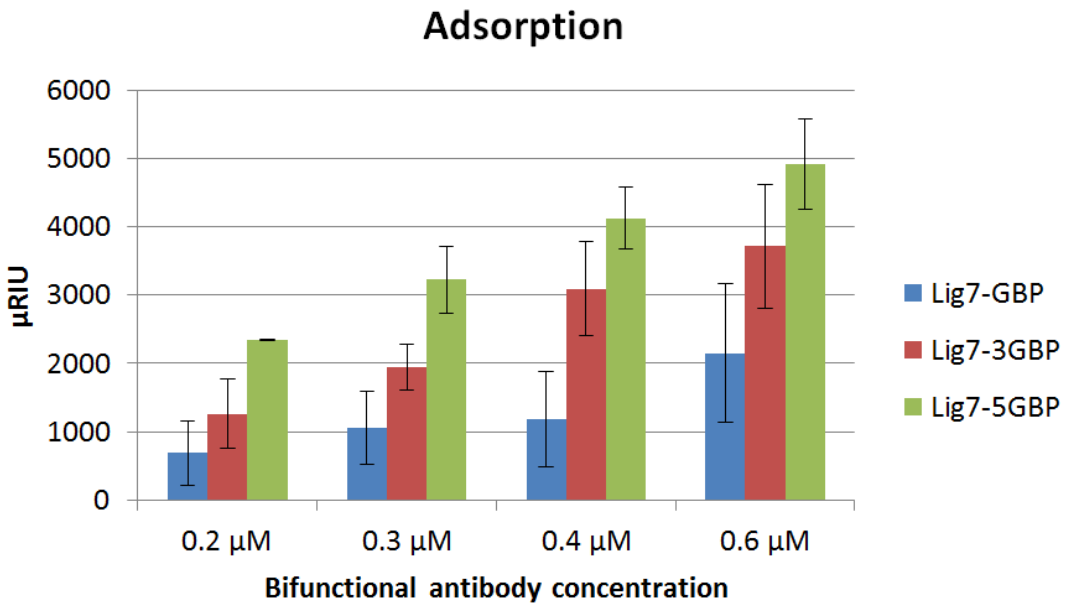

Figure 3.47 : The adsorption of the fusion recombinant antibodies on gold coated SPR sensor chip in refractive index unit.

The uptake and the adsorption values obtained from the SPR sensograms show that these values are dependent on the antibody concentration. The higher is the concentration, the higher is the uptake and the adsorption value. The µRIU ratio calculated between 0.2 µM and 0.6 µM for each bifunctional antibody is varying from 2.21 to 3.17 for the uptake and from 2.1 to 3.12 for the adsorption was observed (Table 3.4). These results show that the µRIU ratio, for 0.6µM/0.2µM antibody ratio, between the uptake and the adsorption is conserved. Therefore, the amount of antibody adsorbed on the surface of the sensor chip is proportional to the antibody flown over the chip. This correlation was expected, and these results showed that the sensor chip was still not fully covered with the antibodies at 0.6 µM concentration.

Since the concentration ratio between 0.2 µM and 0.6 µM is 3 and uptake and adsorption ratio of 3 was expected, in the case of the sensor chip not fully covered. But the results in Table 3.4 shows that even if the uptake and the adsorption ratios for Lig7-GBP are close to 3, the uptake and adsorption ratios are lower than 3 for Lig7-3GBP and Lig7-5GBP. These results indicate that the higher is the size of the antibody flow over the sensor chip the lower is the adsorption rate.One effect for such result might be due to the molecular weight increase, as with the increased molecule size, the steric hindrance effect might be increasing. This may result in adsorption of fewer antibody on the sensor chip surface.

Table 3.4 : The µRIU ratio between 0.2 µM and 0.6 µM antibody concentrations (0.6µM/0.2µM) for the uptake and the adsorption.

	Uptake ratio	Adsorption ratio
Lig7-GBP	3,17	3,12
Lig7-3GBP	2,78	2,94
Lig7-5GBP	2,21	2,10

The SPR sensograms showed that the bifunctional antibodies were adsorbed on the surface of the gold coated SPR sensor chip. The next step was to control if the HBsAg was able to bind to the bifunctional antibodies adsorbed on the sensor chip. For this purpose 0.3µM of recombinant antibodies were flown on the sensor chip then the chip was washed with PBS (3.2 mM Na2HPO4 × 2H2O, 1.4 mM KH2PO4, 2.7 mM KCl and 137 mM NaCl). Once the RIU signal became stabilized, HBsAg at different concentrations (100 nM, 150 nM and 200 nM) was flown over the chip and the binding profile of HBsAg to the bifunctional antibodies was monitored (Figure 3.48 and 3.49).

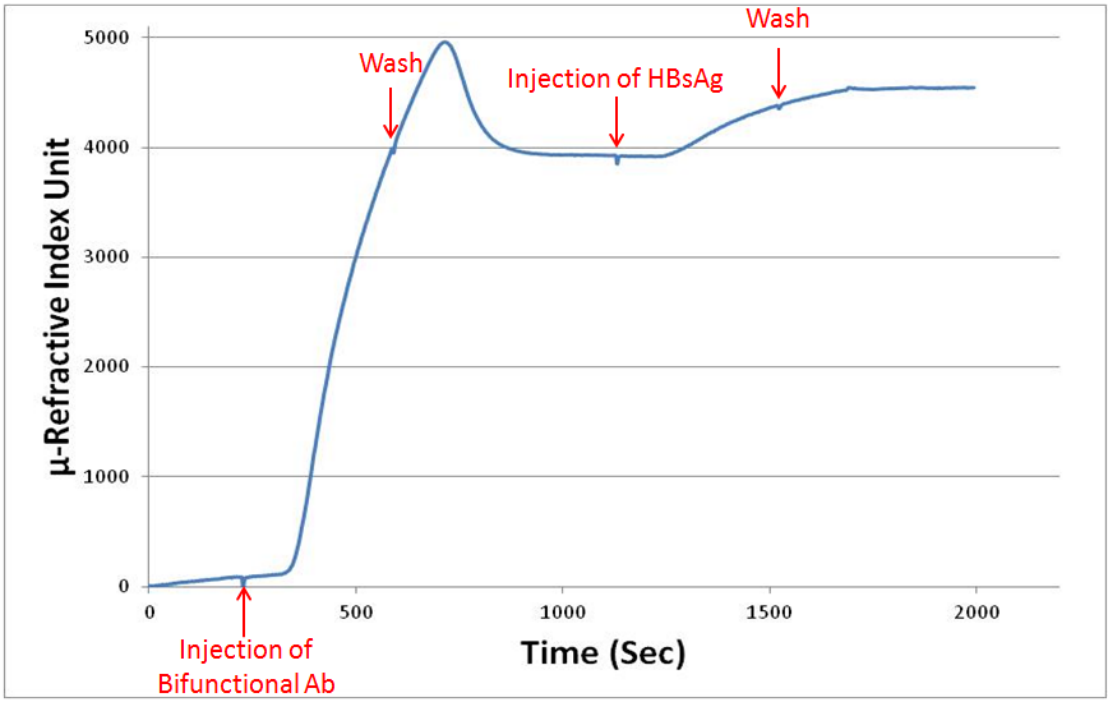

Figure 3.48 : SPR sensorgram of Lig7-GBP (0.3µM) adsorption on the sensor chip and the binding of HBsAg binding to Lig7-5GBP.

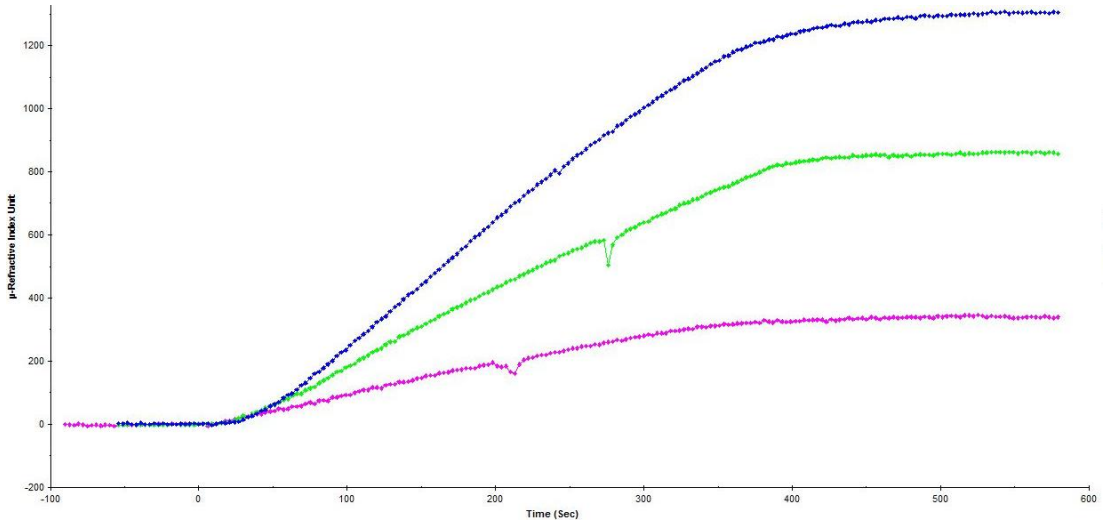

Figure 3.49 : SPR sensorgram of HBsAg binding to Lig7-5GBP adsorbed on the sensor chip. The bifunctional Lig7-5GBP at 0.3μM concentration was adsorbed on the SPR sensor chip. Three different HBsAg concentration was flown over the sensor chip (Blue color; 200 nM, Green color; 150 nM, Purple color; 100 nM).

The HBsAg binding SPR sensograms showed that HBsAg was successfully binding to the bifunctional antibodies. The sensograms also showed a very low desorption of HBsAg indicating that HBsAg was strongly bound to the antibodies. These results demonstrated that the gold binding bifunctional antibodies developed in this work were indeed potential biosensing probes.

The affinity measurements (association rate constant (ka, on), dissociation rate constant (k_d, $_{off}$) and equilibrium dissociation constant K_D) of the bifunctional antibodies to gold surface and to HBsAg were deduced from the SPR sensograms by using BIOevaluation 4.1 software from BIACORE. The calculated ka, kd and K_D values are indicated in Table 3.5.

Table 3.5 : Affinity calculations of the bifunctional antibodies.

Bifunctional antibody	**ka ($M^{-1}s^{-1}$)**	**kd (s^{-1})**	**K_D (M)**	**K_D**
Lig7-GBP/Gold	1.96 E04	9.03 E-03	4.61 E-07	0.46 μM
Lig7-3GBP/Gold	1.84 E04	4.31 E-03	2.34 E-07	0.23 μM
Lig7-5GBP/Gold	1.77 E04	3.46 E-03	1.95 E-07	0.19 μM
Lig7-GBP/HBsAg	7.58 E03	2.39 E-03	3.15 E-07	315 nM
Lig7-3GBP/HBsAg	4.23 E04	1.29 E-03	3.05 E-08	30 nM
Lig7-5GBP/HBsAg	1.21 E04	8.01 E-06	6.62 E-10	0.6 nM

According to the SPR based affinity calculations, similar association rate was observed for the binding of Lig7-GBP, Lig7-3GBP and Lig7-5GBP to the gold

surface. But a higher dissociation rate was observed for Lig7-GBP compared to Lig7-3GBP and Lig7-5GBP. Therefore, even if the bifunctional antibodies are binding to gold at the same rate, Lig7-GBP dissociates at a higher rate compared to the two other antibodies. The equilibrium dissociation constants (K_D) show that all the bifunctional antibodies have the same affinity to gold at μM range slightly. When compared with each other, Lig7-5GBP shows the highest and Lig7-GBP the lowest affinity to gold. This difference might be observed because of the higher copy number of GBP1 within the recombinant antibody consequently the interaction of Lig7-5GBP with a gold surface might be stronger. These results are consistent with the results of Tamerler's group on the characterisation of synthesized 3GBP (Seker, 2009; Tamerler, 2006; Tamerler, 2006). Tamerler's group has calculated the Keq value of 3GBP with plain gold surface as ~10^7M-1 (K_D of ~10-7M) and the binding energy as ~-8.0kcal/mol. The similar equilibrium dissociation constant values obtained for each bifunctional antibodies shows that the fusion of the scFv didn't affect the adsorption of GBP to the gold surface.The potential use of the bifunctional antibodies as biosensing probe was tested by monitoring the binding of HBsAg to the bifunctional antibodies adsorbed on the gold-coated SPR sensor chip. The equilibrium dissociation constant K_D varied from 3.15 E-07 M for Lig7-GBP to 6.62 E-10 M for Lig7-5GBP with a K_D of 3.05 E-08 M for Lig7-3GBP. These results indicate that even if the number of GBP1 repeats has not a very significant effect on the adsorption of the bifunctional antibody, it seems that it has a great influence on the binding of HBsAg to the Lig7 scFv. The higher is the number of repeats the better is the binding of HBsAg to Lig7 scFv. Because Lig7 is the same for all the fusion construct the only possible explanation is that the higher is the repeats number, the better is the conformation of the recombinant antibody or the accessibility to its antigen. These results might also be interpreted such that the GBP1 repeats might act as a linker between the scFv and the GBP1 and/or the repeats immobilized on the gold surface favoriting the optimal conformation of the Lig7 scFv.

Kacar (2009) have developed alkaline phosphatase (AP) with N-terminally fused multiple tandem repeats (n=5, 6, 7 and 9) of GBP1. These gold binding AP fusion molecules were immobilized on the gold surface by adsorption. In that work it was shown that the best AP activity with the highest gold binding ability was obtained with the 5GBP-AP fusion protein and the equilibrium dissociation constant of

5GBP-AP on bare Au gold surface was determined as ~6 nM (Kacar, 2009) . These findings showed that high repeats number (more than 6 repeats) of GBP1 might also have a negative effect on the fusion-protein functions caused by a steric effect generated by the large number of GBP1 repeats. Taken together, all these data show that a gold binding protein fusion construct comprising 5 repeats of GBP1 might be the most appropriate repeats number for an optimal adsorption to gold and a better conformation of the fused protein.

Lig7 was also chemically immobilized on gold coated sensor chip. The affinity of chemically immobilized Lig7 was calculated by flowing various concentrations of HBsAg (50, 100 and 200 nM) on the sensor chip. According to the SPR measurements, an affinity constant (KD) of 31.4 ± 21.4 nM was determined for the binding of HBsAg to the Lig7 scFv. This KD value is 10 times lower than the Lig7 GBP KD value in consequence HBsAg is binding with better affinity to chemically immobilized Lig7 than Lig7-GBP adsorbed on the sensor chip. This result straightens the hypothesis that one GBP1 copy is not sufficient to bind to the gold surface and to maintain the conformation for the fused Lig7 scFv. In the case of Lig7-3GBP fusion construct compared with chemically immobilized Lig7, the KD values are similar, ~30 nM for Lig7-3GBP and ~31 nM for chemically immobilized Lig7. But a 50 times lower KD was observed for Lig7-5GBP compared to chemically immobilized Lig7 for HBsAg binding. Therefore, it seems that HBsAg is more accessible to the Lig7 immobilized on the gold surface via the 5 repeats of gold binding peptide than the chemically immobilized Lig7 scFv.

These results demonstrate that the gold binding bifunctional Lig7 scFv recombinant antibody is adsorbed on plain gold surface and that the number of GPB1 copy does not excessively influence the binding affinity of the construct to gold. In contrary the number of GBP1 copy number has a great influence on presenting the recombinant antibody on the surface of the gold coated sensor chip in the way of favorising the conformation of the scFv as the GBP1 copy number increases.

All these finding are consolidating the hypothesis that the gold binding bifunctional recombinant antibody is immobilized on the surface of plain gold coated sensor chip allowing the correct orientation of the scFv on the sensor chip. In consequence, this construct increases the accessibility of HBsAg to the scFv. Therefore, this self-assembled bifunctional antibody allows a more accurate label-free biosensing probe compared to chemically immobilized antibody-based biosensing devices.

3.3.2 Monitoring HBsAg in *in-vitro* model

In the aim of monitoring HBsAg in mammalian cells. First HBsAg encoding gene was cloned into a mammalian expression vector pCEP4. Then the vector was used for transfection of 4 different mammalian cells lines (HeLa, Hek293 Trex, HepG2 and COS7). One week later the culture medium were collected, and the presence of HBsAg was checked by ELISA (Figure 3.50).

		OD_{405}	
A	Positive control	1.395	
B	Medium of transfected HeLa cells	2.894	
C	Medium of transfected Hek293Trex cells	2.567	
D	Medium of transfected HepG2 cells	0.342	
E	Medium of transfected COS7 cells	0.143	
F	Medium of HeLa cells	0.099	
G	Medium of Hek293Trex cells	0.106	
H	Negative control	0.104	

Figure 3.50 : ELISA results of HBsAg for culture medium of different mammalian cells after transfection.

ELISA results showed that all the transfected cell lines were expressing HBsAg, but COS7 cells were expressing the least with an OD_{405} value of 0.143. THe ELISA results show that HeLa and Hek293 Trex cells were expressing the best with an OD_{405} value of 2.894 and 2.567, respectively. Because HeLa cells were expressing the best, this cell line was selected for further experiments.

Once the HBsAg expression in mammalian cells was confirmed a new transfection was done into HeLa cells grown on sterile coverslips. Twenty-four hours after transfection the growth medium was replaced with fresh medium containing 200 µg Hygromycin B. Then previously expressed Lig7 scFv, mcherry (fluorescent protein) or Lig7-mcherry fusion construct were added to the wells and cells were incubated for 24 hours. The cells were then fixed with methanol, and the nuclei were stained with Hoechst dye. The cell preparations were observed under fluorescence microscope (Figure 3.51 and 3.52).

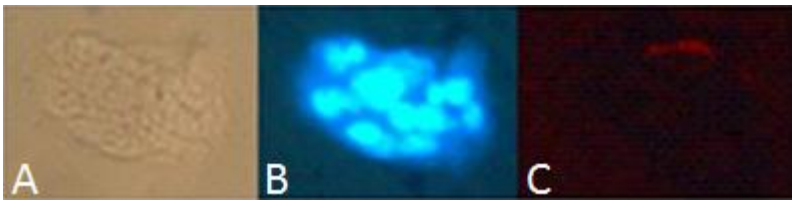

Figure 3.51 : Fluorescence microscope images (10X) of HeLa cells transfected with HBsAg-pCEP4 vector. A; Bright Field, B; A4 filter, C; RFP filter.

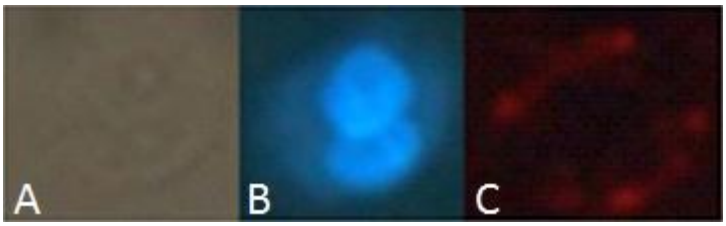

Figure 3.52 : Fluorescenct microscope images (40X) of HeLa cells transfected with HBsAg-pCEP4 vector. A; Bright Field, B; A4 filter, C; RFP filter.

The fluorescence microscopy analysis of the transfected HeLa cells incubated with either Lig7 scFv or mcherry proteins resulted with no fluorescence signal as expected. But the accumulation of the Lig7-mcherry fluorescent recombinant antibodies was observed as spots on the surface of some cells (Figure 3.51 and 3.52). These results showed that HBsAg expressed from HeLa cells were able to be monitored with the Lig7 scFv fused with the fluorescent protein mcherry. These results are indicating that the monitoring of HBsAg expression by using the bifunctional gold binding recombinant antibodies is a possible issue.

4. CONCLUSIONS AND RECOMMENDATIONS

The detection of target molecule by using biological sensing probes is well adapted over the last decades for medical, military, food and environmental applications. Antibodies,i.e. the main biosensing probes, are widely used due to their high and specific affinity to the target molecules. Researches therefore have been mainly focused on either the development of antibodies with better or more specific binding ability or the development of novel ultrasensitive, reliable and cost effective devices. The constant progress in technology leads to the development of new devices but brings also high competition between technological companies.

Regarding the antibody part, the development of new antibodies with higher affinity and specificity than the ones already in the market, becomes more and more difficult. One of the major area left unsloved needs a high attention and get placed under emergent technologies. The coupling methodology of the antibodies on surfaces relies on mainly carbodiimide chemistry, which is a chemical coupling method focused on amino- or carboxyl- groups present on the proteins. Even if this coupling system has great advantages such as covalently coupling antibodies to sensor surfaces hence limiting the antibody leakage as well as the chemicals used might modify the structure of the antibodies. Moreover, such coupling would lead to unoriented coupling of the antibodies. Because several amino- or carboxy- groups might be present on the antibodies, especially at the recognition sites, non specific covalent bonds might be generated at the time of coupling, between the antibody binding sites and the sensor surface leading to unfunctional antibodies.

The recombinant antibody technology has allowed to modify amino acid composition in the intention of developing self-assembled oriented antibodies by adding a cysteine amino acid at the C-terminal end of the antibody heavy chains thereby allowing a coupling between SH groups from the antibody and the ones coated on the sensor surface (Sukhanova, 2012). Other strategies were also successfully done by direct EDC/NHS cross-linking proteins such as protein A or protein G with antibody binding ability to the biosensor chip. Or by linking the

protein G to a single strand DNA and allowing the hybridization with the complementary single strand DNA immobilized on the sensor chip (Wang, 2003; Song, 2011; Jung, 2011; Lee, 2011) . Even if these methods were successful orienting antibodies, they still needed chemical cross-linking steps for immobilizing either the proteins A/G or the DNA.

This thesis provides a new strategy for developing oriented antibody immobilization using biological self-assembly approach on SPR chip for biosensor applications. This approach offers unique strength to control the orientation of the antibody while using a single step surface functionalization under bio-friendly environment without harsh chemicals. For this purpose a well characterized Gold binding peptide (GBP-1) by Prof. Dr. Candan Tamerler's group was selected to be used as molecular linker between the antibody and the gold coated sensor chip. The GBP-1 peptide has been demonstrated to show its gold binding and assembly property in several studies done by the same group or others groups. Up to know GBP-1 was genetically fused with alkaline phosphatase enzyme, Huntingtin protein related to Huntington disease and the DNA binding protein TraI, avian influenza surface antigen or a kinase substrate (Sedlak, 2010, Kacar, 2009) .However, in designing single biomolecules having multifunctional domains, the expected functions might not be present or lost due to structural interferences.

We selected a model antibody having a single chain variable fragment recombinant antibody against Hepatitis B virus surface antigen. Hepatitis B virus (HBV) is one of the major causes of chronic Hepatitis, cirrhosis and liver cancer (hepatocellular carcinoma, HCC). Furthermore an excessive amount of hepatitis B surface antigens (HBsAg) is secreted from HBV-infected host cells to the blood-stream, potentially making from it a good HBV infection marker for biosensor applications.

In this thesis, first an anti-HBsAg scFv was developed by using phage display technology. Within the scope of the thesis, a new cost effective mouse immunization procedure was tried out by infecting mice with HBsAg displaying phages. The successful immune response obtained with this strategy was published in "Advances in bioscience and Biotechnology" journal at the very beginning of year 2014. Then a scFv library was constructed from the mRNA encoding antibody light and heavy chains and screened against HBsAg in the intention of selecting anti-HBsAg scFvs. Several antibodies were selected, but none of them was as good as the previously

developed anti-HBsAg Lig7 recombinant antibody. Owing to its better HBsAg binding ability, Lig7 scFv was chosen for the further development of the gold binding bifunctional recombinant antibody.

Once the anti-HBsAg Lig7 scFv was selected for further studies. The lig7 scFv encoding gene was cloned into the pQE2 expression vector. Then GBP1 encoding region was genetically fused with the Lig7 scFv encoding gene. After cloning expereiments, three different clones, each containing different repeat number of GBP-1 (GBP, 3rGBP and 5r GBP), confirmed by DNA sequence analysis, were obtained and each clone were subjected to protein expression. The SDS-PAGE and western blot studies confirmed the successful expression of all the three bifunctional antibodies.

Unfortunately, the expression products were present as inclusion bodies, therefore, several extra purification steps were necessary causing a decrease in the functional antiobdy yield during the purification steps. Thus, inclusion bodies were solubilized then affinity purified with Cobalt affinity columns. The purified recombinant antibodies were refolded and used for SPR experiments. The adsorption of the antibodies on gold coated sensor chip and the bindnig of HBsAg to the antibodies were monitored in real-time. According to the SPR sensograms, the calculated equilibrium dissociation constants (K_D) show that all the bifunctional antibodies have slightly the same affinity with Lig7-5GBP showing the highest and Lig7-GBP showing the lowest affinity to gold. When looked at the binding of HBsAg to the immobilized recomninant bifunctional antibodies significant changes in the equilibrium dissociation constant was observed. The binding of HBsAg to antibodies was increasing with the number of GBP-1 peptide repeats to reach a K_D of 6.62 E-10 M for Lig7-5GBP which is also 50 times lower than the affinity of chemically cross-linked Lig7 to HBsAg.

Two similar works were published during the thesis, in both studies recombinant antibodies were genetically fused with the GBP-1 peptide. The first group developed a bifunctional recombinant antibody comprising of a heavy chain variable region of the human anti-gold antibody as gold immobilizing molecule fused with either scFv or variable heavy chain antibodies specific to hen egg lysozyme, prostate specific antigen, human chorionic gonadotropin or tumor necrosis factor-R (Ibii, 2010). The group has shown as we have done, that using gold binding protein structures fused

with antibody were increasing the binding efficiency of the immobilized antibodies with its antigen. The group has also measured the gold binding ability of one of their antibodies when the antibody was fused with GBP-1 and its repeats (3GBP and 7GBP). According to their results both three GBP1 based recombinant antibodies were binding at lower affinity compared to their gold binding sensor probes. But no studies were done with 5GBP which, according to our and Dr. Kacar's studies, is the strongest gold binder (Kacar, 2009). And also no further studies regarding the binding ability of the antibody to its antigen were done.

In the literature, one of the study is similar to our research approach. However, this work was based on the genetic fusion of an anti-HBsag scFv fused with a single copy of GBP-1 (Zheng, 2010). Interestingly, the use of a gold binding bifunctional recombinant antibody as a biosensing probe was also confirmed. But no comparative work with different GBP-1 repeats were done and no affinity values were given in the publication.

The results obtained from this work were in correlation with ibii's and Zheng's publications regarding the great potential of using genetically fused gold binding bifunctional antibodies as self-assembled and oriented biosensing probes for the detection of disease related proteins.

The results obtained from this thesis are the first quantitative characterization werre completed, i.e. equilibrium dissociation constant data obtained for the binding of an anti-HBsAg scFv fused with GBP-1, 3GBP or 5GBP.

Future directions

The rapid development of nanotechnology has allowed the generation of nanoparticles with various shape and composition. These nanoparticles are currently being studied to be utilized in cancer diagnosis and therapy (Agarwal, 2008; Katz, 2004a). Gold nanoparticles have great advantages compared to other nanoparticles. First gold nanoparticles are easy to produce at the determined size and shape; they have no toxic effect on cells and they can be coated easily with biomolecules such as proteins and DNA. Gold nanoparticles have also great physical properties, which make it suitable for imaging systems; gold has light scattering and Plasmon resonance properties.

Because of these properties, gold nanoparticles are extensively studied for the detection of different cell types by combining these particles with detecting agents such as antibodies, recombinant antibodies or peptides (El-Sayed, 2005; Katz, 2004b; Tkachenko, 2005). Recently, antibody conjugated gold nanoparticles have been used for the cancer therapy. Cancer cell targeted gold nanoparticles were heated with Infrared laser or radio frequency until the destruction of cancer cells (Gannon, 2008; Huang, 2008). According to our knowledge, no study is done regarding targeted *in-vivo* diagnostic systems by using self assembled oriented bifunctional recombinant antibodies. Therefore, the use of the recombinant antibodies developed during this thesis for the development of a new in-vivo imaging or therapeutic systems based on gold nanoparticles is intended. For this purpose cell lines such as HeLa and Hek293 expressing HBsAg, were already developed during the thesis.

REFERENCES

Agarwal, A., Saraf, S., Asthana, A., Gupta, U., Gajbhiye, V., and Jain, N. K. (2008). Ligand based dendritic systems for tumor targeting. *International journal of pharmaceutics, 350,* 3-13.

Arya, S. K., Solanki, P. R., Datta, M., and Malhotra, B. D. (2009). Recent advances in self-assembled monolayers based biomolecular electronic devices. *Biosensors and Bioelectronics, 24,* 2810-2817.

Ayala, M., Balint, R., Fernandezdecossio, M., Canaan-Haden, L., Larrick, J., and Gavilondo, J. (1995). Variable region sequence modulates periplasmic export of a single-chain fv antibody fragment in escherichia-coli. *Biotechniques, 18,* 832- 842.

Balcioglu B. K., Ozdemir-Bahadir, A., Hinc, D., Tamerler, C., and Erdag, B. (2014). Cost Effective Filamentous Phage Based Immunization Nanoparticles Displaying a full-length hepatitis B virus surface antigen. *Advances in Bioscience and Biotechnology, 5 (1),* 46-53.

Barbas, C., Bjorling, E., Chiodi, F., Dunlop, N., Cababa, D., and Jones, T. (1992). Recombinant human fab fragments neutralize human type-1 immunodeficiency virus in-vitro. *Proceedings of the National Academy of Sciences of the United States of America, 89,* 9339-9343.

Barbas, C., Kang, A., Lerner, R., and Benkovic, S. (1991). Assembly of combinatorial antibody libraries on phage surfaces - the gene-iii site. *Proceedings of the national academy of sciences of the united states of america, 88,* 7978-7982.

Benhar, I. (2001). Biotechnological applications of phage and cell display. *Biotechnology Advances, 19,* 1-33.

Binning, J. M., Leung, D. W., and Amarasinghe, G. K. (2012). Aptamers in virology: recent advances and challenges. *Frontiers in Microbiology, Virology, 3(29),* 1-6.

Bozdayi, G., Turkyilmaz, A. R., Idilman, R., Karatayli, E., Rota, S., Yurdaydin, C., and Bozdayi, A. M. (2005). Complete genome sequence and phylogenetic analysis of hepatitis B virus isolated from Turkish patients with chronic HBV infection. *Journal of Medical Virology, 76,* 476-481.

Braun, R., Sarikaya, M., and Schulten, K. (2002). Genetically engineered gold-binding polypeptides: structure prediction and molecular dynamics. *Journal of Biomaterials Science-Polymer Edition, 13,* 747-757.

Brown, S. (1992). Engineered iron oxide-adhesion mutants of the escherichia-coli phage-lambda receptor. *Proceedings of the national academy of sciences of the united states of america, 89,* 8651-8655.

Brown, S. (1997). Metal-recognition by repeating polypeptides. *Nature Biotechnology, 15*, 269-272.

Brown, S., Sarikaya, M., and Johnson, E. (2000). A genetic analysis of crystal growth. *Journal of molecular biology, 299*, 725-735.

Bruns, M., Miska, S., Chassot, S., and Will, H. (1998). Enhancement of hepatitis B virus infection by noninfectious subviral particles. *Journal of Virology*, 72, 1462-1468.

Cabibbo, A., Sporeno, E., Toniatti, C., Altamura, S., Savino, R., Paonessa, G., and Ciliberto, G. (1995). Monovalent phage display of human interleukin (hil)-6: Selection of superbinder variants from a complex molecular repertoire in the hil-6 D-helix. *Gene, 167*, 41-47.

Celestin, M., Krishnan, S., Bhansali, S., Stefanakos, E., and Goswami, D. Y. (2014). A review of self-assembled monolayers as potential terahertz frequency tunnel diodes. *Nano Research, 7***,** 589-625.

Cesareni, G. (1988). Phage-plasmid hybrid vectors. In R. L. Rodriguez and D. T. Denhardt (Eds.), *Vectors: A survey of molecular cloning vectors and their uses* (pp. 103-111). Stoneham: Butterworth Publishers.

Cetinel, S., Caliskan, H., Yucesoy, D., Donatan, A., Yuca, E., Urgen, M., ….. Tamerler, C. (2013). Addressable self-immobilization of lactate dehydrogenase across multiple length scales. *Biotechnology Journal, 8*, 262-272.

Chasteen, L., Ayriss, J., Pavlik, P., and Bradbury, A. R. (2006). Eliminating helper phage from phage display. *Nucleic Acids Research, 34 (21)*, e145. doi:10.1093/nar/gkl772.

Chechik, V., Crooks, R. M., and Stirling, J. M. (2000). Reactions and Reactivity in Self-Assembled Monolayers. *Advanced Materials, 12*, 1161-1171.

Chen, L., Sheng, Z., Zhang, A., Guo, X., Li, J., Han, H., and Jin, M. (2010). Quantum-dots-based fluoroimmunoassay for the rapid and sensitive detection of avian influenza virus subtype H5N1. *Luminescence, 25*, 419-423.

Chen, Y., Luo, W., Wang, M., Wang, J., Li, L., Yuan, Q., ….. Xia, N. (2007). Isolation of human antibodies against hepatitis E virus from phage display library by immobilized metal affinity chromatography. *Biomedical and Environmental Sciences, 20*, 488-494.

Choi, Y.-H., Lee, G. Y., Ko, H., Chang, Y. W., Kang, M. J., and Pyun, J. C. (2014). Development of SPR biosensor for the detection of human hepatitis B virus using plasma-treated parylene-N film. *Biosensors and Bioelectronics, 56*, 286-294.

Clackson, T., Hoogenboom, H., Griffiths, A., and Winter, G. (1991). Making antibody fragments using phage display libraries. *Nature, 352*, 624-628.

De la Rica, R. & Stevens, M. (2012). Plasmonic ELISA for the ultrasensitive detection of disease biomarkers with the naked eye. *Nature Nanotechnology, 7*, 821-824.

De Wildt, R., Tomlinson, I., Ong, J., and Holliger, P. (2002). Isolation of receptor-ligand pairs by capture of long-lived multivalent interaction complexes. *Proceedings of the National Academy of Sciences of the United States of America, 99*, 8530-8535.

Deng, L. W. & Perham, R. N. (2002). Delineating the site of interaction on the PIII protein of filamentous bacteriophage fd with the F-pilus of Escherichia coli. *Journal of Molecular Biology, 319*, 603-614.

Dimattia, M. A., Watts, N. R., Stahl, S. J., Grimes, J. M., Steven, A. C., Stuart, D. I., and Wingfield, P. T. (2013). Antigenic switching of Hepatitis B virus by alternative dimerization of the capsid protein. *Structure, 21*, 133-142.

El-Sayed, I. H., Huang, X., and El-Sayed, M. A. (2005). Surface plasmon resonance scattering and absorption of anti-EGFR antibody conjugated gold nanoparticles in cancer diagnostics: applications in oral cancer. *Nano letters, 5*, 829-834.

Elliott, C. (2001). Biacore's SPR technology in routine analysis. *Biacore Journal, 2*, 14-15.

Englebienne, P., Van Hoonacker, A., and Verhas, M. (2003). Surface plasmon resonance: principles, methods and applications in biomedical" sciences. *Spectroscopy, 17*, 255-273.

Erdag, B., Balcioglu, B., Bahadir, A., Serhatli, M., Kacar, O., Bahar, A., ….. Baysal, K. (2011). Identification of novel neutralizing single-chain antibodies against vascular endothelial growth factor receptor 2. *Biotechnology and Applied Biochemistry, 58*, 412-422.

Erdag, B., Balcioglu, B. K., Kumbasar, A., and Cirakoglu, B. (2003). Detection of phage displayed peptides with blocking ability in vascular endothelial growth factor (VEGF) model. *Tissue Engineering, Stem Cells and Gene Therapies, 534*, 327-334.

Erdag, B., Balcioglu, K., Kumbasar, A., Celikbicak, O., Zeder-Lutz, G., Altschuh, D., ….. Baysal, K. (2007). Novel short peptides isolated from phage display library inhibit vascular endothelial growth factor activity. *Molecular Biotechnology, 35*, 51-63.

Fields, S. & Song, O. (1989). A novel genetic system to detect protein interactions. *Nature, 340*, 245-246.

Fong, H., White, S. N., Paine, M. L., Luo, W., Snead, M. L., and Sarikaya, M. (2003). Enamel structure properties controlled by engineered proteins in transgenic mice. *Journal of bone and mineral research: the official journal of the American Society for Bone and Mineral Research, 18*, 2052-2059.

Frankel, R. B. & Blakemore, R. P. (1991). *Iron Biominerals*. New York: Plenum Press.

Froussard, P. (1992). A random-PCR method (rPCR) to construct whole cDNA library from low amounts of RNA. *Nucleic acids research, 20*, 2900-2900.

Fuh, G. & Sidhu, S. (2000). Efficient phage display of polypeptides fused to the carboxy-terminus of the M13 gene-3 minor coat protein. *Febs Letters, 480*, 231-234.

Gannon, C. J., Patra, C. R., Bhattacharya, R., Mukherjee, P., and Curley, S. A. (2008). Intracellular gold nanoparticles enhance non-invasive radiofrequency thermal destruction of human gastrointestinal cancer cells. *Journal of nanobiotechnology, 6*, 2.

Gao, X., Huang, Y., and Zhu, S. (1999). Construction of murine phage antibody library and selection of ricin-specific single-chain antibodies. *Iubmb Life, 48*, 513-517.

Gaskin, D., Starck, K., and Vulfson, E. (2000). Identification of inorganic crystal-specific sequences using phage display combinatorial library of short peptides: A feasibility study. *Biotechnology Letters, 22*, 1211-1216.

Giebel, L., Cass, R., Milligan, D., Young, D., Arze, R., and Johnson, C. (1995). Screening of cyclic peptide phage libraries identifies ligands that bind streptavidin with high affinities. *Biochemistry, 34*, 15430-15435.

Goddard, J. M. & Hotchkiss, J. H. (2007). Polymer surface modification for the attachment of bioactive compounds. *Progress in Polymer Science, 32*, 698–725.

Gopinath, S. C. B., Tang, T.-H., Citartan, M., Chen, Y., and Lakshmipriya, T. (2014). Current aspects in immunosensors. *Biosensors and Bioelectronics, 57*, 292-302.

Greenwood, J., Willis, A. E., and Perham, R. N. (1991). Multiple display of foreign peptides on a filamentous bacteriophage. Peptides. *Journal of Molecular Biology, 220*, 821-827.

Griffiths, A. (1993). Building an in-vitro immune-system - human-antibodies without immunization from phage display libraries. *Annales de Biologie Clinique, 51*, 554-554.

Gungormus, M., Branco, M., Fong, H., Schneider, J., Tamerler, C., and Sarikaya, M. (2010). Self-assembled bi-functional peptide hydrogels with biomineralization-directing peptides. *Biomaterials, 31*, 7266-7274.

Gungormus, M., Fong, H., Kim, I. W., Evans, J. S., Tamerler, C., and Sarikaya, M. (2008). Regulation of in vitro calcium phosphate mineralization by combinatorially selected hydroxyapatite-binding peptides. *Biomacromolecules, 9*, 966-973.

Hakami, A. & Ali, A. (2013). Effects of Hepatitis B virus mutations on its replication and liver disease severity. *The Open Virology Journal, 7*, 12-18.

Hall Sedlak, R., Hnilova, M., Gachelet, E., Przybyla, L., Dranow, D., Gonen, T., ….. Traxler, B. (2010). An engineered DNA-binding protein self-assembles metallic nanostructures. *Chembiochem: a European journal of chemical biology, 11*, 2108-2112.

Harkisoen, S., Arends, J. E., van Erpecum, K. J., van den Hoek, A., and Hoepelman, A. I. (2012). Hepatitis B viral load and risk of HBV-related liver disease: from East to West? *Annals of Hepatology, 11 (2)*, 164-171.

Heiat, M., Ranjbar, R., and Alavian S. M. (2014). Classical and Modern Approaches Used for Viral Hepatitis Diagnosis. *Hepatitis Monthly, 14 (4)*, e17632.

Hnilova, M., Karaca, B. T., Park, J., Jia, C., Wilson, B. R., Sarikaya, M., and Tamerler, C. (2012). Fabrication of hierarchical hybrid structures using bio-enabled layer-by-layer self-assembly. *Biotechnology and bioengineering, 109*, 1120-1130.

Hnilova, M., Khatayevich, D., Carlson, A., Oren, E. E., Gresswell, C., Zheng, S., ….. Tamerler, C. (2012). Single-step fabrication of patterned gold film array by an engineered multi-functional peptide. *Journal of colloid and interface science, 365*, 97-102.

Hoess, R. (2001). Protein design and phage display. *Chemical Reviews, 101*, 3205-3218.

Hofschneider, P. H. & Preuss, A. (1963). M 13 bacteriophage liberation from intact bacteria as revealed by electron microscopy. *Journal Molecular Biology, 7*, 450-451.

Holliger, P. & Riechmann, L. (1997). A conserved infection pathway for filamentous bacteriophages is suggested by the structure of the membrane penetration domain of the minor coat protein g3p from phage fd. *Structure, 5*, 265-275.

Homola, J. (2008). Surface plasmon resonance sensors for detection of chemical and biological species. *Chemical reviews, 108*, 462-493.

Homola, J. R. & Dostálek, J.. (2006). *Surface plasmon resonance based sensors*. doi:10.1007/b100321.

Hosseini, S., Ibrahim, F., Djordjevic, I., and Koole, L. H. (2014). Recent advances in surface functionalization techniques on polymethacrylate materials for optical biosensor applications. *Analyst., 139*, 2933-2943.

Huang, X. L., Zhang, B., Ren, L., Ye, S. F., Sun, L. P., Zhang, Q. Q., ….. Chow, G. M. (2008). In vivo toxic studies and biodistribution of near-infrared sensitive Au-Au(2)S nanoparticles as potential drug delivery carriers. *Journal of materials science. Materials in medicine, 19*, 2581-2588.

Hwang, G. Y., Lin, C. Y., Huang, L. M., Wang, Y. H., Wang, J. C., Hsu, C.T., ….. Wu, C. C. (2003). Detection of the hepatitis B virus X protein (hbx) antigen and anti-hbx antibodies in cases of human hepatocellular carcinoma. *Journal Clinical Microbiology, 41*, 5598-5603.

Ibii, T., Kaieda, M., Hatakeyama, S., Shiotsuka, H., Watanabe, H., Umetsu, M., ….. Imamura, T. (2010). Direct immobilization of gold-binding antibody fragments for immunosensor applications. *Analytical Chemistry, 82*, 4229-4235.

Irving, M. B., Pan, O., and Scott, J. K. (2001). Random-peptide libraries and antigen fragment libraries for epitope mapping and the development of vaccines and diagnostics. *Current Opinion in Chemical Biology, 5*, 314-324.

Jacobson, A. (1972). Role of F Pili in the Penetration of Bacteriophage fl. *Journal of Virology, 10*, 835-843.

Jespers, L., dekeyser, A., and Stanssens, P. (1996). Lambda ZLG6: A phage lambda vector for high-efficiency cloning and surface expression of cDNA libraries on filamentous phage. *Gene, 173*, 179-181.

Jonsson, U., Fagerstam, L., Ivarsson, B., Johnsson, B., Karlsson, R., Lundh, K., ….. Ronnberg, I. (1991). Real-time biospecific interaction analysis using surface plasmon resonance and a sensor chip technology. *BioTechniques, 11*, 620-7.

Jung, S., Kim, Y., Kim, S. J., Kwon, T.H., Huh, S., and Park, S. (2011). Bio-functionalization of metal-organic frameworks by covalent protein conjugation. *Chemical Communications, 47*, 2904-2906.

Jung, Y., Lee, J., Jung, H., and Chung, B. (2007). Self-directed and self-oriented immobilization of antibody by protein G-DNA conjugate. *Analytical Chemistry, 79*, 6534-6541.

Kacar, T., Zin, M. T., So, C., Wilson, B., Ma, H., Gul-Karaguler, N., ….. Tamerler, C. (2009). Directed self-immobilization of alkaline phosphatase on micro-patterned substrates via genetically fused metal-binding peptide. *Biotechnology and Bioengineering, 103*, 696-705.

Kacar, T., Ray, J., Gungormus, M., Oren, E., Tamerler, C., and Sarikaya, M. (2009). Quartz Binding Peptides as Molecular Linkers towards Fabricating Multifunctional Micropatterned Substrates. *Advanced Materials, 21*, 295-299.

Kang, A., Barbas, C., Janda, K., Benkovic, S., and Lerner, R. (1991). Linkage of recognition and replication functions by assembling combinatorial antibody fab libraries along phage surfaces. *Proceedings of The National Academy of Sciences of The United States of America, 88 (10)*, 4363-4366.

Katz, E. & Willner, I. (2004a). Biomolecule-functionalized carbon nanotubes: applications in nanobioelectronics. *Chemphyschem: a European Journal of Chemical Physics and Physical Chemistry, 5*, 1084-1104.

Katz, E. & Willner, I. (2004b). Integrated nanoparticle-biomolecule hybrid systems: synthesis, properties, and applications. *Angewandte Chemie, 43*, 6042-6108.

Kausaite-Minkstimiene, A., Ramanaviciene, A., Kirlyte, J., and Ramanavicius, A. (2010). Comparative Study of Random and Oriented Antibody İmmobilization Techniques on the Binding Capacity of İmmunosensor. *Analytical Chemistry, 82*, 6401-6408.

Kay, B. K. & Hoess, R. H. (1996). Principles and Applications of Phage Display. In B. K. Kay, J. Winter, J. Mccafferty (Eds.), *Phage Display of Peptides*

and Proteins: a Laboratory Manual (Vol. 1, pp. 21-34). San Diego, CA: Academic Press Inc.

Kjaergaard, K., Sorensen, J., Schembri, M., and Klemm, P. (2000). Sequestration of zinc oxide by fimbrial designer chelators. *Applied and Environmental Microbiology, 66*, 10-14.

Khatayevich, D., Gungormus, M., Yazici, H., So, C., Cetinel, S., Ma, H., ….. Sarikaya, M. (2010). Biofunctionalization of materials for implants using engineered peptides. *Acta Biomaterialia, 6*, 4634-4641.

Kim, T. K., Oh, S. W., Hong, S. C., Mok, Y. J., and Choi, E. Y. (2014). Point-of-Care Fluorescence Immunoassay for Cardiac Panel Biomarkers. *Journal of Clinical Laboratory Analysis, 00*, 1-9. doi:10.1002/jcla.21704.

Koepsel, J. T. & Murphy, W. L. (2012). Patterned Self-Assembled Monolayers: Efficient, Chemically Defined Tools for Cell Biology. *Chembiochem, 13*, 1717-1724.

Krauland, E., Peelle, B., Wittrup, K., and Belcher, A. (2007). Peptide tags for enhanced cellular and protein adhesion to single-crystal line sapphire. *Biotechnology and Bioengineering, 97*, 1009-1020.

Kubar, A., Yapar, M., Ozyurt, M., Haznedaroglu, T., and Gun, H. (1988). Cloning of hepatitis B virus surface gene region to Escherichia coli. *Flora, 6*, 108-113.

Ladd, J., Taylor, A. D., Piliarik, M., Homola, J., and Jiang, S. (2009). Label-free detection of cancer biomarker candidates using surface plasmon resonance imaging. *Analytical and Bioanalytical Chemistry, 393*, 1157-1163.

Lau, D., Ma, H., Lemon, S., Doo, E., Ghany, M., Miskovsky, E., ….. Hoofnagle, J. (2003). A rapid immunochromatographic assay for hepatitis B virus screening. *Journal of Viral Hepatitis, 10*, 331-334.

Lee, J. H., Choi, H. K., Lee, S. Y., Lim, M. W., and Chang, J. H. (2011). Enhancing immunoassay detection of antigens with multimeric protein Gs. *Biosensors and Bioelectronics, 28*, 146-151.

Lee, S., Choi, J., and Xu, Z. (2003). Microbial cell-surface display. *Trends in Biotechnology, 21*, 45-52.

Lee, S., Mao, C., Flynn, C., and Belcher, A. (2002). Ordering of quantum dots using genetically engineered viruses. *Science, 296*, 892-895.

Liedberg, B., Nylander, C., and Lundstrom, I. (1995). Biosensing with surface plasmon resonance--how it all started. *Biosensors & Bioelectronics, 10*, i-ix.

Light, J. & Lerner, R. (1992). Phophabs - antibody-phage-alkaline phosphatase conjugates for one-step ELISA without immunization. *Bioorganic & Medicinal Chemistry Letters, 2*, 1073-1078.

Lin, Y. H., Wang, Y., Loua, A., Day, G. J., Qiu, Y., Nadala, Jr. E. C. B., ….. Lee, H. H. (2008). Evaluation of a New Hepatitis B Virus Surface Antigen

Rapid Test with Improved Sensitivity. *Journal of Clinical Microbiology, 46 (10),* 3319–3324.

Lok, A. S., Heathcote, E. J., and Hoofnagle, J. H. (2001). Management of hepatitis B: 2000-summary of a workshop. *Gastroenterology, 120*, 1828-1853.

Lopez, J. & Webster, R. E. (1983). Morphogenesis of filamentous bacteriophage f1: orientation of extrusion and production of polyphage. *Virology, 127*, 177-193.

Lowman, H., Bass, S., Simpson, N., and Wells, J. (1991). Selecting high-affinity binding-proteins by monovalent phage display. *Biochemistry, 30*, 10832-10838.

Lowman, H. & Wells, J. (1993). Affinity maturation of human growth-hormone by monovalent phage display. *Journal of Molecular Biology, 234*, 564-578.

Lubkowski, J., Hennecke, F., Pluckthun, A., and Wlodawer, A. (1998). The structural basis of phage display elucidated by the crystal structure of the N-terminal domains of g3p. *Nature Structural Biology, 5*, 140-147.

Lucifora, J., Arzberger, S., Durantel, D., Belloni, L., Strubin, M., Levrero, M., ….. Protzer, U. (2011). Hepatitis B virus X protein is essential to initiate and maintain virus replication after infection. *Journal of Hepatology, 55*, 996-1003.

Luo, Z., Li, L., and Ruan, B. (2012). Impact of the implementation of a vaccination strategy on hepatitis B virus infections in China over a 20-year period. *International Journal of Infectious Diseases, 16*, 82-888.

Lusebrink, J., Schildgen, V., and Schildgen, O. (2009). The human Hepatitis B virus-Classification, biology, life cycle, in vitro and in vivo models. In S. Mauss, T. Berg, J. Rockstroh, C. Sarrazin, H. Wedemeyer (Eds.), *Hepatology - A Clinical Text Book* (2nd ed., pp. 37-57). Germany: Flying Publisher.

Maguire, C., Bovenberg, M., Crommentuijn, M., Niers, J., Kerami, M., Teng, J., ….. Tannous, B. A. (2013). Triple Bioluminescence Imaging for In Vivo Monitoring of Cellular Processes. *Molecular Therapy-Nucleic Acids, 2*, e99. doi:10.1038/mtna.2013.25.

Maier, B. (2005). Using laser tweezers to measure twitching motility in Neisseria. *Current Opinion in Microbiology, 8*, 344-349.

Makowski, L. & Russel, M. (1997). *Structure and assembly of filamentous bacteriophages*. New York: Oxford University Press.

Malmqvist, M. (1993). Surface plasmon resonance for detection and measurement of antibody-antigen affinity and kinetics. *Current Opinion in Immunology, 5*, 282-6.

Marques De Oliveira, R., Ferreira, J., Santos, M. J. L., Faria, R. M., and Oliveira, O. N. (2011). Probing the Functionalization of Gold Surfaces and Protein Adsorption by PM-IRRAS. *Chemphyschem, 12*, 1736-1740.

Marvin, D. A. & Hohn, B. (1969). Filamentous bacterial viruses. *Bacteriological Reviews, 33*, 172-209.

Matthews, D. & Wells, J. (1993). Substrate phage - selection of protease substrates by monovalent phage display. *Science, 260*, 1113-1117.

Mayer, G. & Sarikaya, M. (2002). Rigid biological composite materials: Structural examples for biomimetic design. *Experimental Mechanics, 42*, 395-403.

Mccafferty, J., Jackson, R., and Chiswell, D. (1991). Phage-enzymes - expression and affinity-chromatography of functional alkaline-phosphatase on the surface of bacteriophage. *Protein engineering, 4*, 955-961.

Mcconnell, S., Kendall, M., Reilly, T., and Hoess, R. (1994). Constrained peptide libraries as a tool for finding mimotopes. *Gene, 151*, 115-118.

Mcconnell, S., Uveges, A., Fowlkes, D., and Spinella, D. (1996). Construction and screening of M13 phage libraries displaying long random peptides. *Molecular Diversity, 1*, 165-176.

Mead, D. A. & Kemper, B. (1988). Chimeric single-stranded DNA phage-plasmid cloning vectors. In R. L. Rodriguez, D. T. Denhardt (Eds.), *Vectors: A survey of molecular cloning vectors and their uses* (pp. 85-102). Stoneham: Butterworths Publishers.

Melancon, M. P., Lu, W., Yang, Z., Zhang, R., Cheng, Z., Elliot, A., ….. Li, C. (2008). In vitro and in vivo targeting of hollow gold nanoshells directed at epidermal growth factor receptor for photothermal ablation therapy. *Molecular Cancer Therapeutics, 7*, 1730-1739.

Molenaar, T., Michon, I., de Haas, S., van Berkel, T., Kuiper, J., and Biessen, E. (2002). Uptake and processing of modified bacteriophage M13 in mice: Implications for phage display. *Virology, 293*, 182-191.

Morgan, C. L., Newman, D. J., and Price, C. P. (1996). Immunosensors: technology and opportunities in laboratory medicine. *Clinical chemistry, 42*, 193-209.

Murugaiyan, S. B., Ramasamy, R., Gopal, N., and Kuzhandaivelu, V. (2014). Biosensors in clinical chemistry: An overview. *Advanced biomedical research, 3*, 67.

Naik, R., Brott, L., Clarson, S., and Stone, M. (2002). Silica-precipitating peptides isolated from a combinatorial phage display peptide library. *Journal of Nanoscience and Nanotechnology, 2*, 95-100.

Naik, R. R., Stringer, S. J., Agarwal, G., Jones, S. E., and Stone, M. O. (2002). Biomimetic synthesis and patterning of silver nanoparticles. *Nature materials, 1*, 169-172.

Ng, S. A. & Lee, C. (2011). Hepatitis B virus X gene and hepatocarcinogenesis. *J Gastroenterol, 46*, 974-990.

Nicosia, C. & Huskens, J. (2014). Reactive self-assembled monolayers: from surface functionalization to gradient formation. *Materials. Horizon, 1*, 32-45.

Nourani, S., Ghourchian, H., and Boutorabi, S. M. (2013). Magnetic nanoparticle-based immunosensor for electrochemical detection of hepatitis B surface antigen. *Analytical biochemistry, 441*, 1-7.

Oh, G. Y., Kim, D. G., and Choi, Y. W. (2009). The characterization of GH shifts of surface plasmon resonance in a waveguide using the FDTD method. *Optics express, 17 (23)*, 20714-20720.

Oh, M., Joo, H., Hur, B., Jeong, Y., and Cha, S. (2007). Enhancing phage display of antibody fragments using gill-amber suppression. *Gene, 386*, 81-89.

Onda, T., Laface, D., Baier, G., Brunner, T., Honma, N., Mikayama, T., ….. Green, D. R. (1995). A phage display system for detection of T cell receptor-antigen interactions. *Molecular Immunology, 32*, 1387-1397.

Oren, E. E., Tamerler, C., Sahin, D., Hnilova, M., Seker, U. O., Sarikaya, M., and Samudrala, R. (2007). A novel knowledge-based approach to design inorganic-binding peptides. *Bioinformatics, 23*, 2816-2822.

Ozdemir-Bahadir, A., Balcioglu, B. K., Uzyol, K. S., Hatipoglu, I., Sogut, I., Basalp, A., and Erdag, B. (2011). Phage Displayed HBV Core Antigen with Immunogenic Activity. *Applied Biochemistry and Biotechnology, 165*, 1437-1447.

Pannekoek, H., Vanmeijer, M., Schleef, R., Loskutoff, D., and Barbas, C. (1993). Functional display of human plasminogen-activator inhibitor-1 (pai-1) on phages - novel perspectives for structure-function analysis by error-prone DNA-synthesis. *Gene, 128*, 135-140.

Paschke, M. (2006). Phage display systems and their applications. *Applied Microbiology and Biotechnology, 70*, 2-11.

Pasqualini, R. & Ruoslahti, E. (1996). Organ targeting in vivo using phage display peptide libraries. *Nature, 380*, 364-366.

Prashar, D. (2012). Self-Assembled Monolayers -A Review. *International Journal of ChemTech Research, 4 (1)*, 258-265.

Pei, X., Zhang, B., Tang, J., Liu, B., Lai, W., and Tang, D. (2013). Sandwich-type immunosensors and immunoassays exploiting nanostructure labels: A review. *Analytica Chimica Acta, 758*, 1-18.

Rakonjac, J., Bennett, N. J., Spagnuolo, J., Gagic, D., and Russel, M. (2011). Filamentous bacteriophage: biology, phage display and nanotechnology applications. In *Current Issues in Molecular Biology, 13 (2)*, 51-76).

Ramírez, N. N. B., Salgado, A. N. M., and Valdman, B. (2009). The evolution and developments of immunosensors for health and environmental monitoring: problems and perspectives. *Brazilian Journal of Chemical Engineering, 26 (2)*, 227-249.

Rebar, E. & Pabo, C. (1994). Zinc-finger phage - affinity selection of fingers with new DNA-binding specificities. *Science, 263*, 671-673.

Rehermann, B. & Nascimbeni, M. (2005). Immunology of Hepatitis B virus and Hepatitis C virus infection. *Nature Reviews Immunology, 5(3)*, 215-229.

Revill, P., Yuen, L., Walsh, R., Perrault, M., Locarnini, S., and Kramvis, A. (2010). Bioinformatic analysis of the hepadnavirus e-antigen and its precursor identifies remarkable sequence conservation in all orthohepadnaviruses. *Journal of Medical Virology, 82 (1)*, 104-115.

Rickles, R., Botfield, M., Zhou, X., Henry, P., Brugge, J., and Zoller, M. (1995). Phage display selection of ligand residues important for src-homology-3 domain binding-specificity. *Proceedings of the national academy of sciences of the united states of America, 92*, 10909-10913.

Rosander, A., Bjerketorp, J., Frykberg, L., and Jacobsson, K. (2002). Phage display as a novel screening method to identify extracellular proteins. *Journal of Microbiological Methods, 51*, 43-55.

Russel, M., Lowman, H. B., and Clackson, T. (2004). Introduction to phage biology and phage display. In H. B. Lowman, T. Clackson (Eds.), *Phage Display: A Practical Approach* (pp. 1-26). New York, USA: Oxford University Press.

Sambrook, J. & Russell, D. W. (2001). *Molecular Cloning: A Laboratory Manual* (3rd ed.). New York: Cold Spring Harbour Laboratory Press.

Sano, K., Sasaki, H., and Shiba, K. (2005). Specificity and biomineralization activities of Ti-binding peptide-1 (TBP-1). *Langmuir, 21*, 3090-3095.

Sano, K. & Shiba, K. (2003). A hexapeptide motif that electrostatically binds to the surface of titanium. *Journal of the American Chemical Society, 125*, 14234-14235.

Sarikaya, M. & Aksay, I.A. (1992). Nacre of abalone shell: a natural multifunctional nanolaminated ceramic-polymer composite material. *Results and problems in cell differentiation, 19*, 1-26.

Sarikaya, M., Fong, H., Sunderland, N., Flinn, B.D., and Mayer, G. (2001). Biomimetic model of a sponge-spicular optical fiber - mechanical properties and structure. *Journal of Materials Research, 16*, 1420-1428.

Sarikaya, M., Tamerler, C., Jen, A., Schulten, K., and Baneyx, F. (2003). Molecular biomimetics: nanotechnology through biology. *Nature Materials, 2*, 577-585.

Sarikaya, M., Tamerler, C., Schwartz, D., and Baneyx, F. (2004). Materials assembly and formation using engineered polypeptides. *Annual Review of Materials Research, 34*, 373-408.

Scarselli, E., Esposito, G., and Traboni, C. (1993). Receptor phage - display of functional domains of the human high-affinity ige receptor on the M13 phage surface. *Febs letters*, 329, 223-226.

Schadler, S. & Hildt, E. (2009). HBV Life Cycle: Entry and Morphogenesis. *Viruses, 1*, 185-209.

Schier, R., Balint, R., Mccall, A., Apell, G., Larrick, J., and Marks, J. (1996). Identification of functional and structural amino-acid residues by parsimonious mutagenesis. *Gene, 169*, 147-155.

Scott, J. & Smith, G. (1990). Searching for peptide ligands with an epitope library. *Science, 249*, 386-390.

Sedlak, R., Hnilova, M., Gachelet, E., Przybyla, L., Dranow, D., Gonen, T., ….. Traxler, B. (2010). An Engineered DNA-Binding Protein Self-assembles Metallic Nanostructures. *Chembiochem, 11*, 2108-2112.

Seker, U. & Demir, H. (2011). Material Binding Peptides for Nanotechnology. *Molecules, 16*, 1426-1451.

Seker, U. O., Wilson, B., Dincer, S., Kim, I. W., Oren, E. E., Evans, J. S., ….. Sarikaya, M. (2007). Adsorption behavior of linear and cyclic genetically engineered platinum binding peptides. *Langmuir: the ACS journal of surfaces and colloids, 23*, 7895-7900.

Seker, U.O., Wilson, B., Sahin, D., Tamerler, C., and Sarikaya, M. (2009). Quantitative affinity of genetically engineered repeating polypeptides to inorganic surfaces. *Biomacromolecules, 10*, 250-257.

Sun, Y. S. (2014). Optical biosensors for label-free detection of biomolecular interactions. *Instrumentation Science and Technology, 42 (2)*, 109-127.

Sidhu, S. S. (2001). Engineering M13 for phage display. In *Biomolecular Engineering, 18*, 57-63).

Skladal, P., Kovar, D., Krajicek, V., Siskova, P., Pribyl, J., and Svabenska, E. (2013). Electrochemical immunosensors for detection of microorganisms. *International Journal of Electrochemical Science, 8 (2)*, 1635-1649.

Slocik, J., Moore, J., and Wright, D. (2002). Monoclonal antibody recognition of histidine-rich peptide encapsulated nanoclusters. *Nano Letters, 2*, 169-173.

Smith, G. (1985). Filamentous fusion phage - novel expression vectors that display cloned antigens on the virion surface. *Science, 228*, 1315-1317.

Smith, G. (1993). Surface display and peptide libraries - articles occasioned by a meeting at the banbury-center, cold spring harbor laboratory, April 4-7, 1992-Preface. *Gene, 128 (1)*, 1-2.

Smith, G. & Petrenko, V. (1997). Phage display. *Chemical Reviews, 97*, 391-410.

So, C., Hayamizu, Y., Yazici, H., Gresswell, C., Khatayevich, D., Tamerler, C., and Sarikaya, M. (2012). Controlling Self-Assembly of Engineered Peptides on Graphite by Rational Mutation. *Acs Nano, 6*, 1648-1656.

Song, K. M., Cho, M., Jo, H., Min, K., Jeon, S. H., Kim, T., ….. Ban, C. (2011). Gold nanoparticle-based colorimetric detection of kanamycin using a DNA aptamer. *Analytical biochemistry, 415*, 175-81.

Sousa, S., Cardoso, L., Reed, S.G., Reis, A. B., Martins-Filho, O. A., Silvestre, R., and Silva, A. C. (2013). Development of a Fluorescent Based Immunosensor for the Serodiagnosis of Canine Leishmaniasis Combining Immunomagnetic Separation and Flow Cytometry. *PLOS Neglected Tropical Diseases, 7*, e2371.

Starodub, N. F., Arenkov, P. J., Starodub, A. N., and Berezin, V. A. (1994). Fiber optic immunosensors based on enhanced chemiluminescence and their application to determine different antigens. *Sensors and Actuators B: Chemical, 18*, 161-165.

Sukhanova, A., Even-Desrumeaux, K., Kisserli, A., Tabary, T., Reveil, B., Millot, J. M., ….. Nabiev, I. (2012). Oriented conjugates of single-domain antibodies and quantum dots: toward a new generation of ultrasmall diagnostic nanoprobes. *Nanomedicine: nanotechnology, biology, and medicine, 8*, 516-525.

Sun, Y. S. (2013). Optical Biosensors For Label-Free Detection of Biomolecular Interactions. *Instrumentation Science & Technology, 42*, 109-127.

Sunbul, M., Sugiyama, M., and Kurbanov, F. (2013). Specific mutations of basal core promoter are associated with chronic liver disease in hepatitis B virus subgenotype D1 prevalent in Turkey. *Microbiology and Immunology, 57*, 122-129.

Tamerler, C., Duman, M., Oren, E., Gungormus, M., Xiong, X., Kacar, T., ….. Sarikaya, M.. (2006). Materials specificity and directed assembly of a gold-binding peptide. *Small, 2*, 1372-1378.

Tamerler, C., Khatayevich, D., Gungormus, M., Kacar, T., Oren, E., Hnilova, M., and Sarikaya, M. (2010). Molecular Biomimetics: GEPI-Based Biological Routes to Technology. *Biopolymers, 94*, 78-94.

Tamerler, C., Oren, E. E., Duman, M., Venkatasubramanian, E., and Sarikaya, M. (2006). Adsorption kinetics of an engineered gold binding Peptide by surface plasmon resonance spectroscopy and a quartz crystal microbalance. *Langmuir: the ACS journal of surfaces and colloids, 22*, 7712-7718.

Tamerler, C. & Sarikaya, M. (2009). Molecular biomimetics: nanotechnology and bionanotechnology using genetically engineered peptides. *Philosophical Transactions of the Royal Society a-Mathematical Physical and Engineering Sciences, 367*, 1705-1726.

Tan, G., Yusoff, K., Seow, H., and Tan, W. (2005). Antigenicity and immunogenicity of the immunodominant region of hepatitis B surface antigen displayed on bacteriophage T7. *Journal of Medical Virology, 77*, 475-480.

Tannous, B. A., Kim, D. E., Fernandez, J. L., Weissleder, R., and Breakefield, X. O. (2005). Codon-optimized Gaussia luciferase cDNA for mammalian gene expression in culture and in vivo. *Molecular therapy: the journal of the American Society of Gene Therapy, 11*, 435-443.

Thompson, J., Pope, T., Tung, J. S., Chan, C., Hollis, G., Mark, G., and Johnson, K. S. (1996). Affinity maturation of a high-affinity human monoclonal antibody against the third hypervariable loop of human immunodeficiency virus: Use of phage display to improve affinity and broaden strain reactivity. *Journal of Molecular Biology, 256*, 77-88.

Tkachenko, A., Xie, H., Franzen, S., and Feldheim, D. L. (2005). Assembly and characterization of biomolecule-gold nanoparticle conjugates and their use in intracellular imaging. *Methods in molecular biology, 303*, 85-99.

Url-1 <*http://microgen.ouhsc.edu/biacore.htm*>, date retrieved 30.09.2014.

Url-2 <*http://workbench.sdsc.edu*>, date retrieved 30.09.2014.

Vaisocherova, H., Faca, V., Taylor, A., Hanash, S., and Jiang, S. (2009). Comparative study of SPR and ELISA methods based on analysis of CD166/ALCAM levels in cancer and control human sera. *Biosensors & Bioelectronics, 24*, 2143-2148.

Valenzuela, P., Medina, A., and Rutter, W. (1982). Synthesis and assembly of Hepatitis-B virus surface-antigen particles in yeast. *Nature, 298*, 347-350.

Van Der Merwe, A. (2001). Surface Plasmon Resonance. In S. E. Harding, B. Z. Chowdry (Eds.) *Protein-ligand interactions: hydrodynamics and calorimetry* (pp. 137-170). Oxford: Oxford University Press.

Van Houten, N., Henry, K., Smith, G., and Scott, J. (2010). Engineering filamentous phage carriers to improve focusing of antibody responses against peptides. *Vaccine, 28*, 2174-2185.

Van Weemen, B. K. & Schuurs, A. H. W. M. (1971). Immunoassay using antigen-enzyme conjugates. *Febs Letters, 15*, 232-236.

Van Wezenbeek, P. M., Hulsebos, T. J., and Schoenmakers, J. G. (1980). Nucleotide sequence of the filamentous bacteriophage M13 DNA genome: comparison with phage fd. *Gene, 11*, 129-148.

Vanmeijer, M., Roelofs, Y., Neels, J., Horrevoets, A., vanzonneveld, A., and Pannekoek, H. (1996). Selective screening of a large phage display library of plasminogen activator inhibitor 1 mutants to localize interaction sites with either thrombin or the variable region 1 of tissue-type plasminogen activator. *Journal of Biological Chemistry, 271*, 7423-7428.

Velappan, N., Fisher, H., Pesavento, E., Chasteen, L., D'Angelo, S., Kiss, C., ….. Bradbury, A. R. (2010). A comprehensive analysis of filamentous phage display vectors for cytoplasmic proteins: an analysis with different fluorescent proteins. *Nucleic Acids Research, 38*, 1-16.

Vispo, N., Felici, F., Castagnoli, L., and Cesareni, G. (1993). Hybrid Rop-pIII proteins for the display of constrained peptides on filamentous phage capsids. *Annales de biologie clinique, 51*, 917-922.

Wang, C., Yang, Q., and Craik, C. (1996). Phage display of proteases and macromolecular inhibitors. *Combinatorial Chemistry, 267*, 52-68.

Wang, L. & Yu, M. (2004). Epitope identification and discovery using phage display libraries: Applications in vaccine development and diagnostics. *Current Drug Targets, 5*, 1-15.

Wang, M., Sun, C., Wang, L., Ji, X., Bai, Y., Li, T., and Li, J. (2003). Electrochemical detection of DNA immobilized on gold colloid

particles modified self-assembled monolayer electrode with silver nanoparticle label. *Journal of pharmaceutical and biomedical analysis, 33*, 1117-1125.

Wang, X., Li, Y., Wang, H., Fu, Q., Peng, J., Wang, Y., …. Zhan, L. (2010). Gold nanorod-based localized surface plasmon resonance biosensor for sensitive detection of hepatitis B virus in buffer, blood serum and plasma. *Biosensors & Bioelectronics, 26*, 404-410.

Wang, Z., Zheng, S., Cai, J., Wang, P., Feng, J., Xang, X., ….. Wan, N. (2013). Fluorescent Artificial Enzyme-Linked Immunoassay System Based on Pd/C Nanocatalyst and Fluorescent Chemodosimeter. *Analytical Chemistry, 85*, 11602-11609.

Webster, R. E. (1996). Biology of the filamentous bacteriophage. In B. K. Kay, J. Winter, J. Mccafferty (Eds.), *Phage Display of Peptides and Proteins: a laboratory manual* (Vol. 1, pp. 1-16). San Diego, CA: Academic Press Inc.

Whaley, S., English, D., Hu, E., Barbara, P., and Belcher, A. (2000). Selection of peptides with semiconductor binding specificity for directed nanocrystal assembly. *Nature, 405*, 665-668.

Widersten, M. & Mannervik, B. (1995). Glutathione transferases with novel active-sites isolated by phage display from a library of random mutants. *Journal of Molecular Biology, 250*, 115-122.

Willis, A., Perham, R., and Wraith, D. (1993). Immunological properties of foreign peptides in multiple display on a filamentous bacteriophage. *Gene, 128*, 79-83.

Wittrup, K. (2001). Protein engineering by cell-surface display. *Current Opinion in Biotechnology, 12*, 395-399.

Wu, J., Park, J. P., Dooley, K., Cropek, D. M., West, A. C., and Banta, S. (2011). Rapid Development of New Protein Biosensors Utilizing Peptides Obtained via Phage Display. *PLOS ONE, 6 (10)*, e24948.

Xu, X., Ye, Z. Z., Wu, J., and Ying, Y. B. (2010). Application and Research Development of Surface Plasmon Resonance-based Immunosensors for Protein Detection. *Chinese Journal of Analytical Chemistry, 38*, 1052-1059.

Yang, T., Yang, L., Chai, W., Li, R., Xie, J., and Niu, B. (2011). A strategy for high-level expression of a single-chain variable fragment against TNF alpha by subcloning antibody variable regions from the phage display vector pcantab 5E into pbv220. *Protein Expression and Purification, 76*, 109-114.

Yazici, H., Fong, H., Wilson, B., Oren, E., Amos, F., Zhang, H., ….. Tamerler, C. (2013). Biological response on a titanium implant-grade surface functionalized with modular peptides. *Acta Biomaterialia, 9*, 5341-5352.

Yuca, E., Karatas, A. Y., Seker, U. O., Gungormus, M., Dinler-Doganay, G., Sarikaya, M., and Tamerler, C. (2011). In vitro labeling of

hydroxyapatite minerals by an engineered protein. *Biotechnology and Bioengineering, 108*, 1021-1030.

Yáñez-Sedeño, P., Agüí, L., Villalonga, R., and Pingarrón, J. M. (2014). Biosensors in forensic analysis. A review. *Analytica Chimica Acta, 823*, 1-19.

Zehender, G. & Gabanelli, E. (2012). Spatial and Temporal Dynamics of Hepatitis B Virus D Genotype in Europe and the Mediterranean Basin. *PLOS ONE*, 7, 1-8.

Zhang, Y., Wang, H., Yan, B., Zhang, Y., Li, J., Shen, G., and Yu, R. (2008). A reusable piezoelectric immunosensor using antibody-adsorbed magnetic nanocomposite. *Journal of immunological methods, 332*, 103-111.

Zhao, N., Lange, E., Kubald, S., Grund, C., Beer, M., and Harder, T. (2013). Distinction of subtype-specific antibodies against European porcine influenza viruses by indirect ELISA based on recombinant hemagglutinin protein fragment-1. *Virology Journal, 10*, 1-12.

Zheng, S., Kim, D. K., Park, T. J., Lee, S. J., and Lee, S. Y. (2010). Label-free optical diagnosis of hepatitis B virus with genetically engineered fusion proteins. *Talanta, 82*, 803-809.

Zhu, Z., Rockwell, P., Lu, D., Kotanides, H., Pytowski, B., Hicklin, D., ….. Wittle, L. (1998). Inhibition of vascular endothelial growth factor-induced receptor activation with anti-kinase insert domain-containing receptor single-chain antibodies from a phage display library. *Cancer Research, 58*, 3209-3214.

APPENDICES

APPENDIX A: Primer list.

APPENDIX B: pCANTAB5E vector.

APPENDIX C: pQE2 expression vector.

APPENDIX D: Low Range DNA Ladder.

APPENDIX E: High Range DNA Ladder.

APPENDIX F: Prestained Protein Ladder.

APPENDIX A: Primer list.

HBsAg Forward_SfiI:

5’-ACTCGCGGCCCAGCCGGCCATGGAGAACATCACATCAGG-3’

HBsAg Reverse_NotI:

5’-CATTCTGCGGCCGCTTTGTTTTGTTAGGGTTTAA-3’

HBsAg Forward_BamHI:

5’-ACTCGCGGATCCATGGAGAACATCACATCAGG-3’

HBsAg Reverse_BamHI:

5’-CATTCTGGATCCTTTGTTTTGTTAGGGTTTAA-3’

Light chain primers:

TUB 703: 5’-TATCGAGCTCACCCAGTCTCCA- 3’

TUB 704: 5’- GTTTTATTTCCAACTTTGTCCC- 3’

Heavy chain primers:

TUB 701: 5’- GTGACCGTGGTCCCTTGGCCCC- 3’

TUB702: 5’- AGGTGCAGCTGCAGCAGTCAGG- 3’

TUB 422: 5’- GGGACCACGGTCACCGTCTCCTCA-3’

TUB 423: 5’- TGGAGACTGAGTGAGCTCGATGTC-3’

Lig7 scFv primers:

Lig7_Forw_Ndeİ: 5’-TCGCCATATGCAGGCCCAGGTGCAGCTGCAGGAGTCAGG- 3’

Lig7RevNotI: 5’- GAGTCATTCTGCGGCCGCCCGTTTGATTTCCAGCTTGG- 3’

GBP primers:

GBP1_Not_F: 5’- CTTAAGCGGCCGCATGCATGGAAAAACTCAGGC- 3’

GBP1_HindIII_R:5’- CTTAAAAGCTTGCTCTGGATAGTCCCGCTG- 3’

3GBP_forward: 5’- GGATCCATGCATGGA-3’

3GBP_reverse: 5’- TTAGAATTCGCTCTGG-3’

3GBP_forward_NotI_with tail: 5’-ATTCAGGCGGCCGCGGGATCCATGCATGGA-3’

3GBP_reverse_HindIII_ with tail: 5’-CCATATAAGCTTTTAGAATTCGCTCTGG-3’

Sequencing primers

pDrive vector-specific sequencing primers:

M13 Reverse: 5’ -AACAGCTATGACCATG- 3’

Sp6 promotor: 5’ – CATTTAGGTGACACTATAG-3’

T7 promotor: 5’-GTAATACGACTCACTATAG-3’

PQE2 vector specific sequencing primers:

PQE promotor: 5’- CCCGAAAAGTGCCACCTG -3’

PQE reverse: 5’- GTTCTGAGGTCATTACTGG-3’

pCANTAB5E_specific sequencing primers:

pCANTAB5E_sequencing forward primer: 5’-TATGACCATGATTACGCCAAG-3’

pCANTAB5E_sequencing forward primer: 5’- TTTTGTCGTCTTTCCAGACGTT-3’

APPENDIX B: pCANTAB5E vector.

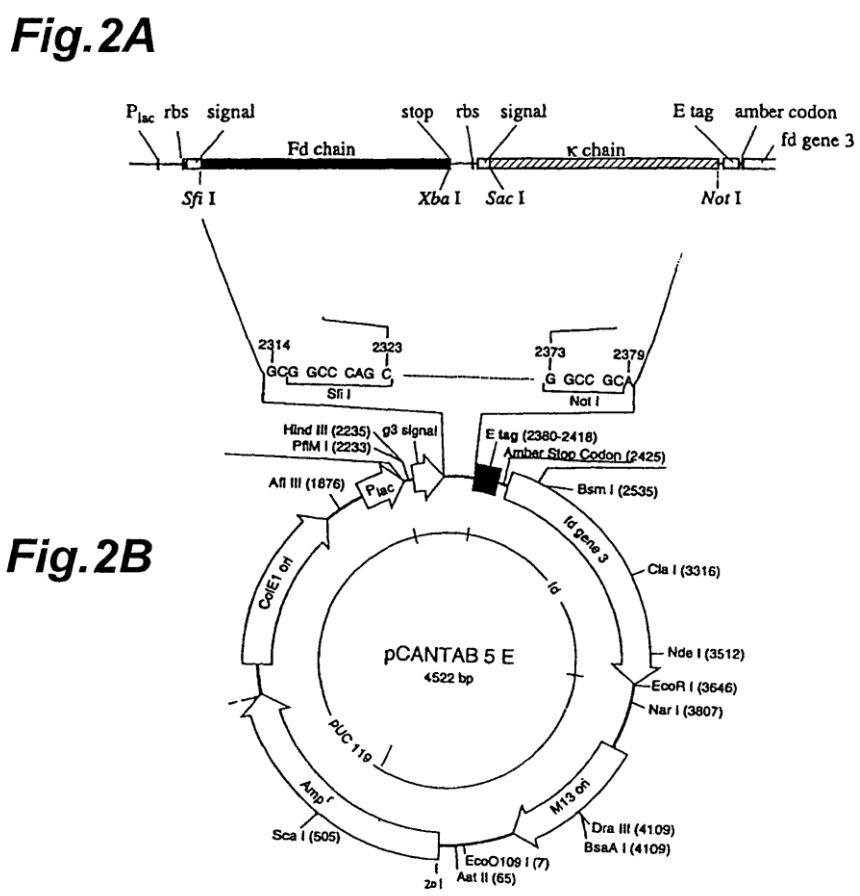

Figure A.1 : pCANTAB5E vector.

APPENDIX C: pQE2 expression vector.

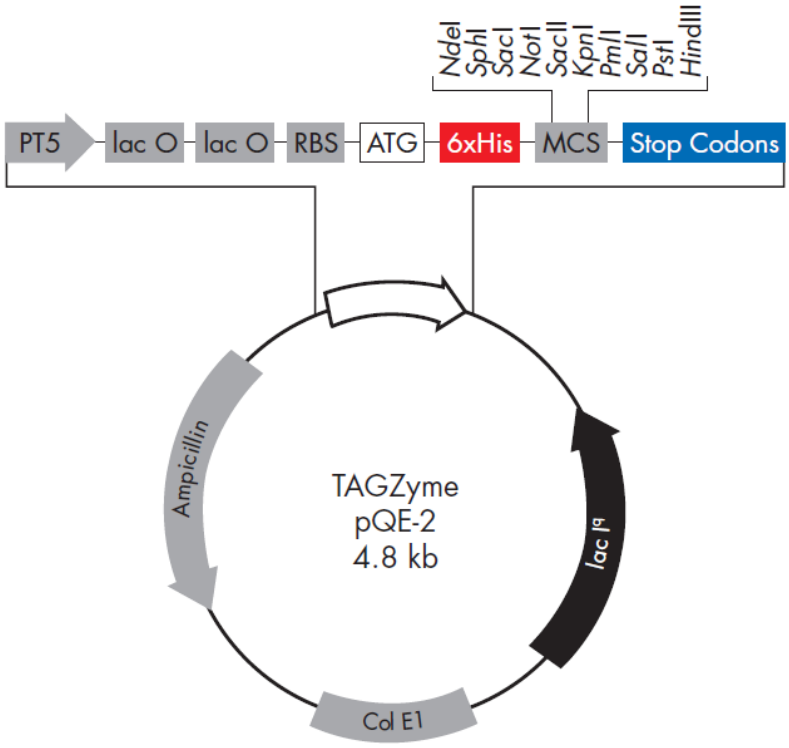

Figure A.2 : pQE2 expression vector (TAGzyme handbook, Qiagen).

APPENDIX D: Low Range DNA Ladder.

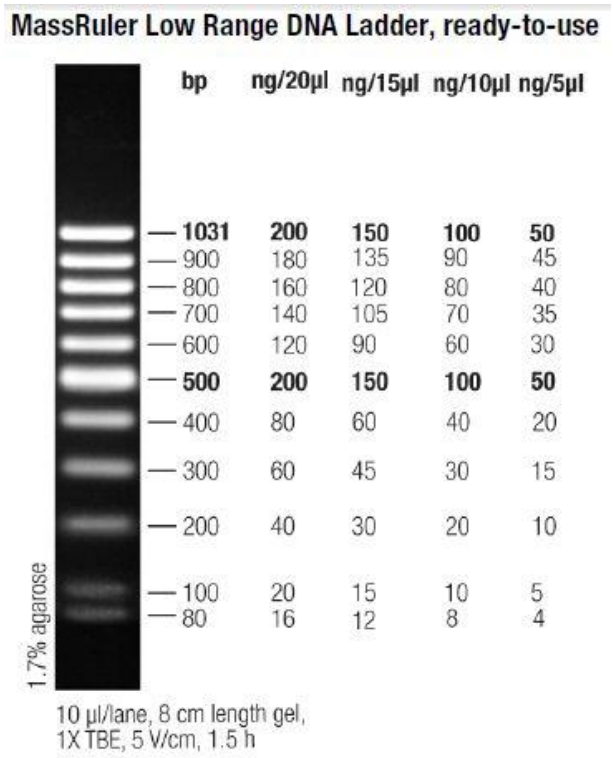

Figure A.3 : MassRuler Low Range, DNA Ladder, ready-to-use, SM0383, Thermo Scientific.

APPENDIX E: High Range DNA Ladder.

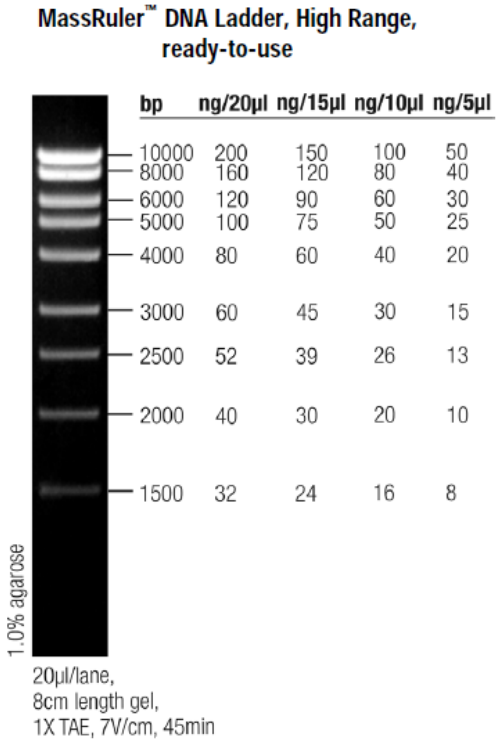

Figure A.4 : MassRuler DNA Ladder, High Range, ready-to-use, SM0393, Fermentas.

APPENDIX F: Prestained Protein Ladder.

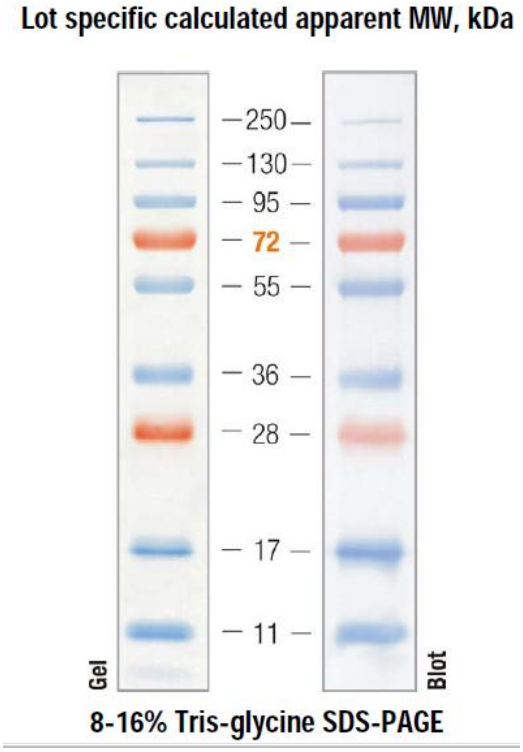

Figure A.5 : PageRuler^{TM} Plus Prestained Protein Ladder, SM1811, Fermentas.

CURRICULUM VITAE

Name Surname: Bertan Koray BALCIOĞLU

Place and Date of Birth: Ankara / 31 January 1976

E-Mail: koray.balcioglu@tubitak.gov.tr

STUDIES:

- **B.Sc.** **:** Claude Bernard University, Cell Biology and Physiology, Lyon, France.
- **M.Sc.** **:** Marmara University, School of Medicine, Medical Biology and Genetics, Istanbul, Turkey.

PROFESSIONAL EXPERIENCE AND REWARDS:

2012- Senior Scientist, Genetic Engineering and Biotechnology Institute, TÜBİTAK-Marmara Research Center, Turkey.

2000- Research Scientist, Genetic Engineering and Biotechnology Institute, TÜBİTAK-Marmara Research Center, Turkey.

Rewards:

- TÜBİTAK MAM, The most successful research team of the year award (28/12/2012).
  Topic: Development of Anti-VEGFR2 antibody structures.

- TÜBİTAK MAM, Success and encouragement award of year 2006 (20/04/2007).
  Topic: Anti-angiogenic anticancer applications on hepatocellular carcinoma transgenic mouse models.

PUBLICATIONS AND PRESENTATIONS RELATED TO THE THESIS:

- **Balcioglu B. K.**, Ozdemir-Bahadir, A., Hinc, D., Tamerler, C. and Erdag, B., 2014. Cost Effective Filamentous Phage Based Immunization Nanoparticles Displaying a full-length Hepatitis B virus surface antigen, *Advances in Bioscience and Biotechnology*, 5(1), 46-53.

- **Balcioglu, B. K.**, Ozdemir-Bahadir, A., Ibrahimoglu, O. , Caliskan, H. B. , Hinc, D. , Tamerler, C. , Erdag, B., 2012. Genetically Engineered Bifunctional Molecular Biosensing Probes: Recombinant antibody against Hepatitis B virus surface antigen on Gold Chips. *International Congress - 15th European Congress on Biotechnology*, September 23-26, 2012 Istanbul, Turkey. (Oral presentation)
- **Balcioglu, B. K.**, Ozdemir-Bahadir, A., Caliskan, H. B., Hinc, D., Tamerler, C., Erdag, B., 2012. Construction of bispecific antibody with gold binding ability for biosensor applications. *International Congress - Molecular Immunology & Immunogenetics Congress*, April 27-29, 2012 Antalya, Turkey.
- **Balcioglu, B. K.**, Ozdemir-Bahadir, A. , Tamerler, C. , Basalp, A. , Erdag, B., 2010. Development of anti-HBsAg recombinant antibody fused with gold binding Peptide. *International Congress - Nanobio Europe, 6TH International congress & exhibition on nanobiotechnology*, June 15-17, 2010 Münster, Germany.

OTHER PUBLICATIONS, PRESENTATIONS AND PATENTS:

- Erdag, B. , **Balcioglu, B. K.**, Ozdemir-Bahadir, A., Serhatli, M., Kacar, O., Bahar, A., Seker, U. O. S., Akgun, E., Ozkan, A., Kilic, T., Tamerler, C. Baysal, K., 2011. Identification of novel neutralizing single-chain antibodies against vascular endothelial growth factor receptor 2. *Biotechnology and Applied Biochemistry*, 58 (6), 412-422.
- Koban, E., Denizci, M., Aslan, O., D. Aktoprakligil, D., S. Aksu, S. , M. Bower, M., **Balcioglu, B. K**., Ozdemir-Bahadir, A., Bilgin, R., Erdag, B., Bagis, H., Arat, S., 2012. High microsatellite and mitochondrial diversity in Anatolian native horse breeds shows Anatolia as a genetic conduit between Europe and Asia. *Animal Genetics*, 43 (4), 401-409.
- Ozdemir-Bahadir, A. , **Balcioglu, B. K.**, Uzyol, K. S. , Hatipoglu, I. , Sogut, I., Basalp, A., Erdag, B. , 2011: Phage Displayed HBV Core Antigen with İmmunogenic Activity. *Appl Biochem Biotechnol*, 165, 1437-1447.
- Erdag, B., B. **Balcioglu, B. K.** , Kumbasar, A. , Celikbicak, O., Zeder-Lutz, G. , Altschuh, D., Salih, B., Baysal, K. , 2007. Novel short peptides isolated from phage display library inhibit vascular endothelial growth factor activity. *Molecular biotechnology*, 35 (1), 51-64.
- Yucel, F., Ozturk, S., Erdag, B., **Balcioglu, K.**, Basalp, A., Baysal K., 2006: Monoclonal Antibodies against Vascular Endothelial Growth Factor (VEGF). *Hybridoma*, 25 (2), 98-99. doi:10.1089/hyb.2006.25.98.
- Erdag, B., **Balcioglu, B. K**., Kumbasar, A., Cirakoglu, B., 2003. Detection of phage-displayed peptides with blocking ability in vascular endothelial growth factor (VEGF) model. In: advances in experimental medicine and biology. Kluwer Academic/Plenum Publishers. New York, 534, 327-334.
- Aksu, S., Aktoprakligil, D., Koban, E., Aslan, O., Denizci, M., **Balcioğlu, K.**, Özdemir-Bahadir, A., Erdağ, B., Bağiş, H., Arat, S., 2010: Gen

Kaynaklarının ve Biyoçeşitliliğin Korunması Kapsamında Yerli At Irklarının Genetik Karakterizasyonu. *BİBAD*, 3 (1), 129-138.

- Erdag, B., **Balcioglu, B. K.**, Bahadir Ozdemir, A., Bahar, A., Baysal, K., Serhatli, M., Kacar, O., Kilic, T., Akgun, E., Ozkan, A., 2010. Recombinant antibody structures binding to and blocking the activity of vascular endothelial growth factor 2 (VEGFR-2/KDR). International patent application number: PCT/IB2010/053109, WO/2012/004631
- Erdag, B., Kumbasar, A., **Balcioglu, B. K.**, Baysal, K., 2007. The peptide structures that bind and block the activity of vascular endothelial growth factor (VEGF). National patent application number 2007/00984.